



# Product Module Rig Test

Louis Chiappetta, Jr., Donald J. Hautman, John T. Ols, Frederick C. Padget IV,  
William O.T. Peschke, John A. Shirley, and Kenneth S. Siskind  
Pratt & Whitney, West Palm Beach, Florida

## The NASA STI Program Office . . . in Profile

Since its founding, NASA has been dedicated to the advancement of aeronautics and space science. The NASA Scientific and Technical Information (STI) Program Office plays a key part in helping NASA maintain this important role.

The NASA STI Program Office is operated by Langley Research Center, the Lead Center for NASA's scientific and technical information. The NASA STI Program Office provides access to the NASA STI Database, the largest collection of aeronautical and space science STI in the world. The Program Office is also NASA's institutional mechanism for disseminating the results of its research and development activities. These results are published by NASA in the NASA STI Report Series, which includes the following report types:

- **TECHNICAL PUBLICATION.** Reports of completed research or a major significant phase of research that present the results of NASA programs and include extensive data or theoretical analysis. Includes compilations of significant scientific and technical data and information deemed to be of continuing reference value. NASA's counterpart of peer-reviewed formal professional papers but has less stringent limitations on manuscript length and extent of graphic presentations.
- **TECHNICAL MEMORANDUM.** Scientific and technical findings that are preliminary or of specialized interest, e.g., quick release reports, working papers, and bibliographies that contain minimal annotation. Does not contain extensive analysis.
- **CONTRACTOR REPORT.** Scientific and technical findings by NASA-sponsored contractors and grantees.

- **CONFERENCE PUBLICATION.** Collected papers from scientific and technical conferences, symposia, seminars, or other meetings sponsored or cosponsored by NASA.
- **SPECIAL PUBLICATION.** Scientific, technical, or historical information from NASA programs, projects, and missions, often concerned with subjects having substantial public interest.
- **TECHNICAL TRANSLATION.** English-language translations of foreign scientific and technical material pertinent to NASA's mission.

Specialized services that complement the STI Program Office's diverse offerings include creating custom thesauri, building customized databases, organizing and publishing research results . . . even providing videos.

For more information about the NASA STI Program Office, see the following:

- Access the NASA STI Program Home Page at <http://www.sti.nasa.gov>
- E-mail your question via the Internet to [help@sti.nasa.gov](mailto:help@sti.nasa.gov)
- Fax your question to the NASA Access Help Desk at 301-621-0134
- Telephone the NASA Access Help Desk at 301-621-0390
- Write to:  
NASA Access Help Desk  
NASA Center for Aerospace Information  
7121 Standard Drive  
Hanover, MD 21076



# Product Module Rig Test

Louis Chiappetta, Jr., Donald J. Hautman, John T. Ols, Frederick C. Padget IV,  
William O.T. Peschke, John A. Shirley, and Kenneth S. Siskind  
Pratt & Whitney, West Palm Beach, Florida

Prepared under Contract NAS3-27235

National Aeronautics and  
Space Administration

Glenn Research Center

Trade names or manufacturers' names are used in this report for identification only. This usage does not constitute an official endorsement, either expressed or implied, by the National Aeronautics and Space Administration.

Note that at the time of research, the NASA Lewis Research Center was undergoing a name change to the NASA John H. Glenn Research Center at Lewis Field. Both names may appear in this report.

Available from

NASA Center for Aerospace Information  
7121 Standard Drive  
Hanover, MD 21076

National Technical Information Service  
5285 Port Royal Road  
Springfield, VA 22100

Available electronically at <http://gltrs.grc.nasa.gov>

## **Product Module Rig Test**

Louis Chiappetta, Donald J. Hautman, John T. Ols, Frederick C. Padget,  
William O. Peschke, John A. Shirley, and Kenneth S. Siskind  
Pratt & Whitney  
West Palm Beach, Florida 33410

# Foreward

This report documents the activities conducted under Work Breakdown Structure (WBS) 1.0.2.7 of the NASA Critical Propulsion Components (CPC) Program under Contract NAS3-27235 to evaluate the low emissions potential of a Rich-Quench-Lean (RQL) combustor for use in the High Speed Civil Transport (HSCT) application. The specific intent was to demonstrate a Rich-Quench-Lean combustor, utilizing reduced scale quench technology implemented in a quench vane concept, capable of achieving the program goal of emissions of nitrogen oxides ( $\text{NO}_x$  EI) less than 5 gm/Kg fuel at the supersonic flight condition while maintaining combustion efficiencies in excess of 99.9%.

The NASA Subelement Task Manager for this task was Mr. David J. Anderson of NASA Lewis Research Center, Cleveland, Ohio. Dr. Robert P. Lohmann was the Pratt & Whitney IPT Team Leader. Mr. Kenneth Siskind and Mr. John Ols were responsible for the design and analysis of the experimental combustor hardware while Dr. Donald Hautman (UTRC) and Mr. Frederick Padget (UTRC) were principal investigators for the experimental assessment of the combustor at United Technologies Research Center. Mr. Edward McCoomb (UTRC) was responsible for design and procurement of the experimental combustor hardware. Mr. Richard B. Ferraro (UTRC) was responsible for fabrication of the experimental combustor hardware. Mr. John Shirley (UTRC) was the principle investigator for the single module rig quench vane parametrics tests in support of the quench vane design activities. Mr. William Peschke (UTRC) was responsible for development of engineering models from the single module rig quench vane parametrics tests in support of the quench vane design activities. Mr. Louis Chiappetta (UTRC) was responsible for the supporting computational fluid dynamics calculations. Combustion tests were conducted at the Jet Burner Test Stand of United Technologies Research Center, with particular acknowledgement of the support of Mr. Jimmey L. Grimes, Mr. James D. Macleod and Mr. Ralph H. Pinney.

# Table of Contents

<b>FOREWARD .....</b>	<b>2</b>
<b>SECTION I - SUMMARY.....</b>	<b>9</b>
<b>SECTION II - INTRODUCTION .....</b>	<b>10</b>
OBJECTIVES.....	11
<b>SECTION III - COMBUSTOR TEST FACILITY .....</b>	<b>13</b>
LAYOUT.....	13
AIRFLOW DELIVERY AND HEATING.....	13
FUEL FLOW .....	14
WATER FLOWS .....	14
NITROGEN FLOW .....	14
<b>SECTION IV - COMBUSTOR HARDWARE DESIGN.....</b>	<b>15</b>
SINGLE MODULE RIG FOR VANE PARAMETRICS .....	15
<i>Fuel Preparation Devices</i> .....	15
Airblast Fuel Injector.....	15
Radial-Inflow High-Shear Injector.....	15
<i>Rich Zone</i> .....	16
<i>Quench Zone</i> .....	16
<i>CFD Analysis of Quench Zone Geometries</i> .....	20
Scope of Effort.....	20
Approach.....	20
Limitations to Approach .....	21
Computational Domains .....	21
Sensitivity of results to grid resolution .....	22
<i>Lean Zone</i> .....	24
PRODUCT MODULE RIG DESIGN .....	24
<i>Build 1 &amp; 1A Design</i> .....	24
<i>Build 2 &amp; 2A Design</i> .....	26
<b>SECTION V - INSTRUMENTATION.....</b>	<b>29</b>
SINGLE MODULE RIG .....	29
<i>Static Pressures</i> .....	29
<i>Temperatures</i> .....	29
PRODUCT MODULE RIG.....	29
<i>Static Pressures</i> .....	29
<i>Temperatures</i> .....	30
EMISSIONS SAMPLING AND ANALYSIS .....	30
<i>Emissions Sampling System</i> .....	30
<i>Emissions Analysis Procedures and Performance Parameters</i> .....	31
<i>Fuel/Air Ratio</i> .....	32
<i>Emissions Index</i> .....	32
<i>Combustion Efficiency</i> .....	33
<b>SECTION VI - COMBUSTOR TEST EVALUATION RESULTS.....</b>	<b>34</b>
SINGLE MODULE RIG TEST CHRONOLOGY .....	34
PRODUCT MODULE RIG TEST CHRONOLOGY .....	35
<i>Build 1 &amp; 1A Test Chronology</i> .....	35
<i>Build 2 Test Chronology</i> .....	40
<i>Build 2a Test Chronology</i> .....	40

DISCUSSION OF VANE PARAMETRICS .....	41
<i>Fuel/Air Excursion</i> .....	41
<i>Pressure Drop Excursion</i> .....	41
<i>Residence Time Excursion</i> .....	41
<i>Emissions Maps</i> .....	42
<i>Effect of Geometric Variations on NO<sub>x</sub> at the Nominal Supersonic Cruise Condition</i> .....	42
Effect of Quench-Air, Injection Orifice Aspect Ratio .....	43
Effect of the Number of Quench-Air, Injection Orifices per Side (Orifice Spacing).....	43
Effect of Quench-Zone Channel Height .....	44
Effect of Momentum-Flux Ratio.....	44
Effect of Single-Direction-Feed.....	45
Effect of Quench-Air Injection Orifice Orientation.....	45
Effect of a Truncated Trailing-Edge .....	45
Effect of Rectangular Rich-Zone .....	46
Particulate Measurements.....	46
Effects of Cooling Air Introduction Post Quench Air Addition .....	46
DISCUSSION OF PRODUCT MODULE RIG .....	46
<i>Build 1 &amp; 1A Test Results</i> .....	46
<i>Build 2 Test Results</i> .....	47
<i>Build 2a Test Results</i> .....	48
<b>SECTION VII - CONCLUSIONS</b> .....	<b>50</b>
<b>REFERENCES</b> .....	<b>51</b>
<b>SECTION II FIGURES</b> .....	<b>52</b>
<b>SECTION IV FIGURES</b> .....	<b>53</b>
<b>SECTION V FIGURES</b> .....	<b>77</b>
<b>SECTION VI FIGURES</b> .....	<b>79</b>

# List of Tables

<i>Table IV - 1 Summary of Reduced Scale Quench Geometries Investigated in Single Module Rig Configuration</i>	18
<i>Table IV - 2 Reduced Scale Quench Vane Orifice Parameters for Single Module Rig Geometries</i>	19
<i>Table IV - 3 Calculated Parameters for Reduced Scale Quench Vane Single Module Rig Geometries</i>	19
<i>Table IV - 4 Inlet Flow Conditions for CFD Analysis of Quench Zone Geometries</i>	21
<i>Table IV - 5 CFD Analyses Assessing the Sensitivity of Results to Grid Resolution</i>	22
<i>Table IV - 6 Rankings of Quench Vane Geometries based on Active Volume Parameter Calculation for Various Fuel/Air Ratio Ranges</i>	23
<i>Table VI - 1 Single Module Rig Run Log and Configuration Summary</i>	34
<i>Table VI - 2 Standard Test Plan for Quench Vane Parametrics Testing in the Single Module Rig Configuration</i>	35
<i>Table VI - 3 Uniform Schedule of Test Points</i>	35
<i>Table VI - 4 Root Cause Investigation Findings for Product Module Rig Build 1</i>	39

# List of Figures

Figure II - 1 Multi-Modular Rich-Quench-Lean Combustor with Reduced Scale Quench Vanes	52
Figure II - 2 Rich Zone Stoichiometry of a Fixed Geometry RQL Combustor (22% rich zone, 73% quench zone, 5% lean zone cooling)	52
Figure IV - 1 RQL Single Module Rig Configuration used for Investigating Quench Vane Parametrics	53
Figure IV - 2 Exploded View of Single Module Rig Configuration	53
Figure IV - 3 Flowpath Feeding Quench Vanes in Single Module Rig Configuration	54
Figure IV - 4 Airblast Fuel Injector Design for Single Module Rig Configuration	55
Figure IV - 5 Airblast Fuel Injector used in Single Module Rig Configuration	55
Figure IV - 6 Schematic of Radial Inflow Swirler/Fuel Injector Concept	56
Figure IV - 7 Relationship of Quench Channel Geometries to Quench and Lean Zone Flow Areas - Single Module Rig	56
Figure IV - 8 Vane Geometry #1	57
Figure IV - 9 Vane Geometry #2	57
Figure IV - 10 Vane Geometry #3	57
Figure IV - 11 Vane Geometry #4	58
Figure IV - 12 Vane Geometry #5	58
Figure IV - 13 Vane Geometry #6	58
Figure IV - 14 Vane Geometry #7	59
Figure IV - 15 Vane Geometry #8	59
Figure IV - 16 Vane Geometry #9	59
Figure IV - 17 Vane Geometry #10	60
Figure IV - 18 Vane Geometry #11	60
Figure IV - 19 Vane Geometry #12	60
Figure IV - 20 Truncated Trailing Edge Quench Vane Geometry	61
Figure IV - 21 Slanted Slot Quench Vane Geometry	61
Figure IV - 22 Single Direction Feed Quench Vane Geometry	62
Figure IV - 23 Parallel Path Vane Geometry with Effusively Cooled Trailing Edge	62
Figure IV - 24 Parallel Path Vane Geometry with Non-Effusively Cooled Trailing Edge	63
Figure IV - 25 Axisymmetric Grid of Rich Zone for Determining Inlet Boundary Conditions for Quench Vane CFD Analyses	63
Figure IV - 26 Full Domain for CFD Analyses of Quench Vane Geometries	64
Figure IV - 27 Quarter Symmetry Domain for CFD Analyses of Quench Vane Geometries	64
Figure IV - 28 Strut-to-Strut Domain for CFD Analyses of Quench Vane Geometries	64
Figure IV - 29 NOx Calculation Sensitivity to Grid Density	65
Figure IV - 30 Active Volume Parameter Insensitivity to Grid Density	65
Figure IV - 31 Active Volume Controlled by Quench Orifice Size and Spacing (Left: Quench Vane Geometry #1; Right: Quench Vane Geometry #3)	66
Figure IV - 32 Calculated Active Volume Parameter Correlated Against Measured NOx Emissions	66
Figure IV - 33 Aft-Looking Forward View of Product Module Rig Build 1	67
Figure IV - 34 Cross Section of Product Module Rig Build 1	67
Figure IV - 35 Exploded View of Product Module Rig Build 1	68
Figure IV - 36 Exploded View of Product Module Rig Combustor Assembly	68
Figure IV - 37 Product Module Rig Bulkhead Assembly	69
Figure IV - 38 Rich Zone Liner for Product Module Rig Build 1	70
Figure IV - 39 Upper & Lower Impingement Shells of Product Module Rig Build 1	70
Figure IV - 40 Quench Vane Assembly for Product Module Rig Build 1	71
Figure IV - 41 Product Module Rig Build 1 Quench Vane FlowPath Views	71
Figure IV - 42 Product Module Rig Build 1 Turning Strip. Forward-Looking-Aft Trimetric View.	71
Figure IV - 43 Aft Trap Plate for Product Module Rig Build 1	72
Figure IV - 44 Comparison of Airflow Paths for Product Module Rig Build 1 versus 2	72
Figure IV - 45 Aft-Looking-Forward View of Product Module Rig Build 2	73

Figure IV - 46 Cross-Section of Product Module Rig Build 2	74
Figure IV - 47 Exploded View of Product Module Rig Build 2	74
Figure IV - 48 Rich Zone Liner for Product Module Rig Build 2	75
Figure IV - 49 Impingement Shells for Product Module Rig Build 2	75
Figure IV - 50 Quench Vane Assembly for Product Module Rig Build 2	76
Figure IV - 51 Sidewall Vane Assembly for Product Module Rig Build 2	76
Figure V - 1 Single Module Rig Instrumentation	77
Figure V - 2 Emissions Sampling Probe System used in Single Module Rig and Product Module Rig Tests	77
Figure V - 3 Aerodynamic Quenching Emissions Probe Tip Design	77
Figure V - 4 Emissions Analysis System Schematic	78
Figure VI - 1 Forward-Looking-Aft View of Product Module Rig Build 1 Combustor Showing Corner Dam Weld Failure and Impact	79
Figure VI - 2 Emissions as a Function of Fuel/Air Ratio for Vane Geometry #3	80
Figure VI - 3 Emissions as a Function of Pressure Drop for Vane Geometry #3	80
Figure VI - 4 Emissions as a Function of Lean Zone Residence Time for Vane Geometry #3	81
Figure VI - 5 Map of Sampling Locations for Single Module Rig Diagnostic Emissions Contours	82
Figure VI - 6 NO <sub>x</sub> Emissions Index Contours for Vane Geometry #3	83
Figure VI - 7 CO Emissions Index Contours for Vane Geometry #3	84
Figure VI - 8 Contours of the Ratio of Emissions-based Fuel/Air Relative to Metered Fuel/Air for Vane Geometry #3	85
Figure VI - 9 NO <sub>x</sub> Emissions as a Function of Orifice Aspect Ratio	86
Figure VI - 10 Active Volume Parameter as a Function of Orifice Aspect Ratio	86
Figure VI - 11 CFD Calculated Fuel/Air Ratio Contours as a Function of Orifice Aspect Ratio	87
Figure VI - 12 NO <sub>x</sub> Emissions as a Function of Orifice Spacing	88
Figure VI - 13 Active Volume Parameter as a Function of Orifice Spacing	88
Figure VI - 14 CFD Calculated Contours of Fuel/Air Ratio as a Function of Orifice Spacing	89
Figure VI - 15 NO <sub>x</sub> Emissions as a Function of Quench Zone Channel Height	90
Figure VI - 16 Active Volume Parameter as a Function of Quench Zone Channel Height	90
Figure VI - 17 CFD Calculated Fuel/Air Ratio Contours as a Function of Quench Zone Channel Height	91
Figure VI - 18 NO <sub>x</sub> Emissions as a Function of Momentum Flux Ratio	92
Figure VI - 19 Active Volume Parameter as a Function of Momentum Flux Ratio	92
Figure VI - 20 CFD Calculated Fuel/Air Ratio Contours as a Function of Momentum Flux Ratio	93
Figure VI - 21 Particle Concentration Measurements at Nominal Supersonic Cruise Condition for Vane Geometry #3 as a Function of Residence Time after Quench	94
Figure VI - 22 Particle Concentration Distributions at Nominal Supersonic Cruise Condition for Vane Geometry #3 as a Function of Residence Time after Quench	94
Figure VI - 23 Effect of Cooling Air Assessed in Single Module Rig with Effusively Cooled Single Direction Feed Vane	95
Figure VI - 24 Emissions as a Function of Combustor Inlet Temperature for Assessment of Cooling Air Impact	96
Figure VI - 25 Emissions as a Function of Residence Time for Assessment of Cooling Air Impact	96
Figure VI - 26 Rich Zone Stoichiometry Comparison at 15% Thrust LTO (Descent) Condition for Product Module Rig Builds 1 & 1A	97
Figure VI - 27 Emissions Data Quality at 15% Thrust LTO (Descent) Condition for Product Module Rig Builds 1 & 1A	97
Figure VI - 28 NO <sub>x</sub> Emissions at 15% Thrust LTO (Descent) Condition for Product Module Rig Builds 1 & 1A	98
Figure VI - 29 CO Emissions at 15% Thrust LTO (Descent) Condition for Product Module Rig Builds 1 & 1A	98
Figure VI - 30 UHC Emissions at 15% Thrust LTO (Descent) Condition for Product Module Rig Builds 1 & 1A	99
Figure VI - 31 Efficiency at 15% Thrust LTO (Descent) Condition for Product Module Rig Builds 1 & 1A	99
Figure VI - 32 Rich Zone Stoichiometry at 5.8% Thrust LTO (Idle) Condition for Product Module Rig Build 2	100

Figure VI - 33 Emissions Data Quality at 5.8% Thrust LTO (Idle) Condition for Product Module Rig Build 2	100
Figure VI - 34 NO <sub>x</sub> Emissions at 5.8% Thrust LTO (Idle) Condition for Product Module Rig Build 2	101
Figure VI - 35 CO Emissions at 5.8% Thrust LTO (Idle) Condition for Product Module Rig Build 2	101
Figure VI - 36 UHC Emissions at 5.8% Thrust LTO (Idle) Condition for Product Module Rig Build 2	102
Figure VI - 37 Efficiency at 5.8% Thrust LTO (Idle) Condition for Product Module Rig Build 2	102
Figure VI - 38 Rich Zone Stoichiometry Comparison at 15% Thrust LTO (Descent) Condition for Product Module Rig Builds 1, 1A & 2	103
Figure VI - 39 Emissions Data Quality at 15% Thrust LTO (Descent) Condition for Product Module Rig Builds 1, 1A & 2	103
Figure VI - 40 NO <sub>x</sub> Emissions at 15% Thrust LTO (Descent) Condition for Product Module Rig Builds 1, 1A & 2	104
Figure VI - 41 CO Emissions at 15% Thrust LTO (Descent) Condition for Product Module Rig Builds 1, 1A & 2	104
Figure VI - 42 UHC Emissions at 15% Thrust LTO (Descent) Condition for Product Module Rig Builds 1, 1A & 2	105
Figure VI - 43 Efficiency at 15% Thrust LTO (Descent) Condition for Product Module Rig Builds 1, 1A & 2	105
Figure VI - 44 Rich Zone Stoichiometry at Nominal Subsonic Cruise Condition for Product Module Rig Build 2	106
Figure VI - 45 Emissions Data Quality at Nominal Subsonic Cruise Condition for Product Module Rig Build 2	106
Figure VI - 46 NO <sub>x</sub> Emissions at Nominal Subsonic Cruise Condition for Product Module Rig Build 2	107
Figure VI - 47 CO Emissions at Nominal Subsonic Cruise Condition for Product Module Rig Build 2	107
Figure VI - 48 UHC Emissions at Nominal Subsonic Cruise Condition for Product Module Rig Build 2	108
Figure VI - 49 Efficiency at Nominal Subsonic Cruise Condition for Product Module Rig Build 2	108
Figure VI - 50 Rich Zone Stoichiometry Comparison at De-rated, Reduced Pressure 100% Thrust LTO (Takeoff) Condition for Product Module Rig Builds 2 & 2A	109
Figure VI - 51 Emissions Data Quality at De-rated, Reduced Pressure 100% Thrust LTO (Takeoff) Condition for Product Module Rig Builds 2 & 2A	109
Figure VI - 52 NO <sub>x</sub> Emissions at De-rated, Reduced Pressure 100% Thrust LTO (Takeoff) Condition for Product Module Rig Builds 2 & 2A	110
Figure VI - 53 CO Emissions at De-rated, Reduced Pressure 100% Thrust LTO (Takeoff) Condition for Product Module Rig Builds 2 & 2A	110
Figure VI - 54 UHC Emissions at De-rated, Reduced Pressure 100% Thrust LTO (Takeoff) Condition for Product Module Rig Builds 2 & 2A	111
Figure VI - 55 Efficiency at De-rated, Reduced Pressure 100% Thrust LTO (Takeoff) Condition for Product Module Rig Builds 2 & 2A	111
Figure VI - 56 Rich Zone Stoichiometry Comparison at Nominal Supersonic Cruise Condition for Product Module Rig Builds 2 & 2A	112
Figure VI - 57 Emissions Data Quality at Nominal Supersonic Cruise Condition for Product Module Rig Builds 2 & 2A	112
Figure VI - 58 NO <sub>x</sub> Emission Comparison at Nominal Supersonic Cruise Condition for Product Module Rig Builds 2 & 2A	113
Figure VI - 59 CO Emission Comparison at Nominal Supersonic Cruise Condition for Product Module Rig Builds 2 & 2A	113
Figure VI - 60 UHC Emission Comparison at Nominal Supersonic Cruise Condition for Product Module Rig Builds 2 & 2A	114
Figure VI - 61 Efficiency Comparison at Nominal Supersonic Cruise Condition for Product Module Rig Builds 2 & 2A	114

## Section I - Summary

The low emissions potential of a Rich-Quench-Lean (RQL) combustor for use in the High Speed Civil Transport (HSCT) application was evaluated as part of Work Breakdown Structure (WBS) 1.0.2.7 of the NASA Critical Propulsion Components (CPC) Program under Contract NAS3-27235. Combustion testing was conducted in cell 1E of the Jet Burner Test Stand at United Technologies Research Center. Specifically, a Rich-Quench-Lean combustor, utilizing reduced scale quench technology implemented in a quench vane concept in a product-like configuration (Product Module Rig), demonstrated the capability of achieving an emissions index of nitrogen oxides ( $\text{NO}_x$  EI) of 8.5 gm/Kg fuel at the supersonic flight condition (relative to the program goal of 5 gm/Kg fuel). Developmental parametric testing of various quench vane configurations in the more fundamental flametube, Single Module Rig Configuration, demonstrated  $\text{NO}_x$  EI as low as 5.2. All configurations in both the Product Module Rig configuration and the Single Module Rig configuration demonstrated exceptional efficiencies, greater than 99.95%, relative to the program goal of 99.9% efficiency at supersonic cruise conditions.

Sensitivity of emissions to quench orifice design parameters were determined during the parametric quench vane test series in support of the design of the Product Module Rig configuration. For the rectangular quench orifices investigated, an aspect ratio (length/width) of approximately 2 was found to be near optimum. An optimum for orifice spacing was found to exist at approximately 0.167 inches, resulting in 24 orifices per side of a quench vane, for the 0.435 inch quench zone channel height investigated in the Single Module Rig. Smaller quench zone channel heights appeared to be beneficial in reducing emissions. Measurements were also obtained in the Single Module Rig configuration on the sensitivity of emissions to the critical combustor parameters of fuel/air ratio, pressure drop and residence time. Minimal sensitivity was observed for all of these parameters.

## Section II - Introduction

Environmental impacts will dictate substantial constraints on the High Speed Civil Transport (HSCT) aircraft that will in turn establish its economic viability. Emissions output, and in particular the oxides of nitrogen generated during supersonic flight in the stratosphere, is especially significant because of their potential for participating in the destruction of ozone at these high altitudes. These concerns lead to the need to severely constrain the output of  $\text{NO}_x$  from the engines for this aircraft. Comprehensive studies of the dynamics of the upper atmosphere as it influences ozone concentrations are being conducted under the NASA sponsored Atmospheric Effects of Stratospheric Aircraft program (Ref. 1). The initial results from these studies have led to a goal of an emissions index of 5 gm of  $\text{NO}_x$ /kg fuel at the supersonic cruise flight condition. Since this level is five to eight times lower than that achievable with current engine combustor technology only the most aggressive and advanced low emissions technology can be considered for the power plants for this aircraft. Pratt & Whitney and General Electric are studying two combustor concepts in the NASA-sponsored High Speed Research program to define a burner that achieves this  $\text{NO}_x$  emissions goal at the supersonic cruise operating condition. Such a burner must also preserve high efficiency, broad operability, and low emissions at all other operating conditions as well as being durable and economically competitive.

The effort at Pratt & Whitney has focused on the Rich-Quench-Lean (RQL) combustor. A conceptual embodiment of this combustor is shown in Figure II - 1. This combustor concept incorporates separated zones of combustion to preserve combustor stability while achieving emission control. The combustion process is initiated in a fuel-rich combustion zone and completed in a fuel-lean combustion zone, with a rapid transition between them. All of the fuel is introduced in the rich zone but with only a fraction of the air required for complete combustion. The rich combustion process provides the combustor stability and, being deficient in oxygen, completes a significant portion of the overall energy release without forming oxides of nitrogen. The combustion products proceed to a quench section where the remainder of the combustion air is introduced in a rapid, intense mixing process. The downstream lean zone is used to complete CO and soot burn-off. Low  $\text{NO}_x$  emissions will be achieved only if the quench or transition process between the zones is sufficiently vigorous to avoid significant flow residence time near stoichiometric mixture proportions. Sub-scale testing of a single injector or modular version of the RQL combustor at the HSCT engine supersonic cruise operating conditions has demonstrated the low emissions potential of this concept and generated a significant design data base. This effort has been conducted at United Technologies Research Center (UTRC) and was performed as Task 3, HSR Low  $\text{NO}_x$  Combustor, of NASA Lewis Research Center contract NAS3-25952, Aero-Propulsion Technology Research Program, with Pratt & Whitney of the United Technologies Corporation (Ref. 2).

For the High Speed Civil Transport engine application the aerothermal design point of the Rich-Quench-Lean combustor is the supersonic cruise condition. The results of the evaluations performed in Ref. 2 indicate that the equivalence ratio in the rich zone should be about 2.0. This equivalence ratio is sufficiently high to preclude  $\text{NO}_x$  emissions at the exit of the rich zone while minimizing the proclivity for smoke formation. To minimize  $\text{NO}_x$  production in the quench and lean zones, liner cooling airflow to the lean zone is minimized and the remainder of the combustor air enters through the quench air system. Based on an overall fuel/air ratio of 0.030 at nominal supersonic cruise, these considerations lead to a combustor airflow distribution of about 22% in the rich zone, 73% through the quench system and 5% for lean zone liner cooling. Figure II - 2 shows the rich zone operating characteristics, on a stoichiometry diagram, for a fixed geometry combustor that incorporates this airflow distribution. It is evident that the characteristic of any combustor with a fixed rich zone airflow fraction is a line that must pass through the origin of the graph. For the particular engine cycle under consideration, both the high-power, supersonic cruise operating point and the low-power, ground-idle point are shown on the characteristic line. This range of "rich zone" equivalence ratios, from 0.6 to 2.0, is similar to many gas turbine combustors typically used for subsonic aircraft, implying that a fixed geometry combustor with 22% combustor airflow in the "rich" zone might satisfy the operational requirements of this engine.

However, while this airflow distribution is optimized from the point of view of supersonic cruise operation, as the engine is operated at fuel/air ratios less than supersonic cruise, the mixture strength in

the rich zone would approach and eventually pass through stoichiometric proportions. Since the highest gas temperatures occur in the products of stoichiometric or near-stoichiometric combustion, steady state operation at points in this regime could have adverse effects on durability of the rich zone liner and on the emissions output at some intermediate power levels. This effect is demonstrated graphically on Figure II - 2, where a regime of prohibited steady state operation, labeled "Durability", is indicated around stoichiometric proportions.

While not immediately relevant to the fixed geometry 22% rich zone airflow configuration, Figure II - 2 also indicates another area of prohibited steady state operation. This second prohibited region occurs at low, overall engine fuel/air ratios and high rich zone equivalence ratios. This regime indicates the operation of the rich zone at above stoichiometric conditions that will generate large quantities of CO and smoke but for which there is inadequate temperature levels in the quench and lean zones to oxidize these products. Consequently, the so-called "rich" zone (at high power) can only be operated at lean, or below stoichiometric proportions at low power to avoid large quantities of CO and smoke in the exhaust. Providing for the operational capability of a flight engine while satisfying the constraints of avoiding steady state operation in the prohibited zones of the rich zone stoichiometry diagram is a subject addressed in other tasks of the program (Ref. 3) and are not addressed here since the focus of this task was to develop the Rich-Quench-Lean combustor to satisfy the goals of low NO<sub>x</sub> emissions at supersonic cruise conditions.

## **Objectives**

The objective of the task reported herein, which was conducted as Work Breakdown Structure (WBS) 1.0.2.7 of the NASA Critical Propulsion Components (CPC) Program under Contract NAS3-27235, was to evaluate the low emissions potential of a Rich-Quench-Lean (RQL) combustor for use in the High Speed Civil Transport (HSCT) application. The specific intent was to demonstrate a Rich-Quench-Lean combustor, utilizing reduced scale quench technology implemented in a quench vane concept, capable of achieving the program goal of emissions of nitrogen oxides (NO<sub>x</sub> EI) less than 5 gm/Kg fuel at the supersonic flight condition while maintaining combustion efficiencies in excess of 99.9%.. Emphasis was also placed on robust designs that could be introduced with minimal additional development and refinement because of the rapid-paced High Speed Research program requirements. Specific objectives of the task were to:

- Design and fabricate various quench vane configurations, that implement reduced scale quench technology, parametrically varying key geometric and flow variables and evaluate their performance in the Single Module Rig combustor in support of development of a product-like implementation of reduced scale quench technology.
- Conduct computational fluid dynamic (CFD) analyses and water flow visualization of quench vane configurations to aid the engineering comprehension of the flow field impacts associated with various reduced scale quench parameters.
- Design and fabricate a combustor that represents an inner module of the full scale Two-Bank Modular RQL combustor design for testing in the Product Module Rig.
- Design and fabricate a combustor that is a single nozzle representation an inner bank of the full scale Dual Annular Reduced Scale Quench Vane RQL combustor design for testing in the Product Module Rig.
- Perform combustion tests with each configuration at nominal supersonic cruise condition and at other critical conditions in the flight envelope, including airport vicinity and subsonic cruise conditions, to determine performance, emissions and operability of these concepts.

The activities performed in this program were consistent with the above objectives. The design activities for both the parametric quench vane series for the Single Module Rig and the product-like implementation for the Product Module Rig were conducted as a joint activity between Pratt & Whitney and United Technologies Research Center. CFD analyses were conducted by United Technologies

Research Center. Combustion tests of the Single Module Rig and Product Module Rig were conducted in dedicated facilities at the United Technologies Research Center. This facility was located in Cell 11E of the Jet Burner Test Stand at United Technologies Research Center. The facility is capable of testing at combustor pressures up to 200 psia, combustor inlet air temperatures of 1400°F, and contained airflow control features to alter the airflow rates delivered to the rich-zone combustor and to the quench mixer. An existing high inlet air temperature Rich-Quench-Lean combustor rig used in the concept demonstration and design base data acquisition activities of Ref. 2 was the test vehicle for the performance, emissions and operability assessment of the parametric series of quench vane evaluations conducted in the Single Module Rig combustion tests. The combustor rig contained a modular, 5-inch diameter RQL combustor that allowed evaluation of quench vane geometry components in a size scale consistent with a product implementation of reduced scale quench vane technology for an RQL combustor under development in the High Speed Research program. The Product Module Rig combustors were designed fabricated specifically for this task and were targetted as a representative section of the full scale RQL combustor concepts. The Product Module Rig combustor was designed as a drop-in replacement section for the Single Module Rig combustor making efficient use of the existing test facility and to support the rapid development process in support of the forthcoming combustor downselect in the High Speed Research Critical Propulsion Components Program.

This report details the activities and results of the evaluation of the reduced scale quench vane technology development towards a Product Module Rig combustor demonstration. Section I provides a Program Summary, while Section II includes introductory and background information. Section III provides a description of the test facility and Section IV provides a description of the combustor hardware, including the Single Module Rig combustor and the Product Module Rig combustor. Section V describes the instrumentation and emissions systems used in the evaluation of the performance of the combustor concepts while the results of the combustion test programs are discussed in Section VI. Conclusions are presented in Section VII.

## Section III - Combustor Test Facility

### *Layout*

The reduced-scale-quench (RSQ), rich-quench-lean (RQL) combustor test facility included a high-temperature airflow distribution and control system, the RQL combustor, an emissions system and an exhaust system.

The total combustor airflow (WAT) was supplied to the test facility installed in Cell 1E of the Jet Burner Test Stand at United Technologies Research Center by continuous-flow compressors. This flow was metered by a venturi and heated by a series of two non-vitiated air heaters. For the Single Module Rig configuration, the airflow exiting the second heater was divided into the rich-zone airflow (WAR) and the quench-zone airflow (WAQ). The rich zone airflow traveled through a 6 inch pipe to a metering orifice plate while the quench zone airflow was routed through a 3 inch pipe to the quench air manifold. The quench-zone airflow rate was calculated as the difference between WAT and WAR. In the Product-Module Rig configuration, the total airflow traveled through a 6 inch pipe to the combustor and the rich zone and quench zone airflows were set by the combustor hardware and determined by the relative effective flow areas of the passages leading into each zone of the combustor.

A water-cooled emissions probe support section was located at the exit of the combustor. The emissions sampling system is described in Section V. Downstream of the probe support section, the combustor exhaust passed through a diffuser and transition section located upstream of the combustor back-pressure control valve. The transition section diverted the flow through two 90-deg. turns prior to the introduction of high-pressure water sprays to cool the flow before entering the back-pressure valve. An axially-traversing, circumferentially-rotating emissions sampling probe was mounted in the transition section along the combustor centerline. A small window was also mounted in the OD wall of the transition section to provide indication of a combustor flame.

### *Airflow Delivery and Heating*

Four centrifugal air compressors, capable of delivering airflow rates up to 20 lb/s at pressures of 400 psia, supplied the high pressure airflow required for the RQL combustor tests. These airflow rates were established by using a large capacity regulator to provide a fixed pressure to a total airflow metering venturi. A secondary system, also supplying airflow at 400 psi, delivered unmetered cooling air to the proof-of-light viewing window.

Combustor inlet air temperatures (T3) of 1200F were achieved with multiple, non-vitiated heating systems. An indirect, natural gas-fired heater and an electrical resistance heater were plumbed in series to obtain the 1200F inlet temperatures. The first heater, rated at 15.1 BTU/hr, was capable of raising the airflow temperature from ambient to approximately 850F delivered temperature to the test cell. The second unit, a 480 Volt, 3 phase, 650 KW system provided the additional energy required to boost the air temperature from 850F to 1200F.

For the Single Module Rig configuration, the total airflow was split into two separate flows downstream of the electric heater and directed to either the rich zone or the quench zone. A metering orifice plate, placed in the rich zone airflow leg, provided the desired airflow split of approximately 23% to the rich zone and 77% to the quench-zone. A new orifice plate was sized for each vane configuration during the parametric test series, as necessary, to maintain the desired flow split.

The Product Module Rig configuration was designed to control the airflow split via the effective areas of the fuel injector/bulkhead assembly and the rich zone liner cooling/quench air flow passages. These flow passages were designed to provide the desired rich zone flow of approximately 23% of the total combustor air flow.

## ***Fuel Flow***

Jet-A fuel was supplied to the test cell from above ground storage tanks using a 1200 psi positive displacement pump capable of flow rates of 4800 lb/hr. The fuel was delivered to the test combustor by independently controlled primary and secondary systems. The primary system delivered flow rates of 200 to 550 lb/hr and the secondary system delivered flow rates to 200 lb/hr. Fuel flows for each system were controlled with a pressure-reducing regulator in series with an appropriately sized orifice and metered with a turbine flow meter.

## ***Water Flows***

Most of the Single Module Rig RQL combustor was cooled by low pressure water. The internal, cast ceramic liner reduced the heat loss from the combustor and maintained a hot combustor wall. However, the cast ceramic was not a sufficient insulator to restrict metal temperatures of the pressure vessel spool sections to acceptable limits. The required water flow rate was minimal and was set to a conservative level of nominally 10 GPM for each combustor section. High pressure water was injected upstream of the back-pressure valve. This flow reduced the combustor exhaust gas temperature and suppressed noise. It was supplied from the facility closed loop cooling system by a high pressure, centrifugal water pump capable of flows up to 350 GPM at pressures of 700 psi.

## ***Nitrogen Flow***

High pressure gaseous nitrogen, used for fuel injector purge and sampling probe purge, was supplied from a 15000 SCF storage tank that was charged to 2400 psi by a liquid nitrogen vaporizer-compressor system. The nitrogen was regulated to provide adequate pressures and flows for purge.

## Section IV - Combustor Hardware Design

### *Single Module Rig for Vane Parametrics*

The Single Module Rig combustor configuration consisted of a fuel injection device, a rich zone, a quench zone and a lean zone as shown in Figure IV - 1. An exploded 3-d view of the combustor is shown in Figure IV - 2. The quench zone air flow was bled off of the inlet piping, upstream of an orifice plate, for delivery to the inlet of the quench zone spool piece. The flowpath details of the quench zone are shown in Figure IV - 3. While this flowpath is not the most ideal configuration for fundamental testing, expedient use of existing hardware for rapid quench vane development testing in support of the Product Module design was necessary. The orifice plate was used to set the desired air flow split between the rich and quench zones. An emissions sampling probe system at the exit of the combustor provided diagnostic emissions performance of the combustor. Details of each section are described below.

### **Fuel Preparation Devices**

In the Single Module Rig configuration, the rich zone airflow was delivered to the fuel preparation spool that housed the fuel injector. The fuel preparation spool was constructed of an 8.5 inch long, 6 inch diameter schedule 40 pipe with a 6 inch, 300-lb class flange on the inlet and an 8 inch, 400-lb class flange on the exit. The material for the spool was Type 304H Stainless Steel.

### *Airblast Fuel Injector*

The fuel injector employed for nearly all of the Single Module Rig tests was an axial-flow swirler with an airblast fuel nozzle that passed all of the rich zone airflow. This fuel injector had been designed and fabricated under a prior contract (NAS3-25952) (Ref. 2) and was tested in the Modular RQL combustor rig as part of the baseline testing of the variable geometry concepts testing under a prior contract (NAS3-26618) (Ref. 4). The technology base of this airblast injector is well established in commercial engine application including PW2000 and PW4000 models. The fuel injector, shown in Figure IV - 4 and Figure IV - 5, was attached to a water-cooled bulkhead such that the fuel injector aircap extended approximately 0.16 inches into the rich zone. This assembly was secured to a mounting flange that had a 4.32 inch ID and comprised the rich zone bulkhead. Air was introduced through two concentric annular passages, each of which was equipped with independent, vane swirlers. The outer swirler contained 20 curved vanes, with a final turning angle of 60 deg. These outer vanes were located in a flow annulus with a 2.50 inch OD and a 1.89 inch ID. The central swirler contained 5 straight vanes, inclined to a turning angle of 50 deg., in a flow annulus with a 1.25 inch OD and a 0.75 inch ID. The two swirl passages induced co-rotating flow in the rich zone.

Fuel was supplied through a single 0.25 inch OD by 0.035 inch thick wall tube welded to an internal plenum that fed fifteen 0.020 inch diameter holes angled at 45 deg. and equally spaced on a 1.525 inch diameter. The fuel was introduced to the combustor in a thin annular film between the central air stream and the outer air stream. High speed airflows impinging onto and shearing the low speed fuel sheet enabled a high level of atomization. The flow number of the fuel injector was 52 and the effective airflow area of the fuel injector assembly was 0.81 in<sup>2</sup>.

### *Radial-Inflow High-Shear Injector*

While conducting the parametric assessment of quench vane design parameters, effort was also directed at the evaluation of an alternate fuel injector for the Single Module Rig combustor. The intent of the evaluation was to establish a database on the influence of fuel-air mixture preparation on the performance and emissions characteristics of the RQL combustor concept. A radial inflow swirler/fuel injection systems had been designed and fabricated for this purpose.

A schematic view of a radial inflow swirler/injector is shown in Figure IV - 6. This concept is a variation of a standard design that has been under investigation at Pratt & Whitney and United Technologies

Research Center for some time. An extensive database on its definition was evolved in the effort of Ref 5. The configuration consists of radial inflow swirlers with air introduced through inner and outer passages. Each of these passages contained tangential slots through which the air was admitted, imparting a swirl component to the flow. A centrally mounted fuel injector delivered fuel through radial jets, spaced at even azimuthal intervals. These fuel jets penetrated through the inner airflow and impinged on the inner side of the wall between the two air passages. There, a film of fuel was developed, flowing axially downstream until it left the surface of that wall and was sandwiched between the two high-speed shearing air flows. The radial inflow swirler/fuel injector system was used in two Single Module Rig tests as well as in both Product Module Rig combustor configurations.

## **Rich Zone**

The rich zone section consisted of a cylindrical length followed by a transition to the rectangular quench zone entrance. The cylindrical length was 4.5 inches long and had a 5 inch inner diameter (ID). The transition had an axial length of 1.5 inches long over which the combustor transitioned smoothly from a 5 inch ID cylindrical cross-section to a 4.06 inch wide by 5.10 inch high rectangular cross-section to match the quench zone entrance. This section provided approximately 9 milliseconds of hot rich zone residence time to the transition section at the nominal supersonic cruise condition.

The rich zone combustor section was fabricated as a double-wall spool with 8 inch, 300 psi flanges. The section was specified to use commercially available carbon steel pipe or tube and achieve a 0.125 inch high annular gap to pass an axially-flowing water coolant. Spacer wires were used during fabrication to preserve the gap uniformity of the water cooling passage. The active water cooling enabled a usable test section pressure rating of 200 psia. Typically, the spool was fed by four, 0.5 inch water coolant delivery lines and four lines were also used for the water coolant exhaust. A nominal water cooling flow rate of 10 GPM was utilized.

The rich combustor section contained a castable ceramic liner to provide thermal insulation and achieve the internal dimensions mentioned above. The insulating liners were cast from Plibrico Plicast 40, a commercially available ceramic consisting of mostly alumina. This material was selected because of its favorable thermal shock properties and its ability to withstand combustor temperatures up to 3400F.

## **Quench Zone**

The objective of the reduced-scale-quench vane design was to achieve the most rapid mixing of the rich-zone flow with the quench air, so that minimal nitric oxides ( $\text{NO}_x$ ) are formed as the local conditions in the quench zone pass through an equivalence ratio of 1 and regions of high, mixed-gas temperatures. Optimum mixing is generally taken to mean mixing to nearly a homogeneous flow within the minimum time (i.e., flow distance). There have been a number of studies directed at determining flow geometries and parameters which lead to optimum mixing. Of particular relevance to this investigation are those studying normal jets in confined flows. While it could be argued that reduced-scale-quench vanes (typically non-aerodynamically shaped) have flow expansion and the potential for some downstream recirculation, mixing needs to be completed within the confined jet region of the quench zone in order to achieve low  $\text{NO}_x$  emissions and, therefore, these confined jet flow studies have relevance for supporting this design.

To assess the impact of the many design variables associated with quench air introduction many reduced-scale-quench designs were committed to fabrication prior to the initiation of the Single Module Rig testing so that rapid changes in hardware could be accomplished, in most cases overnight, to facilitate efficient use of the combustion test facility. . Therefore, there was not extensive feedback of test results to affect the evolution of the design, but a broader range of parameters were assessed. Nevertheless, several considerations can be described which were important in the design of a reduced-scale-quench vane, such as jet penetration analysis and mixing optimization.

Mixing studies of jets in crossflow found that the most significant flow variables are the momentum flux ratio,  $J$ , and the ratio of the orifice spacing to the channel height,  $S/H$ . Ultimately, these variables determine jet penetration, which has been identified as an important variable for mixedness performance.

If the jets do not penetrate, then quench air is confined to the boundary layer next to the reduced-scale-quench vane. If the jets over penetrate a stratified region of quench air is formed on the centerline where the opposed jets meet. Therefore, for a given geometry an optimum  $J$  is expected. Optimum mixing is generally assumed to mean leading to a uniform distribution of conserved scalar quantities in a minimum downstream distance. It is presumed that achieving this degree of mixing should also result in the lowest  $\text{NO}_x$  emissions because most of the  $\text{NO}_x$  is formed in the quench mixing zone of a rich-quench-lean combustor.

Studies of the penetration of a circular jet normal to an unconfined flow generally correlate the coordinates of the jet as a power law function in the normalized axial direction (Ref. 6) and have been extended here for non-circular jet shapes:

$$\frac{y_0}{d_h} = K\sqrt{J}(x/d_h)^{0.33}$$

where:

- $y_0$  = jet penetration in the unconfined flow;
- $d_h$  = jet orifice hydraulic diameter;
- $J$  = jet-to-crossflow momentum flux ratio in the unconfined flow;
- $x$  = distance downstream of injection location.

The constant,  $K$ , depends on the point within the jet that is being followed, i.e. centerline or the inner or outer boundaries. A recommend value of  $K = 0.56$  is used to track the penetration of the centerline of the jet.

A jet injected into a confined flow, as found in the quench zone, locally accelerates the crossflow, which in turn reduces the penetration. Ultimately, the jet mixes with the crossflow and a general flow acceleration results from the jet mass addition. Near the plane of injection, the jets are coherent and represent a blockage to the crossflow. Downstream the jets spread and mix so the blockage effects change as the flow develops.

A model was developed in the early phases of the RQL development (Ref. 2) to estimate blockage effects of penetrating jets in a confined flow. In this model, a correction is applied to the jet-crossflow momentum flux ratio to compensate for blockage and the penetration is defined as before:

$$\frac{y}{d_h} = K\sqrt{J_b}(x/d_h)^{0.33}$$

where:

$$J_b = J \left( \frac{A_Q - N \cdot w \cdot y}{A_Q} \right)^2$$

and  $A_Q$  is the crossflow area with no jet blockage and  $N$  is the number of jets and  $w$  is the transverse-width projection of the jet.

A key parameter in mixing, therefore, is the jet-to-crossflow momentum flux ratio,  $J$ . The momentum flux ratio is defined as:

$$J = \frac{\rho_J u_J^2}{\rho_R u_R^2}$$

where the parameters with  $R$  subscript are defined as the flow in the quench zone immediately upstream of the quench-air jets, designated by parameters with the subscript  $J$ . It can be shown that:

$$J = \frac{\rho_R}{\rho_J} \left( \frac{\dot{m}_J}{\dot{m}_R} \right)^2 \left( \frac{A_Q}{C_d A_J} \right)^2$$

where:

$\rho_R$  = density of the rich gas

$\rho_J$  = density of the jet gas

$\dot{m}_J$  = mass flow of jet

$\dot{m}_R$  = mass flow of crossflow, i.e. rich flow

$A_Q$  = crossflow area

$A_J$  = total area of jets

$C_d$  = discharge coefficient of jets.

The ratio of the mass flow rates in the last equation may be replaced with  $(1/s - 1)^2$ , where  $s$  is the flow split between the rich zone and the quench zone. Once the design point parameters for the combustor are chosen (in this particular case, supersonic cruise), that is, the flow split and the desired  $f/a$  overall, then the first factor, the density ratio, and the second factor, the mass flow ratio, are fixed and the only remaining free variables are the areas of the crossflow and jets.

The flow areas are determined based on the design goal pressure drop for the system and the target mass flows as described by the fuel/air ratio and split. Therefore, once all these parameters are specified independent control of  $J$  is not possible. The momentum flux,  $J$ , is defined by the above described flow parameters and an optimum mixing design must be sought with this constraint taken into consideration. In other words, specifying the pressure drop across the reduced-scale-quench vanes and the quench mass flow sets the total quench-jet area and the optimizing variables must focus on the quench jet orifice configuration.

A number of reduced-scale-quench vane geometries were designed, fabricated and tested in this program to assess key quench jet orifice parameters and their effect on  $\text{NO}_x$  emissions. The greatest number of configurations consisted of four vanes equally spaced in the quench zone: two in the center and two vanes buried half way into the wall. Configurations incorporating five vanes were also tested, in two quench zone channel heights. All reduced-scale-quench vanes had the same dimension in the spanwise (i.e., quench zone channel length) direction, 4.06 inches. Table IV - 1 summarizes the flow areas of the vane geometries investigated and Figure IV - 7 shows the relation of the different quench height geometries to the quench section.

Number of Vanes per Set	Number of Quench Channels	Quench Zone Channel Height, H (inches)	Total Quench Zone Crossflow Area, $A_Q$ ( $\text{in}^2$ )	Total Jet Area, $A_J$ ( $\text{in}^2$ )	$A_Q/A_J$
4	3	0.580	7.064	3.375	2.09
4	3	0.580	7.064	4.590	1.54
5	4	0.435	7.064	3.375	2.09
5	4	0.300	4.872	2.336	2.09

Table IV - 1 Summary of Reduced Scale Quench Geometries Investigated in Single Module Rig Configuration

Mixing studies are helpful for the selection of relevant parameters and the initial design of the vanes. In this program the mixing study results were taken as a starting point about which design variations were made to seek an optimum design. A number of vanes were made in the four vane configuration in an effort to find the optimum mixing geometry as determined by emission measurements in the Single Module Rig combustor. The important geometric variables of the reduced-scale-quench vanes that were tested are summarized in Table IV - 2 and Table IV - 3. The shape of the orifices for these vanes were rectangular, characterized by a width crosswise to the flow and a length. The web is the width between adjacent orifices.

Vane Geometry Number	# of Jets, N, per side of vane	Channel Height, H (in)	Width, W (in)	Length, L (in)	Total Quench Jet Area, $A_J$ (in <sup>2</sup> )	Web (in)	Spacing, S (Pitch) (in)	Haudraulic Diameter (in)
1	6	0.580	0.375	0.250	3.375	0.340	0.715	0.300
2	12	0.580	0.153	0.306	3.371	0.176	0.329	0.204
3	18	0.580	0.125	0.250	3.375	0.100	0.225	0.167
4	18	0.580	0.094	0.334	3.391	0.133	0.227	0.147
5	18	0.580	0.180	0.170	3.305	0.042	0.222	0.175
6	18	0.580	0.170	0.250	4.590	0.052	0.222	0.202
7	32	0.580	0.070	0.250	3.360	0.055	0.125	0.109
8	5	0.580	0.742	0.140	3.116	0.060	0.802	0.236
9	16	0.435	0.115	0.230	3.386	0.140	0.255	0.153
10	24	0.435	0.094	0.188	3.393	0.073	0.167	0.125
11	32	0.435	0.081	0.163	3.380	0.042	0.123	0.108
12	24	0.300	0.078	0.156	2.336	0.090	0.168	0.104

Table IV - 2 Reduced Scale Quench Vane Orifice Parameters for Single Module Rig Geometries

Vane Geometry Number	# of Jets, N, per side of vane	Channel Height, H (in)	Aspect Ratio (L/W)	S/H	$A_Q/A_J$	(S/H)*( $A_Q/A_J$ )
1	6	0.580	0.67	1.233	2.09	2.580
2	12	0.580	2	0.568	2.10	1.189
3	18	0.580	2	0.388	2.09	0.812
4	18	0.580	3.55	0.391	2.08	0.815
5	18	0.580	0.94	0.383	2.14	0.818
6	18	0.580	1.47	0.383	1.54	0.589
7	32	0.580	3.57	0.216	2.10	0.453
8	5	0.580	0.19	1.383	2.27	3.135
9	16	0.435	2	0.586	2.09	1.223
10	24	0.435	2	0.383	2.08	0.799
11	32	0.435	2	0.284	2.09	0.591
12	24	0.300	2	0.560	2.09	1.168

Table IV - 3 Calculated Parameters for Reduced Scale Quench Vane Single Module Rig Geometries

Quench vane geometry #8 was intended to represent a full slot. However, for structural integrity, four webs were designed to bridge across from the leading edge to the trailing edge to prevent distortion of the vane outer shell, and hence its characteristics are listed as a five quench jet per side configuration. In addition to variations in quench-orifice number and dimensions, there were designs that were constructed with different shapes and different flow paths to change the jet injection angle. The design variants included a truncated trailing-edge (i.e., squared-off), orifices slanted at 20 degrees, and variations in the flow channel feeding the quench-air injection orifice. All of these variants essentially maintained the quench-orifice pattern similar to vane geometry #3. Drawings of these geometries are shown in Figure IV - 8 to Figure IV - 24.

A number of geometries were also designed and fabricated with smaller quench-zone channel heights. Quench-zone channel heights of 0.435 and 0.300 inches were tested in configurations that incorporated five vanes. The various geometries that were made with these reduced quench-zone channel height are shown in Table IV - 2 and Table IV - 3.

## CFD Analysis of Quench Zone Geometries

Since the technology to make reacting mixing-measurements at pressures and temperatures is not available, water-tunnel-flow visualization, chemical-kinetic-reactor-network calculations, computational fluid dynamics(CFD) calculations, and a review of non-reacting mixing results for jets-in-crossflow were identified (in addition to additional JBTS combustion testing) as program elements of this effort. All elements needed to be done concurrently, since there was limited time to gain this understanding.

Simultaneously, reacting, three-dimensional CFD calculations were made using the commercially-available code, FLUENT, for these geometries. The objective of these calculations was to obtain detailed, spatially-resolved, reacting, mixing information for the new designs. When coupled with the JBTS combustion tests these calculations would lead to the improved understanding of the mixing and NO<sub>x</sub> formation process.

### *Scope of Effort*

Computation Fluid Dynamics(CFD) calculations were performed to determine the influence of geometric and flow boundary condition changes on the details of the flow field, thereby providing a basis for correlating measured NO<sub>x</sub> levels. The initial attempt to predict directly NO<sub>x</sub> levels proved to be unsuccessful since the predicted levels were found to be extremely sensitive to such changes while the measured levels showed much smaller variations. An alternative means of correlating measured NO<sub>x</sub> levels with a relatively easy-to-compute flow field parameter was developed.

CFD calculations were made for the rich-quench-lean geometric family known as reduced-scale-quench. Three-dimensional temperature and species distributions were obtained. Thermal NO<sub>x</sub> levels were also calculated. However, for reasons presented in the following discussion, the predicted NO<sub>x</sub> values were not used in the final assessment of performance. For the reduced-scale-quench geometries, a single flow condition was used as the boundary condition. However, the effects of changes in strut number, slot length, slot width, number of slots, and slot orientation were modeled. The sensitivity of results to numerical issues was also examined.

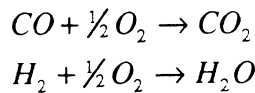
### *Approach*

CFD solutions were provided using the commercial code, FLUENT, as it was the only code available to the program that was capable of providing two-phase, reacting flow simulations (the fuel was modeled as a liquid injected into the air flow stream). In anticipation of performing NO<sub>x</sub> calculations, it was also necessary to have a reasonably accurate heat release model to provide the temperature distribution. FLUENT has a probability-density function (PDF) model that uses a thermodynamic data base so that a reasonable number of chemical species can be used to provide accurate temperature and species estimates near the fuel injector; for the cases discussed herein, Jet-A, CO, CO<sub>2</sub>, H<sub>2</sub>, H<sub>2</sub>O, O<sub>2</sub> and N<sub>2</sub> were included. Finally, the code contains a thermal NO<sub>x</sub> model that may also be run with a PDF model to incorporate the effects of fluctuating temperature and major species on NO<sub>x</sub> levels.

The fuel spray droplet size distribution was determined experimentally and fitted with a Rosin-Rammler distribution with a width parameter of 1.7 and characteristic size of 60 microns; these parameters correspond to a Sauter Mean Diameter of 28 microns. The spray boundary conditions were specified at the same axial and radial position as the fuel injection site of actual injector. At this position, eleven droplet size classes were specified. A stochastic spray model was used in which the effects of gas-phase turbulence on droplet trajectories was simulated. Each droplet class was sampled ten times, so that 110 trajectories were computed for each iteration of the liquid phase.

CFD calculations with the reduced-scale-quench geometries took advantage of the upstream axisymmetric geometry to simplify the problem. An axisymmetric, two-phase flow case was first run upstream of the reduced-scale-quench mixing section with flow conditions at the exit of the swirlers assigned. The axisymmetric profiles at the end of this section were then used as boundary conditions for the three-dimensional flow through the reduced-scale-quench mixing section. Note that the fuel was completely vaporized well upstream of the reduced-scale-quench mixing section. The PDF model was

used for the axisymmetric calculation; however, through the reduced-scale-quench mixing section a two-step, mixed-is-burned model was used with the chemical reaction set as follows:



Therefore, a total of six chemical species were used for the reduced-scale-quench mixing section: CO, CO<sub>2</sub>, H<sub>2</sub>, H<sub>2</sub>O, O<sub>2</sub> and N<sub>2</sub>.

CFD calculations were made for a single flow condition (see Table IV - 4) for a variety of reduced-scale-quench mixing geometries.

P3	150	psia
T3	1200	deg F
Rich Zone Air flow rate	0.66	pps
Fuel flow rate	324	pph
Quench Zone Air flow rate	2.34	pps

Table IV - 4 Inlet Flow Conditions for CFD Analysis of Quench Zone Geometries

### **Limitations to Approach**

Since a commercial code was used, all calculations were performed using a single workstation. Therefore, it was necessary to limit the maximum number of grid points to about 200000. As a consequence, it was not possible to resolve adequately all of the important regions of the flow field. In the discussion of computational domains (below), the various approaches used to provide higher-resolution results are presented. To the extent possible, trends of results are made using comparable grid resolution.

It was found that the predicted NO<sub>x</sub> levels were very sensitive to grid resolution and no satisfactory remedy was found. This limitation motivated the search for an alternative way of assessing performance. The active volume parameter method described later shows much less sensitivity to grid resolution.

### **Computational Domains**

For reduced-scale-quench mixing geometries a large number of slot length, width and number combinations were modeled, together with different strut-to-strut spacing variations. For these calculations three basic computational domains were modeled: full section, quarter section, and strut-to-strut.

The rich zone for the reduced-scale-quench geometry calculations was modeled using an axisymmetric computational domain with 95 cells in the axial direction and 64 cells in the radial direction (see Figure IV - 25). Flow conditions at the end of the rich zone were then used as boundary conditions for the three-dimensional flow calculations through the reduced-scale-quench mixing zone and into the lean zone.

Initial cases were run with the entire reduced-scale-quench mixing section and lean zone simulated. A typical example is presented in Figure IV - 26. Use of the entire geometry was motivated by the fact that the axisymmetric flow calculations showed a large amount of residual swirl at the end of the rich zone. While it was anticipated that the struts removed essentially all of the swirl, there was no way to determine a priori what effect the residual swirl had on performance.

There was also concern that the limitation of maximum grid number did not provide for adequate resolution of the flow in the span-wise direction, especially as the number of slots increased. Therefore, several additional cases were run using a quarter section, an example of which is shown in Figure IV - 27. This approach obviously changed the nature of the swirling flow as the flow approached the struts; viewed in terms of the full domain (Figure IV - 26), one large vortex is thereby replaced by four smaller, counter-rotating ones. Finally, to increase grid resolution even further, strut-to-strut domains were used, an example of which is presented in Figure IV - 28. Here, all effects of swirl were ignored and the inlet

boundary conditions were replaced by uniform, mass-averaged conditions from the axisymmetric case. Finally, for selected cases advantage was taken of additional symmetries in the simplified domain. For example, it was possible to use only one-half of the domain in the span-wise direction, provided that the slots were symmetrically distributed in the span-wise and strut-to-strut directions. Also, it was also possible in those cases to model only one-half of the distance between struts.

### ***Sensitivity of results to grid resolution***

For a reduced-scale-quench geometry calculation in which the grid was progressively refined in the strut-to-strut direction (see Table IV - 5), the NO<sub>x</sub> levels increased proportionally. However, the flow fields showed little sensitivity to grid density. However, it is known that NO<sub>x</sub> levels are very sensitive to local conditions. This sensitivity of results led to the examination of alternative means of assessing performance or correlating measured NO<sub>x</sub> levels with geometric changes - see the discussion of the active volume parameter, below.

Case	Description
1	Full Domain with Coarse Grid
11	Full Domain with Higher Mid-Span Resolution
12	Quarter Symmetry Domain with Fine Grid
39	Strut-to-Strut (Half-Span) Domain with Coarse Grid
40	Strut-to-Strut (Half-Span) Domain with Finer Grid
41	Strut-to-Strut (Half-Span) Domain with Finest Grid

*Table IV - 5 CFD Analyses Assessing the Sensitivity of Results to Grid Resolution*

Some differences were also observed for the reduced-scale-quench geometry calculations depending on whether the domain in Figure IV - 26, Figure IV - 27, or Figure IV - 28 was used. Of course, some sensitivity is expected due to the different boundary conditions required for these different calculation domains. Again, the active volume parameter was less sensitive to such changes.

Initially, CFD was used to compute NO<sub>x</sub> levels for each of the cases modeled. However, it was found that the levels were very sensitive to grid density, the type of computational domain (see Figure IV - 26, Figure IV - 27 and Figure IV - 28), etc. For example, consider the case consisting of three struts with 18 slots per surface; each slot had length of 0.25-in and a width of 0.18-in. Table IV - 5 summarizes the variations in gridding density made for this reduced-scale-quench geometry.

Case 1 was the baseline case using the full strut section (as in Figure IV - 26). Somewhat higher grid resolution in the span-wise direction was used for one of the slots in case 11. In case 12, the quarter section (Figure IV - 27) was used together with higher span-wise resolution throughout. In cases 39-41, the strut-to-strut configuration was used (Figure IV - 28) with an increasing number of grid nodes in that direction.

The computed NO<sub>x</sub> levels for all of these calculations are shown in Figure IV - 29. Note the extreme sensitivity to grid density of the results for cases 39 through 41. As the grid cell size was reduced, non-convergent behavior of the predicted NO<sub>x</sub> is apparent. For reference purposes, the measured NO<sub>x</sub> level was 106 ppm.

### **Active volume parameter**

Recall that computed NO<sub>x</sub> levels showed large sensitivity to changes in slot length, width, number, etc. as well as to changes in grid density or the geometry of the computational domain. The measured NO<sub>x</sub> values were much less sensitive slot geometry. After reviewing the CFD results for a large number of cases, an alternative approach was developed.

$$AVP = \sum \Delta V_i, \quad (F/A)_{MIN} \leq (F/A)_i \leq (F/A)_{MAX}$$

Each control volume in a CFD solution can be viewed as a miniature chemical reactor that has the potential for producing NO<sub>x</sub>. For fixed inlet conditions, NO<sub>x</sub> production rates depend on the local fuel-air ratio, or equivalently, local temperature. In its simplest form (the manner in which it is used here), the active volume parameter considers only those control volumes with a fuel-air ratio within a specified range. Based on knowledge of the NO<sub>x</sub> generation processes, attention was restricted to fuel-air ratios between 0.055 and 0.075, the latter being somewhat higher than the stoichiometric value. Specifically, the active volume parameter (AVP) is the total volume of gas within the specified fuel-air ratio range.

Here, the fuel-air ratio is that implied from the elemental composition of the gas in the control volume. NO<sub>x</sub> production rates are extremely temperature dependent so it is likely that the control volumes should be weighted in some manner to account for this sensitivity; the form used here can be viewed as a non-weighted method. No account was taken of the effect of residence time in each control volume. Given these limitations, the simple form used here still provides a good correlation with measured NO<sub>x</sub> levels and has the advantage that it is easily computed.

In Figure IV - 30, the range of variation for the active volume parameter is shown for the baseline configuration, but using different modeling assumptions (grid density, size of computational domain, etc.). In contrast to the variation of computed NO<sub>x</sub> levels for these cases (Figure IV - 29), the Active Volume Parameter shows much less variation.

Figure IV - 31 shows the volume represented by the Active Volume Parameter for two different reduced-scale-quench mixing geometries. One geometry has 6 quench-air injection orifices per side of the strut and the other geometry has 18 quench-air injection orifices. The 6 quench-air injection orifices per side geometry has more volume at fuel-air ratios between 0.055 and 0.075 than the 18 quench-air injection orifices per side geometry. Consequently, the mixing was better and the NO<sub>x</sub> emissions would be expected to be lower.

Table IV - 2 and Table IV - 3 summarizes the reduced-scale-quench mixing geometries that CFD calculations were made. The effect of quench-air injection orifice size, quench-air injection orifice aspect ratio, momentum-flux ratio, quench-zone gap, single-direction-feed quench-air injection, slanted and staggered quench-air, injection orifices, and a truncated trailing-edge were investigated by these CFD calculations. Test data were available for all of these geometries.

Table IV - 6 shows the effect of changing the fuel-air ratio range in the calculation of the Active Volume Parameter. This table shows that the ranking of the geometries with respect to the value of the Active Volume Parameter is relatively independent of the fuel-air ratio range selected.

Vane Geometry Number	0.055 < f/a < 0.075	0.055 < f/a < 0.07	0.035 < f/a < 0.075
12	1	1	1
10	2	2	2
3	3	4	5
4	4	3	3
11	5	6	4
9	6	7	9
5	7	5	6
6	8	8	7
7	9	9	8
1	10	10	10

Table IV - 6 Rankings of Quench Vane Geometries based on Active Volume Parameter Calculation for Various Fuel/Air Ratio Ranges

The measured NO<sub>x</sub> versus the Active Volume Parameter is plotted in Figure IV - 32 for the reduced-scale-quench geometries given in Table IV - 2 and Table IV - 3. In Figure IV - 32 the CFD calculations used the strut-to-strut domain configuration (Figure IV - 28). It is observed that the measured NO<sub>x</sub>

decreases with decreasing Active Volume Parameter. It was also observed that the measured  $\text{NO}_x$  trend with respect to the Active Volume Parameter was independent of the calculation domain.

### **Limitations of the Active Volume Parameter**

While the Active Volume Parameter as used here provides a reasonable basis for correlating measured  $\text{NO}_x$  values, some limitations should be noted. First,  $\text{NO}_x$  levels are sensitive to temperature; however, no account has been made of variations in the range of fuel-air ratio used for defining the active volume. One possible solution is to assign a weighting factor proportional to a representative Arrhenius factor,  $e^{(E/RT)}$ . Second, no account has been taken of the effect of residence time in each control volume. Finally, the results do show some sensitivity to grid density and computational domain geometry. This variation is readily seen in Figure IV - 30.

Some care is required to eliminate regions of the flow field that do not contribute to the overall  $\text{NO}_x$  level. Recall that the reduced-scale-quench geometry were initiated near the end of the fuel-rich zone. Therefore, there are no contributions to the Active Volume Parameter from those control volumes near the fuel injector that are within the specified fuel-air ratio range.

### **Lean Zone**

The lean zone section consisted of a transition at the quench zone exit followed by a cylindrical length. This transition section had an axial length of 1.5 inches long over which the combustor cross-section transitioned from a 4 inch wide by 5 inch high rectangle to a 5 inch ID cylinder. The cylindrical length was 7.5 inches long for a total spool section length of 9 inches. The lean zone exit was defined by the location of the probe tips of the axially-traversable, emissions probe system. In the furthest downstream position, the probe tips penetrated 3 inches into the lean zone cylindrical section. Thus, the maximum effective axial length of the lean zone was 6 inches and provided a maximum lean zone residence time of approximately 3.3 milliseconds at the nominal supersonic cruise condition. However, this time could be shortened by traversing the probe system forward, hence making lean zone residence time a primary variable of focus in the combustion test program.

The lean zone combustor section was fabricated as a double-wall spool with 8 inch, 300 psi flanges. The section was specified to use commercially available carbon steel pipe or tube and achieve a 0.125 inch high annular gap to pass an axially-flowing water coolant. Spacer wires were used during fabrication to preserve the gap uniformity of the water cooling passage. The active water cooling enabled a usable test section pressure rating of 200 psia. Typically, the spool was fed by four, 0.5 inch water coolant delivery lines and four lines were also used for the water coolant exhaust. A nominal water cooling flow rate of 10 GPM was utilized.

The lean combustor section contained a castable ceramic liner to provide thermal insulation and achieve the internal dimensions mentioned above. The insulating liners were cast from Plibrico Plicast 40, a commercially available ceramic consisting of mostly alumina. This material was selected because of its favorable thermal shock properties and its ability to withstand combustor temperatures up to 3400F.

## ***Product Module Rig Design***

The RQL Product Module Rig was designed to approximate 1 inner bank module of the RQL 3770.54 Product Engine. The product engine design consisted of two banks radially with the inner bank flowing approximately 40% of the total combustor air flow. The inner bank was composed of 24 trapezoidal modules. The Product Module Rig was therefore designed to fit within a 15-degree sector with an inner radius of 13.150 inches and an outer radius of 19.595 inches.

### **Build 1 & 1A Design**

This RQL Configuration incorporates the Reduced Scale Quench concept by utilizing quench vanes to break up the quench zone into 3 channel which are 0.500 inches wide by 4.797 inches long as can be seen in Figure IV - 33. These 0.500 inch channels are created by two quench vanes and by two sidewall

turning strips. A cross-section of the rig is shown in Figure IV - 34. A 3-d solid model exploded view of the combustor and the assembly into the rig pressure vessel are shown in Figure IV - 35 and Figure IV - 36, respectively.

The main test section is a 15.44 inch length of 8 inch nominal diameter tubing (7.980 inch approximate inner diameter) with flanges welded at both ends. A fuel nozzle boss is welded at top dead center. An ignitor boss is installed at the bottom. Instrumentation egress bosses are also installed in this section. The exit transition zone is water cooled and has a cast ceramic flowpath. The cast ceramic transitions the flowpath from a trapezoid to a 5 inch diameter. The rotating/translating emissions probe protrudes into the lean zone. The probe rotates about the pressure vessel centerline and can be translated up to the trailing edge of the quench vanes. The combustor housing is a solid 7.86 inch diameter stainless steel plug approximately 7.8 inches long with a mounting flange. The trapezoidal flowpath for the 15 degree sector has been cut into this piece. Mounting holes for the quench vanes and impingement shells are machined into the aft face.

The bulkhead assembly consists of the bulkhead structure, the heatshield, and the swirler as shown in Figure IV - 37. The bulkhead structure is machined from Inconel 625 bar stock and contains the mounting hole for the swirler and ignitor and 484 impingement cooling holes that are 0.030 inches in diameter (not shown). The spent impingement air travels radially inward and mixes with the swirler air. Angled stand-offs (not shown) were placed on the bulkhead to add swirl to the spent impingement air, co-rotating with the outer swirler air. The bulkhead heatshield is machined from a directionally solidified nickel alloy casting (PWA 1422) and contains four Inconel threaded studs which are pressed in and secured with a tack weld. These studs fit through oversized holes in the bulkhead to allow for thermal growth. The hot surface of the bulkhead heatshield is coated with a thermal barrier coating (PWA 265). The swirler is a radial inflow device with an measured effective flow area of 0.850 in<sup>2</sup>. The swirler is welded to the bulkhead. The fuel injector is a radial jet injector with 6 fuel orifices that are 0.060 inches in diameter and spray the fuel onto the filming surface of the radial inflow swirler. The fuel injector used was an existing PW engine fuel injector.

The rich zone liner is a wire edm (electrical discharge machining) directionally solidified nickel alloy (PWA 1422) in a basic trapezoidal sector shape (Figure IV - 38). The liner overall length is 6.588 inches. Two alignment tabs are positioned on the aft end of the side walls to provide axial constraint of the liner. Two slots to accept the quench vanes are machined on the aft edge. The inner surface of the liner was TBC (thermal barrier coating) coated over the region that is exposed to flame. The upper and lower surfaces of the liner are impingement cooled. The spent impingement air is exhausted rearwards and convectively cools the area of the liner in between the quench vanes before it is dumped into the exit transition zone. The side walls of the liner are convectively cooled. The upper & lower impingement shells (see Figure IV - 39) are rolled Inconel 625. A 0.250 inch flange is welded to the aft end. Two attachment holes are placed in the front edge to connect the shells to the bulkhead structure. Scallop for the quench vanes are machined into the aft end. The upper & lower shells have a staggered array of 0.025 inch diameter holes installed to impinge on the hot region of the liner. The approximate density is 36 holes per square inch. The upper shell has 728 holes, the lower shell has 481 holes. Corner dams are tack welded to the upper & lower impingement shells. These dams are thin bent sheet metal devices which are intended to separate the convectively cooled liner sidewalls from the impingement cooled upper and lower surfaces of the liner.

An exploded view of the quench vane assembly is shown in Figure IV - 40. The platforms and supports are brazed to the outer vane shell with a gold-nickel braze. The vane impingement baffle is then electron beam (EB) welded to this assembly. The vane outer shell is wire EDM cut from a single-crystal, nickel casting (PWA 1484). The shell profile is a tapered racetrack shape. The axial length is a constant 1.896 inches while the width of the vane tapers at a 7.5 degree angle from 1.284 inches at the OD to 0.644 inches at the ID. After the platforms and supports are brazed to it the outer surface is TBC coated and the quench orifices are laser cut. There are 22 main quench orifices on each side of the vane, each 0.123 inches wide by 0.250 inches axially. Upstream and downstream of the main orifices are exhaust slots for the spent impingement cooling air. These slots are 0.123 inches wide by 0.054 inches axially and are located in line with the main orifices. The upper and lower platforms are wire EDM cut from directionally solidified nickel castings (PWA 1422). The hot surface of these parts are TBC coated. The

upper and lower supports are machined from Inconel 625 bar stock. The supports include some impingement holes to provide cooling to the platforms. The lower support flange has a machined slot to allow thermal growth differentials between the vane and the combustor housing. The vane impingement baffle is a 0.030 inch thick structure wire cut from Inconel 625 bar stock. A staggered impingement hole array of 299 holes, 0.025 inches in diameter each, is laser cut into the leading edge and trailing edge of the shell (598 total holes per vane). The impingement baffle was welded at one end and allowed to move thermally at the other end. The vane baffle is machined with rails which mate with a longitudinal pad on the inside of the vane outer shells to separate the impingement air from the main quench air as seen in Figure IV - 41. A cruciform splitter is placed inside the impingement baffle. This cross shaped piece separates the ID and OD sides of the vane after slot 17 out of 22 (with slot 1 toward the OD side of the vane). The cruciform also separates the left and right sides of the baffle as shown in Figure IV - 41.

The turning strips (Figure IV - 42) take air that was used to convectively cool the liner sidewalls and turns the air 90 degrees into the rich gas path. As the air is turned it is also broken up into 22 discreet jets, each 0.123 inches wide by 0.250 inches long axially. The aft end of the turning strip consists of an effusively cooled sidewall so that the turning strip ends at the same axial plane as the quench vanes.

The aft trap plate is a 0.125 inch thick 9.15 inch diameter circular plate with a trapezoidal hole as seen in Figure IV - 43. This trapezoid is a 15 degree sector from a 13.550 inch radius to 18.767 inch radius. This plate covers the aft face of the combustor, outside of the flowpath. The rear surface of this plate and the inside edges of the trapezoid are TBC coated.

A modification to the Build 1 design was intended to perturb the split within the combustor in an attempt to bring the split in line with the design intent. The modification of Build 1 into Build 1A was accomplished by installing a blockage ring at the inlet to the radial inflow swirler, a standard practice for parametric variations of flow split while conducting development combustor testing. This blockage ring was installed such that it reduced the airflow to only the inner swirler of the radial inflow swirler. To facilitate rapid test turn-around during this development phase of combustion testing, the blockage ring was tack-welded in place while the combustor was still installed in the test facility centerline. The installation of the blockage ring resulted in a net reduction in the overall bulkhead effective flow area (including inner swirler passage, outer swirler passage and bulkhead cooling) from 1.11 in<sup>2</sup> for Build 1 to 0.90 in<sup>2</sup> for Build 1A.

## **Build 2 & 2A Design**

Build 2 of the Product Module Rig focused on the following major changes: smaller quench zone channel height for improved emissions, simulation of an annular RQL configuration with improved feed of sidewall quench orifices, and improved rich zone liner cooling control (Figure IV - 44). The design of Build 2 has 4 quench zone channels, 0.3 inches wide, as shown in Figure IV - 45, relative to the Build 1 design that had 3 channels, 0.5 inches wide. The Build 2 design also incorporates "half vanes" instead of turning strips at the sidewalls to simulate a representation of an annular rich zone design in this single fuel injector rig. The rich zone liner was cooled on all four sides with impingement air. The spent impingement air was extracted from the rig and separately valved and measured through a venturi for improved liner durability. A cross section of the Build 2 design is shown in Figure IV - 46. Figure IV - 47 shows an exploded 3-d solid model view of the components that comprise the Build 2 combustor.

To facilitate a rapid redesign for this second build, many components were re-used or designed with similar features to Build 1. The main test section was reused from Build 1. Additional egress ports were added to plumb the bypassed cooling air out of the rig. The exit transition zone was reused from Build 1 without any change. The combustor housing for Build 2 was similar to Build 1 except additional material was removed to provide room for the impingement exhaust tubes and to provide better flow of air to the liner impingement holes. The fuel injector was reused from Build 1. The bulkhead assembly was similar to Build 1 as shown in Figure X and consisted of the same components. The aft trap Plate is effectively identical to Build 1.

The following describes the significant differences between Build 1 and Build 2 designs.

The bulkhead heatshield for Build 2 was machined from Inconel 625 plate stock instead of from a DS Nickel casting. The swirler was a radial inflow device with a measured effective flow area of 0.51 in<sup>2</sup>. The impingement cooling hole pattern was changed to 427 holes 0.028 inch diameter each (from 484 holes 0.030 inch diameter in Build 1).

The rich zone liner for Build 2 is shown in Figure IV - 48. While the ID and OD radius remained the same, Build 2 incorporated tapered "half vanes" on the two sidewalls rather than straight turning strips. As a result, the sidewall angle for build 2 is slightly different. In addition, 3 vane slots are required for Build 2 rather than the two slots required for Build 1. The rich zone liner contained four threaded studs on each wall of the liner. These studs tie the liner to the impingement shells (Figure IV - 49) maintaining the desired gap and also provided the axial constraint of the liner. The two tabs which existed in the Build 1 liner were not required. The upper and lower impingement shells are similar to Build 1. The average hole density for all four shells is approximately 57 holes per square inch in Build 2 as opposed to approximately 36 holes/in<sup>2</sup> in Build 1. All impingement holes are 0.025" diameter. The upper shell has 1,108 holes and the lower shell has 754 holes. The sidewall impingement shells each have 1,264 impingement holes. The sidewall shells also have provisions for extracting the spent cooling air. Along the top and bottom edge of each side shells a transfer block is attached which contains a cavity 0.180 inches wide by 4.93 inches long. These cavities each feed a 1 inch diameter tube which brings the air axially forward. The aft end of these tubes is closed off. The front edge of these tube enter an elbow (not shown) which brings the air out of the pressure vessel. The four tubes are then connected to a manifold and single exhaust tube runs through a orifice for measuring air flow and a control valve before dumping into the rig exhaust stack.

Figure IV - 50 shows an exploded view of the quench vane assembly. The upper and lower supports are welded to the outer shell with an EB weld. The vane impingement baffle is then EB welded to this assembly. The Vane Outer Shell is wire EDM cut from Inconel 625 bar stock. The shell profile is a tapered racetrack shape. The axial length is a constant 1.896 inches while the width of the vane tapers at a 3.75 degree angle from 0.854 inches at the OD to 0.540 inches at the ID. After the supports are welded to it the outer surface is TBC coated and the quench orifices are laser cut. There are 37 main quench orifices on each side of the vane, each 0.073 inches wide by 0.150 inches axially. Upstream and downstream of the main orifices are exhaust slots for the spent impingement cooling air. The upstream slots are 0.073 inches wide by 0.064 inches axially and the downstream slots are 0.073 inches wide by 0.032 inches axially. Both sets of exhaust slots are located in line with the main orifices. The Upper and Lower Supports are machined from Inconel 625 bar stock. Separate platform pieces are not required in Build 2 as the supports perform the same function as both the supports and platforms did in Build 1. The supports include some effusion holes to provide cooling to the platform area. The lower support flange has a machined slot to allow thermal growth differentials between the vane and the combustor housing. The vane impingement baffle is a 0.030 inch thick structure wire cut from Inconel 625 bar stock. A staggered impingement hole array of 543 holes, 0.020 inches in diameter each, is laser cut into the leading edge and 276 holes, also 0.020 inch diameter on the trailing edge of the shell (819 total holes per vane). The impingement baffle was welded at one end and allowed to move thermally at the other end. As in Build 1 the vane baffle is machined with rails which mate with a longitudinal pad on the inside of the vane outer shells to separate the impingement air from the main quench air. The cruciform splitter was located after slot 28 out of 37.

The sidewall vanes (Figure IV - 51) are designed to simulate one half of a normal quench vane. Because they are mounted flush with the sidewall of the rich zone liner, they have a square leading edge, rather than a rounded front like the main quench vanes. In order to provide better feed of the quench air to the sidewall vanes, air is allowed to enter the sidewall vane baffle structure through holes machined in the outer face in addition to feed from the ID and OD sides. Extended flanges are incorporated into the aft end to attach the half vanes to the combustor housing and to close off the back of the rig and prevent air from bypassing the quench zone and leaking directly into the exit transition zone.

Build 2A was a modification of Build 2 in which the 0.51 in<sup>2</sup> ACd swirler was removed and a 0.68 in<sup>2</sup> swirler was installed, changing the airflow split between the rich and quench zones. Because an increase in effective flow area was required for this design modification, more extensive modifications to the hardware were required than was pursued between the Build 1 and Build 1A modifications (installation

of a blockage ring). To facilitate a quick change over between swirlers, it was decided to leave the entire combustor assembled in the pressure vessel, complete with instrumentation, during this modification. The entire pressure vessel was removed from the test facility centerline and the existing Build 2 swirler was machined out of the bulkhead. The increased flow capacity swirler for Build 2A was then EB welded in place of the original swirler. The entire process required a downtime of only 4 days, from completion of Build 2 testing to the initiation of testing for Build 2A, a tribute to the personnel performing this re-work with un-precedented turn-around.

## Section V - Instrumentation

### *Single Module Rig*

#### **Static Pressures**

The pressure instrumentation for the Single Module Rig configuration is shown in Figure V - 1. Pressures were recorded via a combination of individual transducers and scanners. Combustor inlet static pressure (P3) was measured in the plenum just upstream of the fuel injector. The rich zone static pressure (PRICH) was measured near the exit of the rich zone and the lean zone static pressure (PLEAN) was measured approximately 4.5 inches downstream of the lean zone entrance. A static pressure (PUPORIF) was measured upstream of the orifice plate located in the rich zone airflow leg. The difference between PUPORIF and P3, along the effective area of the orifice plate, was used to calculate the rich zone airflow and, hence, the airflow split. Dual measurements of inlet pressure, rich zone pressure and lean zone pressure were made for redundancy. Two static pressure measurements (P3Q) were recorded in the quench air plenum that fed the quench vanes and were diametrically opposed. In most quench vane configurations, two of the vanes (one wall vane and one center vane) were instrumented to record the static pressure (PBaffle) just upstream of the main quench orifices. These taps were placed between the quench vane impingement shell and the outer shell.

For all locations where redundant measurements were acquired, the readings were assessed and analyzed for validity. All readings determined to be valid were averaged to obtain the measurement value for that location.

#### **Temperatures**

The temperature instrumentation for the Single Module Rig configuration is also shown in Figure V - 1. Because of the use of cast ceramic, high-temperature capable liners in the rich and lean zones and based on previous combustion experience with this liner material, the requirements for temperature measurements in the Single Module Rig configuration were minimized to measure only the essential gas path air flow temperatures. Temperatures were recorded via a combination of individual thermocouples and scanners. Combustor inlet stagnation temperature (T3) was measured in the plenum just upstream of the fuel injector. Dual measurements of inlet temperature were made for redundancy. Two stagnation temperature measurements (T3Q) were recorded in the quench air plenum that fed the quench vanes and were diametrically opposed. The combustor inlet temperature setpoint corresponded to a mass averaged value of T3 and T3Q.

For all locations where redundant measurements were acquired, the readings were assessed and analyzed for validity. All readings determined to be valid were averaged to obtain the measurement value for that location.

### *Product Module Rig*

#### **Static Pressures**

Pressures were recorded via a combination of individual transducers and scanners. Combustor inlet static pressure (P3) was measured in the plenum just upstream of the fuel injector. The rich zone static pressure (PRICH) was measured just downstream of the fuel injector bulkhead and the lean zone static pressure (PLEAN) was measured approximately 4.5 inches downstream of the lean zone entrance. Dual measurements of inlet pressure, rich zone pressure and lean zone pressure were made for redundancy.

Two pressure taps were located between the fuel injector bulkhead impingement shell and the heatshield to measure the spent-impingement cooling air pressure of the bulkhead heatshield. Two static pressure taps were welded into each impingement shell surrounding the rich zone liner to measure the pressure of the spent-impingement cooling air in the impingement passage. The taps affixed to the top and bottom

shells were also located approximately 1.6 inches and 4.5 inches axially downstream of the bulkhead. The pressure taps along the top shell were positioned 0.25 inches to the right of the liner centerline and the taps on the lower shell were located 0.2 inches to the left of the centerline when viewed from an aft-looking-forward position. For build 2, the two taps attached to each side shell were located along the liner centerline and positioned approximately 1.6 inches and 4.5 inches axially downstream of the bulkhead.

Each of the quench vanes was fitted with four static pressure taps. Two of the taps were located just upstream of the main quench orifices; one on the OD end and one on the ID end. The other two taps were intended to measure the spent-impingement coolant air pressure between the quench vane impingement baffle and the outer shell. One of these taps measured the annulus pressure on the leading edge of the quench vane and the other measured the annulus pressure on the trailing edge.

For all locations where redundant measurements were acquired, the readings were assessed and analyzed for validity. All readings determined to be valid were averaged to obtain the measurement value for that location.

## **Temperatures**

Temperatures were recorded via a combination of individual thermocouples and scanners. Combustor inlet stagnation temperature (T3) was measured in the plenum just upstream of the fuel injector. Dual measurements of inlet temperature was made for redundancy.

Two surface thermocouples were welded to the backside of the bulkhead heatshield to measure the backside metal temperature of the bulkhead heatshield. Two surface thermocouples were welded to each wall of the rich combustor liner to measure the backside metal temperature of the rich zone liner. The thermocouples attached to the top and bottom walls were located along the liner centerline and positioned approximately 1 inch and 4 inches axially downstream of the bulkhead. The two thermocouples affixed to each side wall were also located approximately 1 inch and 4 inches axially downstream of the bulkhead. However, the upstream thermocouple was positioned 1.2 inches radially inboard of the liner centerline and the downstream thermocouple was located 1.2 inches radially outboard of the centerline.

For all locations where redundant measurements were acquired, the readings were assessed and analyzed for validity. All readings determined to be valid were averaged to obtain the measurement value for that location.

## ***Emissions Sampling and Analysis***

### **Emissions Sampling System**

The principle focus of the combustion test program was to document combustor emissions levels achieved at operating conditions, primarily the nominal supersonic cruise condition, representative of an HSCT aircraft engine. Emissions samples were acquired in the lean zone at multiple radial, circumferential and axial locations.

The lean zone sampling probe (Figure V - 2) consisted of an array of five emissions sampling ports attached to a common housing and cooling supply tube. The emissions system was designed and configured to allow each of the five ports to be sampled individually or, through control system valving, any number of ports, up to and including all five ports, could be ganged together to obtain a representative ganged sample along a diamtral line across the combustor gas path.

Four of the probe tips were positioned at radii of 0.562", 1.125", 1.687" and 2.000" and a fifth was placed on the centerline. The ports at the 0.562" and 1.687" radial locations were positioned on one side of the centerline port while the ports at the 1.125" and 2.000" radial locations were placed diamtrally across the centerline port on the other side. These port locations were not positioned at centers of equal areas, as might be found in more traditional emissions systems. Instead, the position of these ports was

designed to provide the capability of performing detailed diagnostic evaluation and mapping at planes close to the quench air injection location.

Driven by a motorized Velmex Unislide axial positioning system and rotary table, the probe was axially traversable over a 6 inches length. The zero position was defined as beginning at the leading edge of the lean zone and increasing values of probe axial position indicate that the probe system was moved aft of its zero position. This feature allowed emissions levels to be obtained at various lean zone residence times for a given operating condition or permitted emissions to be acquired at a constant residence time while conditions were varied. The probe was also capable of rotating  $\pm 180$  deg. Combining this flexibility with the individual port sampling capability provided the capability to obtain a detailed point-by-point profile of the emissions concentration at a plane defined by the probe's axial position.

Each probe tip was designed to provide an aerodynamic quenching of the gas sample. The probe system was operated to maintain a choked inlet at the sampling port orifice during acquisition of gas samples for emissions analysis. The quenching process was accomplished by a rapid expansion of the gas sample to supersonic conditions, reducing the static temperature of the gas sample and thereby freezing its composition. Energy was extracted from the sample by convective heat transfer to the probe's water coolant flow which further reduced the gas sample total temperature. The sample flow was then shocked to a subsonic condition at a stabilization step. The probe tip was design to remove sufficient energy from the sample such that the sample's static temperature after the shock would be low enough to inhibit further chemical reactions. The aerodynamic-quenching probe concept is described in more detail in Ref. 2.

The probe tip (Figure V - 3), designed to minimize  $\text{NO}_x$  formation and CO oxidation, included a 0.030 inch diameter sample inlet, a supersonic expansion area ratio of 4.27 and a supersonic quenching length of 1.97 inches. Each probe tip consisted of three concentric, 304 Stainless Steel tubes: 1) an outer tube having a 0.375 inch OD x 0.028 inch wall; 2) a mid-tube having a 0.25 inch OD x 0.016 inch wall; and 3) an inner tube having a 0.094 inch OD x 0.016 inch wall. Water cooling, necessary to insure durable and reliable probe operation in the combusting flow, especially in the near stoichiometric mixture regions at locations close to the quench air addition plane, and for heat extraction from the sample as described above, was supplied to the entire probe at a nominal flowrate of 10 GPM, with the tips receiving approximately 2 GPM each.

### **Emissions Analysis Procedures and Performance Parameters**

The UTRC emissions sampling and analysis system is maintained and operated in accordance with ARP 1256A specifications. The emissions cart employed is capable of continuous monitoring of emissions of carbon monoxide (CO), oxygen ( $\text{O}_2$ ), carbon dioxide ( $\text{CO}_2$ ), unburned hydrocarbons (UHC) and oxides of nitrogen ( $\text{NO}_x$ ) as shown in Figure V - 4. CO and  $\text{CO}_2$  levels are determined from individual Milton Roy Model 3300 nondispersive infrared analyzers. A Thermo Environmental Model 10 chemiluminescence analyzer is used to measure  $\text{NO}_x$  composition. A Rosemount Model 755 paramagnetic device is used for oxygen analysis and a Beckman Model 402 flame ionization detector is used to monitor unburned hydrocarbons.

Emissions samples were routed from the probe through electrically heated lines to a valving system, where the samples could either be combined or extracted individually, and then delivered to the gas analyzers. The samples were then transferred from the valving system to the emissions cart through an externally insulated 304 Stainless Steel line that was maintained at 350F. The transfer line had a 0.18 inch ID and was approximately 75 feet long. At the cart the sample was divided for distribution to the five analyzers. The  $\text{NO}_x$  and UHC samples were plumbed directly to the corresponding analyzers and measured as wet samples. The  $\text{CO}_2$ , CO and  $\text{O}_2$  samples passed through a capillary dryer which was used to remove the moisture before those samples were analyzed. The composition of  $\text{NO}_x$ , CO, UHC,  $\text{CO}_2$  and  $\text{O}_2$  were determined from the appropriate analyzer reading and a corresponding calibration curve.

The results from analyses of the emission sample were used to calculate the primary performance parameters for a combustion test. These parameters included the fuel/air ratio, emissions indices, flame temperature and combustion efficiency. Since each of these parameters was based on the sample

analysis, the parameter reflected either a local value when individual probe samples were analyzed, or a global value, along a diametral line across the combustor gas path, when all probes were ganged together.

### Fuel/Air Ratio

The fuel/air ratio calculated from the emissions analysis followed the technique outlined by Spindt (Ref. 3). This procedure has been used by UTRC for analysis of emissions-based fuel/air ratio because it is based on ratios of the component concentrations and is, therefore, not sensitive to small errors in gas sample analysis. Furthermore, no correction for condensed water is necessary, as long as all components are treated the same. This method can be applied to exhaust gas analysis without regard to the degree of combustion encountered, which is appropriate for the detailed diagnostic evaluations conducted when sampling the potentially near-stoichiometric mixture regions at locations near the quench plane air addition. The fuel/air ratio ( $f/a$ ) was calculated as:

$$f/a = \left\{ F_b \left( 11.492 F_c \cdot \frac{1 + R/2 + Q}{1 + R} + \frac{120(1 - F_c)}{3.5 + R} \right) \right\}^{-1}$$

where:

$$F_b = \frac{\text{PPM}_{\text{CO}} + \text{PPM}_{\text{CO}_2}}{\text{PPM}_{\text{CO}} + \text{PPM}_{\text{CO}_2} + \text{PPM}_{\text{UHC}}}$$

$$F_c = \frac{12.01}{12.01 + 1.008 \left( \frac{H}{C} \right)}$$

$$R = \frac{\text{PPM}_{\text{CO}}}{\text{PPM}_{\text{CO}_2}}$$

$$Q = \frac{\text{PPM}_{\text{O}_2}}{\text{PPM}_{\text{CO}_2}}$$

and:

$\text{PPM}_i$  = parts per million molar concentration of species  $i$   
 $C, H$  = number of carbon and hydrogen atoms, respectively, contained in the fuel.

The Spindt technique combined  $\text{CO}$ ,  $\text{UHC}$ ,  $\text{CO}_2$ , and  $\text{O}_2$  emissions to determine the fuel/air ratio, but as for any similar procedure, the result was largely influenced by the  $\text{CO}_2$  and  $\text{O}_2$  concentrations.

### Emissions Index

An emissions index of specie  $i$  ( $\text{EI}_i$ ) was calculated for  $\text{NO}_x$ ,  $\text{CO}$ ,  $\text{UHC}$ ,  $\text{CO}_2$  and  $\text{O}_2$  according to:

$$\text{EI}_i = \frac{\text{PPM}_i}{1000} \cdot \frac{\left( 1 + \frac{f}{a} \right)}{\frac{f}{a}} \cdot \frac{\text{MW}_i}{\text{MW}_{\text{comb}}}$$

where:

$\text{PPM}_i$  = parts per million molar concentration of specie  $i$   
 $\text{MW}_i$  = molecular weight of specie  $i$

$f/a$  = fuel/air ratio based on the sample analysis

$MW_{comb}$  = molecular weight of the combustor composition

For the Single Module Rig Configuration tests, the CO, CO<sub>2</sub> and O<sub>2</sub> emissions indices are reported in an as measured state, i.e. semi-dry (sample passed through a capillary dryer). This was deemed acceptable for parametric testing where only back-to-back comparisons are made for configurations tested in the same facility. For the Product Module tests, all emissions are reported, consistent with ICAO Annex 16 procedures, in an in-situ state, i.e. wet (accounting for water vapor in the combustion products). This was agreed upon to facilitate comparisons with the LPP MRA combustor tests for Combustor Downselect. The correction for water vapor for CO, CO<sub>2</sub> and O<sub>2</sub> essentially amounts to approximately a 5% correction to the emissions indices.

### Combustion Efficiency

The combustion efficiency ( $\eta_{comb}$ , with units of percent) was calculated from the sample analysis, where inefficiencies were represented by emissions indices of the incompletely oxidized species, CO and UHC:

$$\eta_{comb} = 100 - 0.1(0.235 EI_{CO} + EI_{UHC})$$

The efficiency calculation assumed that the unburned hydrocarbons had the same heat of combustion as the Jet-A fuel, 18500 BTU/lb.

# Section VI - Combustor Test Evaluation Results

## Single Module Rig Test Chronology

The series of parametric tests in support of the quench vane design were conducted in Cell 1E of the Jet Burner Test Stand at United Technologies Research Center. The test series was initiated on October 9, 1997 and progressed through February 12, 1998. During this period, a series of 27 tests were conducted and are documented in Table VI - 1.

CPC Run	Vane Geometry Number	ACd N/S	Nozzle/Swirl Configuration	Additional Comments
93	3	0.81	60 Deg Airblast	
94	3	0.81	60 Deg Airblast	rectangular rich zone
96	6	0.81	60 Deg Airblast	
98	3, Single Direction Feed	0.81	60 Deg Airblast	
99	5	0.81	60 Deg Airblast	
100	3, Slanted Slots	0.81	60 Deg Airblast	
101	8	0.81	60 Deg Airblast	
102	7	0.81	60 Deg Airblast	
103	3, Truncated Trailing Edge	0.81	60 Deg Airblast	rig leak
104	6	0.81	60 Deg Airblast	
105	3, Truncated Trailing Edge	0.81	60 Deg Airblast	
106	4	0.81	60 Deg Airblast	
110	3	0.81	60 Deg Airblast	particulates
112	3	0.81	60 Deg Airblast	
113	3	0.81	60 Deg Airblast	reversed quench section
115	3	0.81	60 Deg Airblast	split parametric test
117	3	0.81	60 Deg Airblast	split parametric test
118/9	3	0.81	60 Deg Airblast	
121	Parallel Path with Effusion	0.81	60 Deg Airblast	Feed mal-distribution noted
122	10	0.81	60 Deg Airblast	
124	3	0.84	Radial Inflow Swirler	
126	2	0.86	60 Deg Airblast	
127	9	0.86	60 Deg Airblast	
128	11	0.86	60 Deg Airblast	
129	ParallelPath no Effusion	0.86	60 Deg Airblast	added shroud conditioner Feed mal-distribution still noted
130	12	0.51	Radial Inflow Swirler	rig leak

Table VI - 1 Single Module Rig Run Log and Configuration Summary

A standard test plan was used for these parametric tests and is shown in Table VI - 2. This standard test plan focused on permutations about the nominal supersonic cruise condition. It provided for lean zone residence time evaluations, fuel/air excursions and evaluation of the sensitivity to pressure drop. In addition, a 40 sample detailed map of the exit plane emissions was obtained to provide diagnostic information to aid in the assessment of the configurations.

Wa total	P3-baffle	T3A	Wf	dP/P	f/a-oa	Probe Axial Position	Probe Angular Position	Probe
(pps)	(psia)	(deg F)	(pph)	(%)		(in)	(deg)	
2.25	150	1200	255	4.0	0.0315	2	-180, -135, 22.5, 90	All
2.25	150	1200	255	4.0	0.0315	4	-180, -135, 22.5, 90	All
2.25	150	1200	243	4.0	<b>0.0300</b>	6	-180, -135, 22.5, 90	All
2.25	150	1200	275	4.0	<b>0.0340</b>	6	-180, -135, 22.5, 90	All
2.25	150	1200	292	4.0	<b>0.0360</b>	6	-180, -135, 22.5, 90	All
2.60	150	1200	295	<b>5.0</b>	0.0315	6	-180, -135, 22.5, 90	All
2.00	150	1200	227	<b>3.0</b>	0.0315	6	-180, -135, 22.5, 90	All
<b>2.25</b>	<b>150</b>	<b>1200</b>	<b>255</b>	<b>4.0</b>	<b>0.0315</b>	<b>6</b>	-180, -135, -67.5, -22.5, 22.5, 67.5, 90, 135	All, 1,2,3,4,5

Table VI - 2 Standard Test Plan for Quench Vane Parametrics Testing in the Single Module Rig Configuration

## Product Module Rig Test Chronology

### Build 1 &1A Test Chronology

After assembly of build 1 of the Product Module Rig, the combustor section was installed in Cell 1E of the Jet Burner Test Stand at United Technologies Research Center. Instrumentation was connected and testing began on February 27, 1998 as run 132 of the CPC program. Testing was focused on conditions taken from the HSR/CPC Program Coordination Memo GE97-002-C, summarized in Table VI - 3, with the primary intent of obtaining supersonic cruise emissions in support of the Combustor Downselect.

	T3 (F)	P3 (psia)	f/a
Nominal Supersonic Cruise	1200	150	0.0300
Nominal Subsonic Cruise	630	80	0.0200
100% Thrust LTO (Takeoff)	919	301	0.0329
65% Thrust LTO (Climb)	740	212	0.0248
34% Thrust LTO (Approach)	588	134	0.0187
15% Thrust LTO (Descent)	446	82	0.0141
5.8% Thrust LTO (Idle)	295	45	0.0113

Table VI - 3 Uniform Schedule of Test Points

Initially, non-combusting warmflow data points were taken to assess the flow split within the combustor. Results showed that the percentage of combustor airflow entering the rich zone, the SPLIT, was high, approximately 31%-33% relative to the design intent of 22%-23%. Despite this maldistribution of airflow, the decision was made to acquire some data prior to shutting down to correct the split. (A correction would be necessary prior to proceeding to supersonic cruise conditions since the higher than intended flow splits would result in leaner stoichiometry at the rich, high temperature conditions, resulting in an over-temperaturing of the rich zone liner.) Inlet conditions for the 15% LTO Descent condition were set and the combustor was lit off using the spark igniter. A fuel/air excursion at the descent condition was conducted and ganged emissions acquired. The fuel/air excursion, conducted by a change in fuel flow, spanned the range from a lean to a rich front end, simulating both sets of modules operating in a fuel shifted mode. (A discussion of the emissions results can be found below in the Test Results section.) The rig was then shut down to allow correction of the split.

A blockage ring was installed on the swirler to modify the airflow distribution of the combustor, with the intent of reducing the split. This blockage ring was positioned to block the inner passage of the radial inflow swirler since this passage was the predominant passage for airflow entering the rich zone. A brief

inspection of the combustor was conducted during this shutdown and no signs of distress appeared on the liner or quench vanes. However, it was observed at this time, that two of the four corner dams had apparently broken some welds and were out of position as shown in Figure VI - 1.. The two corner dams located on the ID side of the rich zone were lifted up, partially blocking the sidewall/turning-strip air flow passage. These corner dams separate the sidewall/turning-strip flow from the top and bottom spent-impingement cooling air. The corner dams were simply pushed down, back into place, appearing to stay seated in their original position, so that combustion testing could continue.

Build 1A testing, with the blockage ring on the swirler, began as run 133 on March 2, 1998. Again, non-combusting, coldflow and warmflow data were acquired and showed splits of 23%-26%, and were deemed acceptable to proceed on with combustion tests. Inlet conditions for the 15% LTO Descent condition were set and the combustor was again lit off using the spark igniter. A fuel/air excursion at the descent condition was conducted and ganged emissions acquired. At lightoff, the split was recorded at approximately 33% and persisted for a few data points before settling back in to the 23%-25% range for the remaining descent test points. (A discussion of the emissions results can be found below in the Test Results section.) The increase and then subsequent decrease in split at the descent condition remains an unexplained phenomenon. After testing at the descent condition, the combustor was blown out so that the inlet conditions could be raised to the supersonic cruise condition. Warmflow data taken during this period showed that the split remained in the 21%-25% range. Auto-ignition was used to light the combustor at the supersonic cruise condition (as had been done during all of the Single Module Rig tests). Again, the split was high at 29%. Two data points were acquired and based on the observed split and emissions behavior, the rig was shut down for inspection. During cool-down, warmflow data showed splits of 25%.

Post test inspection of the build 1A hardware showed significant distress to the rich zone liner and quench vanes. The sidewalls of the rich zone liner appeared bowed inwards for the trailing last third of the liner. In addition, a section approximately 2 inches by 1.5 inches was oxidized away on the trailing edge of the left sidewall, as viewed from an aft-looking-forward position. A burn-through approximately 1 inch by 0.5 inches was found in the OD surface of the liner approximately 2.5 inches downstream of the bulkhead. The ID surface also bowed inward towards the combustion zone and showed axially cracking and liner oxidation beginning at about 2 inches down stream from the bulkhead and progressing towards the leading edge of the quench vanes. Thermal barrier coating (TBC) was found spalled from the leading edge of the the quench vanes and each vane showed cracking and oxidation of regions of approximately 0.5 inches in diameter on the leading edge. The bulkhead heatshield showed no signs of distress and the turning strips appeared to be unaffected by the liner distress except for some spattering of quench vane material on one of the turning strips which may have subsequently caused damage to a few quench teeth on the right turning strip (aft-looking forward view). All distress was limited to the heat shield surfaces of the combustor and the major structural components, bulkhead, outer shell, inner shell and quench vane impingement baffles were all in nominal condition, showing no distress. The corner dams were again found lifted from their nominal position, blocking a portion of the lower sidewall flow. A root-cause investigation was conducted to determine the probable cause of the distress and the findings and corrective actions are documented in Table VI - 4. The root cause of the combustor distress is believed to be fundamentally associated with the corner dams. These dams were known to have been mis-positioned from inspection after running build 1 and were placed back into position (welding could not be applied without significant disassembly) and subsequently found out of place after testing of build 1A. Their resultant position significantly blocked the sidewall flow, preventing adequate convective cooling of the sidewall causing subsequent over-temperaturing and thermal distortion of the liner with subsequent hardware damage occuring as a result of the flow field of the entire combustor being significantly disturbed from the design intent. Build 1/1A testing was terminated and lessons-learned applied to the next build of the Product Module Rig.

<i>Observation</i>	<i>Impact</i>	<i>Comments</i>	<i>Recommended Corrective Action</i>	<i>Implemented</i>
corner dams loosened (Root Cause)	block sidewall convective air  crosstalk between spent impingement and convective air streams	re-design eliminates need for corner dams  damage was noticed after first day of running... decision was made to push back into place and continue to run due to time constraints to acquire data prior to PDR	improved weld process for dam structures  shut down and repair at any sign of damaged hardware	yes, where applicable  yes
split (%Wa in rich zone) was greater than design (29% vs 22%) at supersonic cruise condition	lower $\Phi_{rich}$ (1.7* vs 2.0) higher $T_{flame,rich}$ (300-500 deg)	*during operation, $\Phi_{rich}$ was maintained $1.6 < \Phi_{rich} < 1.8$ by operating at higher $f/a$ (0.035 vs 0.030)	smaller swirler  increase shroud area (see Mn,shroud observation)  verify split with cold flow and warm flow  utilize all pressure instrumentation during cold/warm flow to characterize shroud losses and all flow splits simultaneously  cold/warm flow at higher pressure to increase $\Delta P$ accuracy  shut down if split too high  Install $\Delta P$ transducers for increased accuracy of $\Delta P$ measurement	yes yes yes yes yes yes yes
split varied during heat up (19% - 25%)	none...non-combusting		verify split with warm flow  warm flow at higher pressure to increase $\Delta P$ accuracy  confirm behavior with Fuel Shifting Sector Rig  do not light off if split too high shut down if split too high	yes yes yes yes
split varied as a function of rich or lean front end	split must ultimately determined under rich combusting environment at condition  fuel shifting schedule of operation must account for this behavior	behavior also observed in Fuel Shifting Sector Rig	determine split under rich combusting environment at condition	yes
split abruptly changed (33%-->25%) during operation at approach condition ( $T_3=450F$ ) with a lean front end: $0.5 < \Phi_{rich} < 0.7$	unknown	no observed change in Rig ACd monitored on-line  similar condition run previous day with no observed damage  possible unplugging of rich zone pressure tap	shut down if split changes abruptly  run with a lean front end prior to shutting down	yes  yes... procedure followed in

		after shutting down from a cold, rich condition the previous day	after a test shift	Fuel Shifting Sector Rig
Prich pressure taps not attached to rich zone liner	loss of reliable split reading	loss of 1 tap noted and corrected in data system during testing  build 1 configuration used a low profile pressure tap routed in the convective sidewall channel and attached to the liner via strapping that is tack welded to the liner and brazed to the hypo	attach/route rich zone pressure taps through bulkhead/heatshield  weld pressure tap to liner	yes  yes
Shroud Mn greater than design (0.1 vs 0.07)	higher pressure losses in quench path potentially causing higher split  lower static pressure in shroud could reduce impingement cooling or potentially reverse cooling flow		increase shroud area to bring shrouds in-line with design Mn or below	yes
Liner temperatures increased as $\Phi_{rich}$ was increased during rich front end operation at approach condition (T3=450F)	unknown...possible sign of reversal of quench air	behavior inconsistent with previous experience	perform flow visualization to inspect for quench flow reversal	yes (no flow reversal observed)
stain pattern on TBC of liner shows minor possibility of reverse quench flow along sidewall in one corner	unknown...possible sign of reversal of quench air		perform flow visualization to inspect for quench flow reversal	yes (no flow reversal observed)
TBC thickness less than design (0.008" vs 0.025")	rich zone liner operates above design temperatures		re-confirm TBC specification with vendor  increase inspection of parts	yes  yes
insufficient impingement cooling on upper and lower shells	rich zone liner operates above design temperatures	exhaust spent may have been too restrictive	exhaust spent impingement air out of rig through venturi for measurement  increase cooling	yes  yes
insufficient vane cooling	vanes operate above design temperatures		increase vane cooling on build 2 to build 1 levels (build 2 vanes have reduced surface area and enhanced impingement hole pattern)	yes
sidewall convective cooling not effective, sensitive to differential thermal growth	rich zone liner operates above design temperatures		impingement cool sidewalls	yes
lost TC's	unknown liner temperatures	shutdown due to lost TC's could significantly impact run efficiency	incorporate improved TC attachment methods  shutdown at sign of lost TC for replacement	no  no
$\Delta P/P < 0$ across lower shell, stain pattern on lower shell shows signs of flow in incorrect direction	cooling flow reversal	cooling flow split from coldflow ACd calibration was obtained as P3--> Plean value and was implemented as %Wa in the on-line data system	exhaust spent impingement air out of rig through venturi for measurement  increase shroud area (see Mn, shroud observation)  monitor $\Delta P$ across all	yes  yes  yes

			impingement shells (see comment)	
			utilize $\Delta P$ across all impingement shells during cold/warm flow ACd calibration	yes
			install $\Delta P$ transducers for increased accuracy of $\Delta P$ measurement	yes
			shut down at sign of low $\Delta P/P$ (<1%)	yes
liner bending or buckling due to overconstraint	loss of cooling effectiveness		provide increased provisions for liner thermal growth	yes
			accomodate for up to a vane that is 400F cooler than the liner without overstressing the liner-->0.020" thermal growth allowance on ID	yes
			accomodate greater circumferential growth-->0.010" thermal growth allowance on sidewall vane/liner interface	yes
			perform detailed FEM analysis	yes
liner walls warped or bowed inward	loss of cooling effectiveness		re-designed liner/shell construct to allow impingement shell to float with liner...maintaining impingement gap height..stiffen construct	yes
			add studs to liner to attach shell to liner (similar construct to undamaged bulkhead/heatshield) shells have oversized holes to allow for in-plane thermal growth	yes
			impingement cool sidewalls	yes
liner shifted forward 0.100"	leakage at quench plane uncontrolled split	tabs can disengage from shell	improve axial attachment of liner with studs	yes
downstream shroud pressure higher than upstream pressure on ID	unknown flowfield	potential for reversed instrumentation connections	flow verification of pressure tap instrumentation	yes
blockage ring loose	loss of split modification	still in place at rig disassembly	none	n/a
blockage rings on radial inflow swirlers cause flowfield distortion	flowfield distortion		undersize swirler and correct flowsplit with shroud/vane endcap restrictions if necessary	yes

Table VI - 4 Root Cause Investigation Findings for Product Module Rig Build 1

## **Build 2 Test Chronology**

Testing of Build 2 began on April 7, 1998 as run 138 with coldflow and warmflow checkout up to full supersonic cruise inlet conditions as had been recommended from the root cause investigations of build 1. Splits were recorded as 20%-21% during this checkout run, slightly lower than design intent. Combustion testing included operation at idle, descent, subsonic cruise, a de-rated low pressure takeoff (facility limited to 150 psia maximum inlet pressure), and nominal supersonic cruise conditions. Data from these conditions were acquired during runs 139, 142, 145 and 146. The last cumbusting run, run 146, was conducted on May 13, 1998. Throughout the combustion testing, splits remained in the 18% - 20% range.

Post-test inspection showed minor spallation of TBC in a 1 inch by 0.5 inch region about 2 inches downstream from the bulkhead on the lower right side of the sidewall (aft-looking-forward view). Two of the three center quench vanes (left-center and center) showed spallation of TBC along their leading edge for about 50%-75% of the ID to OD length but no damage to the metallic surfaces underneath the spalled TBC regions. The left-center quench vane showed some through surface oxidation (less than 0.25 inches by 0.25 inches), with some progression (less than 0.1 inch diameter) through the impingement baffle, occuring about 0.5 inches downstream of the quench air addition orifices and about 0.5 inches radially inboard from the OD platform. The liner, sidewall vanes and bulkhead heatshield, along with all structural components showed no signs of distress.

The split change between build 2 and 2A was accomplished by machining out the build 2 swirler and attaching the build 2A swirler (with a larger effective flow area) to the bulkhead with an EB-weld. All of this reconstruction was performed with the rig fully assembled and installed in the pressure vessel housing, minimizing the disassembly time. The left-center quench vane was also replaced prior to proceeding with testing of build 2A. TBC was also reapplied to the leading edges of the three center quench vanes and was applied in-situ to the rich zone liner in the region of spallation. The entire re-operation, re-TBC and re-installation into the test cell centerline was accomplished in an unprecedented four day turn-around.

## **Build 2a Test Chronology**

Build 2A testing was conducted on May 18, 1998 as run 147 of the CPC program. Testing included coldflow conditions to verify the proper split. Results showed a split of 22%-23% as anticipated from the change in effective inlet area to the rich zone resulting from the swirler change. Testing then proceeded to the de-rated low pressure takeoff condition, followed by a combustor inlet temperature excursion up to nominal supersonic cruise conditions. Subsequent to tesing at the nominal supersonic cruise conditions, the rig was shut down for inspection.

Post-test inspection showed spallation and through-surface oxidation (approximately 0.5 inches in diameter) on the leading edge of the left-center quench vane at approximately the 50% span location. Spallation was also apparent on the leading edge of the center quench vane for about one-half the radial height from the ID platform towards the OD platform. No oxidation of the metallic surface underneath the spalled TBC of the center quench vane was observed.

## **Discussion of Vane Parametrics**

Combustion tests were performed with the reduced-scale-quench vane geometries to assess the performance of the various designs with respect to  $\text{NO}_x$  and CO emissions at the supersonic cruise condition. The vane designs, previously described, were tested using a set of parameter variations around the nominal supersonic cruise condition:  $P_3 = 150$  psia,  $T_3 = 1200$  F, fuel/air = 0.0315. Parameter variations included excursions in:

- fuel/air ratio
- combustor pressure drop
- lean zone residence time

In addition to these parametric variations, detailed maps of emissions were acquired at the nominal supersonic cruise condition six inches downstream of the quench-zone exit. These maps were obtained by sequentially rotating the sampling probe and collecting emissions from each of the individual sampling orifices. In this manner a detailed map of 40 samples within the 5 inch diameter was developed and used to assess the quality of mixing of the different vane designs. Typical test results for these parametric variations and emissions maps are described below for the reduced-scale-quench vane design with Geometry #3.

### **Fuel/Air Excursion**

The nominal fuel/air ratio for the Single Module Rig combustion tests was 0.0315. This value accounts for the 5 % air required for lean-zone cooling, so that the fuel/air ratio entering the turbine section including the lean-zone cooling air would be 0.030 for the nominal supersonic cruise condition. Emissions were also obtained at fuel/air ratios of 0.030, 0.0340, and 0.0360, at a  $T_3 = 1200$ F, a 4 % pressure drop (see Pressure Drop Excursion Section, below, for a description of the location of this pressure drop), and  $P_3 = 150$  psia.

The fuel/air excursion emissions results are shown in Figure VI - 2 for the geometry #3 vanes with a 0.58 inch quench-zone gap. Both  $\text{NO}_x$  and CO emissions show an increasing trend with increasing fuel/air ratio. The fuel/air ratio on the abscissa of this plot (metered fuel/air ratio) is determined from the fuel turbine meter and the air venturi measurements. The individual points represent the results of ganged samples collected at four sampling probe angles (i.e. 180, -135, 22.5 and 90 degrees).

### **Pressure Drop Excursion**

The variation of the measured emission levels as a function of pressure drop is shown in Figure VI - 3. The pressure drop, in percent, is based on the pressure drop across the quench-air orifices: baffle pressure - lean zone pressure normalized to the baffle pressure. The baffle pressure is measured at two positions in the space between the inner impingement baffle and the outer vane shell containing the quench-air injection orifices. The average of these two pressure is used. The pressure drop is controlled by the overall air flowrate. Therefore, increasing pressure drop means increasing air flow. The quench-air jet to rich-zone flow momentum-flux ratio remains relatively constant as the pressure drop is changed.  $\text{NO}_x$  is seen to decrease slightly with increasing pressure drop. The CO remained relatively constant as the pressure drop increased.

### **Residence Time Excursion**

The dependence of the measured emission indices on the lean-zone residence-time is shown in Figure VI - 4. These data were obtained by sampling at 2, 4 and 6 inches downstream of the quench-zone exit while inlet conditions were maintained constant. The lean-zone residence-time is computed using the distance to the sampling probe from the quench-zone exit and the calculated one-dimensional velocity in the lean zone. The lean-zone velocity is calculated using the cross-sectional flow area and the gas

density, which is calculated from the measured lean-zone pressure and the calculated flame temperature for the metered fuel/air ratio.

Previous measurements have shown that an extremely low level of  $\text{NO}_x$  is formed in the rich zone. The fact then that the  $\text{NO}_x$  EI does not extrapolate to a value of 0 EI at zero residence time, in Figure VI - 4, indicates that either the majority of the  $\text{NO}_x$  emissions are formed in the quench mixing process and/or that there are significant recirculation regions in the lean zone. Water flow visualization measurements showed only small lean-zone recirculation regions with the reduced-scale-quench vane geometries, so it is therefore likely that most of the  $\text{NO}_x$  is formed in the quench zone.

## Emissions Maps

Detailed maps of  $\text{NO}_x$  and CO emissions were measured by rotating the probe and acquiring emissions from individual probe positions. These maps were made 6 inches downstream of the quench-zone exit. Data are represented by contours of emissions index versus position in a plane perpendicular to the flow. Forty individual measurements were used to generate the contour plots. The resulting contours represent the flowfield as would be seen in cross-section when aft-looking-forward (i.e., looking towards the rich zone from the lean zone). The reduced-scale-quench vanes in this view are horizontal. Figure VI - 5 shows how this contour relates to the reduced-scale-quench geometry.

Figure VI - 6 shows contours of  $\text{NO}_x$  EI for the test of the geometry #3 vanes at the nominal supersonic cruise condition. As can be seen in the figure,  $\text{NO}_x$  was formed to a greater extent at the top of the combustor, while lower levels were observed at the bottom of the combustor.

The CO map typically shows features that are opposite to the  $\text{NO}_x$  features, meaning that where the  $\text{NO}_x$  is high, the CO is low and vice-versa. The CO contours for vane geometry #3 are illustrated in Figure VI - 7. At the top of the combustor the CO is low where as the  $\text{NO}_x$  was high there. The CO is high towards the bottom of the combustor.

Figure VI - 8 plots contours of the ratio of the fuel/air calculated from the emissions relative to the fuel/air ratio calculated from flow measurements, FARR. This ratio indicates regions of the flow that are high or low in fuel/air ratio with respect to the average fuel/air ratio. FARR contours were found to be generally correlated with the CO contours, which is supported by comparing Figure VI - 8 and Figure VI - 7.

## Effect of Geometric Variations on $\text{NO}_x$ at the Nominal Supersonic Cruise Condition

Since the  $\text{NO}_x$  and CO emissions levels vary across the flow, an appropriate average or other suitable performance index was needed to rate and compare the performance of the various reduced-scale-quench vane designs. The performance of reduced-scale-quench vane designs were compared by determining the  $\text{NO}_x$  EI at a metered fuel-air ratio (based on the air and fuel flow measurements) of 0.0315 from an exponential curve fit of the  $\text{NO}_x$  emissions measured during the fuel/air ratio excursion tests.

There were a total of nineteen different reduced-scale-quench vanes designed and fabricated for the supersonic cruise condition testing phase of the Single Module Rig Vane Parametrics program. Eighteen of these vane designs were tested in a total of 38 different tests. The rich zone was cylindrical except for one test that had a rectangular rich-zone.

Three quench-zone gaps were investigated as described in the previous section describing the reduced-scale-quench vane designs. Most of the tests were with a four vane design with a quench-zone channel height of 0.580 inches. Four tests were conducted with the five vane design - three at a quench-zone channel height of 0.435 inches and one at a quench-zone channel height of 0.300 inches.

The vane designs tested under this program generally fall into four somewhat broad classes. There were eight designs of the four-vane design which involved variations in the number of holes, size of the holes and aspect ratio (see Table IV - 1). There was one design with a truncated trailing-edge. There were four designs with variations in the jet orientation: a single-direction-feed design, a design with slanted, quench-air, injection orifices, and two designs to test the effect of auxiliary jets located in front and

behind the main quench jets. These two vanes were intended to evaluate the effect of cooling air injection in the Product Module configuration and were not tested. Finally, there were four designs of the five-vane design, representing three variations in number of orifices per side and one set of vanes with even a smaller quench-zone channel height. The next section discusses some of the results of these geometric variations.

Vane Geometry Number	# of Jets	Channel Height H (in)	Active Volume Parameter	NO <sub>x</sub> EI
1	6	0.580	3.54	11.1
2	12	0.580	0.86	8.2
3	18	0.580	0.51	5.8
3	18	0.580	1.93	7.2
slanted slots				
3	18	0.580	3.43	10.3
truncated trailing edge				
3	18	0.580	2.20	8.8
single direction feed				
4	18	0.580	0.53	7.1
5	18	0.580	0.59	6.6
6	18	0.580	0.68	8.3
7	32	0.580	1.03	8.7
8	5	0.580	0.54	6.9
9	16	0.435	0.58	9.1
10	24	0.435	0.41	5.2
11	32	0.435	0.53	6.6
12	24	0.300	0.22	6.2

*Reduced-Scale-Quench Vane Orifice Calculated Parameters for Geometries*

### ***Effect of Quench-Air, Injection Orifice Aspect Ratio***

Geometries #3, #4, and #5 investigated the effect of aspect ratio. The quench-zone channel height was 0.58 inches and the number of orifices per side was 18. Figure VI - 9 summarizes the results of these tests. An optimum aspect ratio was found with respect to NO<sub>x</sub> emissions. The NO<sub>x</sub> EI decreased from approximately 6.6 to 5.8 and then increased to 7.1 as the aspect ratio changed from 0.94 to 2 to 3.55. Both the Active Volume Parameter (Figure VI - 10) and the measured NO<sub>x</sub>EI indicate that an aspect ratio of 2 is optimal. Achieving a quench-air, jet penetration that balances the amount of rich-zone gas that passes between the quench jets in the vertical direction with the amount that passes in the transverse direction is critical in minimizing the nitric oxides emissions. Figure VI - 11 shows the effect of quench-air, injection orifice aspect ratio (length/width) on the fuel-air distribution downstream of the quench-air, injection orifices.

### ***Effect of the Number of Quench-Air, Injection Orifices per Side (Orifice Spacing)***

Geometries #9, #10, and #11 investigated the effect of the number of quench-air orifices per side with a constant quench-zone channel height and a constant quench-air injection orifice aspect ratio (length/width). The quench-zone channel height was 0.435 inches and the quench-air injection orifice aspect ratio was 2. Figure VI - 12 summarizes the results of these tests. An optimum number of quench orifices per side (or quench orifice spacing) exists with respect to the nitric oxides emissions. The nitric oxides emission index decreased from approximately 9.1 to 5.2 and then increased to 6.6 as the number of quenchair injection orifices per side changed from 16 to 24 to 32 (orifice spacing of 0.255 inches, 0.167 inches and 0.123 inches, respectively or an S/H of 0.586, 0.383 and 0.284, respectively). In Figure VI - 13 the Active Volume Parameter calculation also indicates this behavior of an optimal orifice spacing. Figure VI - 14 gives CFD calculations with a quench-zone gap equal to 0.435 inches, an aspect

ratio of 2, and for different numbers of quench-air, injection orifices. Three axial planes of fuel-air ratio distributions are given in these figures. The planes of fuel-air ratio are given at various axial locations downstream of the quench-air, injection orifices. The first observation is that fairly rapid mixing occurs and that the end of the quench vane a significant amount of mixing has occurred. The second observation is that an optimum number of quench-air injection orifices exists that balances the amount of rich gas that passes between the quench-air jets in the vertical direction with the amount that passes in the transverse direction.

### ***Effect of Quench-Zone Channel Height***

Geometries #3 and #10 varied the quench-zone channel height. The quench-air injection orifice aspect ratio was maintained constant at 2 and the ratio between the quench-air injection orifice pitch and the quench-zone gap was held constant at 0.39. The number of quench orifices changed from 18 to 24 as the quench-zone channel height decreased from 0.580 inches to 0.435 inches. Figure VI - 15 shows the results of these tests. The NO<sub>x</sub> EI decreased slightly from 5.8 to 5.2 as the quench-zone channel height decreased from 0.580 inches to 0.435 inches.

Geometry #12 was also tested and had a quench-zone channel height of 0.300 inches. The measured NO<sub>x</sub> EI was 6.2 which was higher than with the 0.435 inch and 0.58 inch quench-zone channel height geometries. However, vane geometry #12 did not have the same ratio between the quench-air injection orifice pitch and the quench-zone channel height as that of vane geometries #3 and #10. Also, it was noted that the calculated discharge coefficient for the quench-air injection orifices was greater than 1 for the test conducted with vane geometry #12. This calculation indicates that a leak of the quench air into the lean or rich zone existed before that air had reached the quench-air injection orifices.

Figure VI - 16 plots the Active Volume Parameter versus the quench-zone gap. The Active Volume Parameter is observed to continue to decrease as the quench-zone gap decreased. However, there exists some doubt about the test with the 0.3 inch quench-zone gap as explained in the previous section. The quench-air, injection orifices had a larger than designed effective area and therefore a lower momentum-flux ratio. These observations lead to the hypothesis that the reduced-scale-quench vane-holder was leaking. As will be discussed later, a lower momentum-flux ratio increased NO<sub>x</sub>.

Figure VI - 17 shows the effect of quench-zone gap on the fuel-air distribution downstream of the quench-air, injection orifices. The aspect ratio was kept constant at 2 for these geometries. Figure VI - 17 indicates that the level of fuel-air uniformity increased as the quench-zone gap decreased.

### ***Effect of Momentum-Flux Ratio***

Geometries #3 and #6 investigated the effect of momentum-flux ratio on NO<sub>x</sub> emissions. The variation in momentum-flux ratio was accomplished by increasing the width of the vane geometry #3 quench-air injection orifice from 0.125 inches to 0.17 inches. Consequently, the quench-air injection orifice aspect ratio changed in addition to the momentum-flux ratio. Figure VI - 18 shows the results that the higher aspect ratio and momentum-flux geometry (vane geometry #3) resulted in lower NO<sub>x</sub> EI. The decrease is larger than expected from a change in the aspect ratio alone (see Figure VI - 9). Therefore, a lower momentum-flux ratio resulted in a higher NO<sub>x</sub> EI.

Figure VI - 19 is a plot of the Active Volume Parameter versus the quench-air to rich-zone gas momentum-flux ratio that was measured during the test. The measured quench-air to rich-zone gas momentum-flux ratio was 18.8 for geometry #3 and 14.7 for geometry #6. The change in measured quench-air to rich-zone gas momentum-flux ratio is not consistent with a 1.4 factor change in the quench-air, injection orifice area. However, the plots in Figure VI - 18 and Figure VI - 19 indicate that both the Active Volume Parameter and the measured Nitric Oxides Emission Index decreased with increasing quench-air to rich-zone gas momentum-flux ratio.

Figure VI - 20 shows the effect of quench-air to rich-zone gas momentum-flux ratio on the fuel-air distribution downstream of the quench-air, injection orifices. These results are for geometries #3 and #6. The number of quench-air, injection orifices was 18, the quench-air, injection length was 0.25 inches, and the quench-air, injection orifice width varied from 0.125 inches to 0.17 inches. This change in orifice

area resulted in an approximately factor of 2 change in the momentum-flux ratio (i.e. from 15.5 to 8). Figure VI - 20 shows that the quench-air jet penetration decreased with decreasing quench-air to rich-zone gas momentum-flux ratio. This trend is consistent with past jet penetration studies.

### ***Effect of Single-Direction-Feed***

A single-direction-feed, reduced-scale-quench vane design was also investigated (see Figure IV - 22). The back side of this geometry was rounded and effusion cooled. The quench-air injection orifices had single-direction-feed. The  $\text{NO}_x$  EI increased from approximately 5.8 to 9 when compared with vane geometry #3. Based on computational fluid dynamics results the single-direction-feed resulted in non-normal quench-air injection, which was probably responsible for most of this increase, since jet penetration is significantly impacted by the normality of the jet injection.

In order to investigate the effect of single-direction feed, the design in Figure IV - 22 was analyzed using computational fluid dynamics. The flow splits for this design are as follows: 90% of the air entering the vane passes through the upstream impingement-shell to cool the leading edge of the vane. This air then enters the quench zone through the quench-air, injection orifices. 10% of the quench air passes through the downstream impingement-shell to cool the trailing edge of the vane. This air enters the combustor by effusion holes on the trailing edge of the vane. Grids were generated in the internal passage between the impingement shell and leading-edge outer-shell up to the quench-air, injection orifices for the computational fluid dynamics calculations. The computational fluid dynamics calculation indicated that the quench air entered the quench zone at an angle relative to the more perpendicular quench jets of quench vane geometry #3. The Active Volume Parameter increased from approximately 0.51 to 2.2 which shows the same behavior as the measured nitric oxides emission index increased from approximately 5.8 to 9. Most of this increase is due to the angled, quench-air injection.

### ***Effect of Quench-Air Injection Orifice Orientation***

A reduced-scale-quench geometry that had slanted quench-air injection orifices (see Figure IV - 21) was also investigated. This geometry had a 0.580 inch quench-zone channel height and 18 quench-air injection orifices per side. The quench-air injection orifice aspect ratio was 2. Therefore, this geometry differed from vane geometry #3 only in the orientation of the quench-air injection orifices. The geometry with the slanted quench-air injection orifices had a measured  $\text{NO}_x$  EI of approximately 7.2. This measured value is greater than the 5.8 measured with the vane geometry #3.

The design in Figure IV - 21 was investigated using computational fluid dynamics to assess the effect of this design on the nitric oxides emissions index. Each side of the vane had the quench-air, injection orifices slanted 90 degrees out of phase to one another. The geometry with the slanted, quench-air, injection orifices had a larger Active Volume Parameter consistent with the higher measured nitric oxides relative to vane geometry #3.

### ***Effect of a Truncated Trailing-Edge***

A truncated-trailing-edge, reduced-scale-quench vane design was also investigated (see Figure IV - 20). The back side of this geometry was effusion cooled. The quench-air injection orifices also had single-direction-feed. The  $\text{NO}_x$  EI increased to approximately 10 relative to 5.8 for vane geometry #3. This increase was larger than observed with the single-direction-feed geometry. The reduction in the amount of confined mixing resulted in an increase of approximately 1 EI.

The design in Figure IV - 20 was investigated using computational fluid dynamics to assess the effect of this design on the nitric oxides emissions index. The flow splits for the design in Figure 34 are as follows. 90% of the air entering the vane passes through the upstream impingement-shell to cool the leading edge of the vane. This air then enters the quench zone through the quench-air, injection orifices. 10% of the quench air passes through the downstream impingement-shell to cool the trailing edge of the vane. This air enters the combustor by effusion holes on the trailing edge of the vane. The active volume parameter increased from approximately 0.51  $\text{in}^3$  for vane geometry #3 to 3.5  $\text{in}^3$  for the truncated trailing-edge geometry. This increase in the active volume parameter was similar in behavior

to the increase in nitric oxides emission index observed in combustion testing from approximately 5.8 to 10.

### ***Effect of Rectangular Rich-Zone***

Since the rich-zone of the Product Module configuration was trapezoidal, a test was conducted with a rectangular rich-zone. The reduced-scale-quench vane geometry #3 were used. The measured NO<sub>x</sub> EI were only slightly higher with the rectangular rich-zone.

### ***Particulate Measurements***

Particulate measurements were acquired in the Single Module Rig configuration with quench vane geometry #3 installed. Data acquisition was focused on the nominal supersonic cruise condition with investigation of the effects of residence time on particle concentration and concentration distribution. Total particle concentrations were low for this configuration, on the order of 1-1.5 million per cm<sup>3</sup>. Figure VI - 21 shows the decreasing concentration of particles as the combustion products progress through the aft end of the combustor. Based on the particle concentration distributions obtained also as a function of residence time (Figure VI - 22) it is apparent that the larger particles are the ones significantly oxidized beyond the quench region. By 3 milliseconds after the quench air introduction, particles in the 100-200 nm size range have already approached the background concentration levels. The peak of approximately 20-25 nm in size distribution is apparently typical for rich burning front end combustors.

### ***Effects of Cooling Air Introduction Post Quench Air Addition***

To assess the impact of exit transition zone cooling air on RQL quench vane emissions, additional tests were conducted with the Single Module Rig configuration with the Single Direction Feed quench vane geometry installed. This geometry was chosen because the effusive cooling on the trailing surface simulated the air introduction effects of exit transition zone air. This configuration is shown in Figure VI - 23. Cold combustor inlet temperatures were set while the combustor was operating in a rich front end mode. This is considered a severe condition for CO oxidation as cold cooling air might be likely to quench the CO reaction, resulting in high CO emissions. As shown in Figure VI - 24, CO emissions slightly increased from approximately 10 EI to 25 EI for inlet temperatures ranging from 660F down to 490F. This behavior shows that the cooling air introduction downstream of the quench air addition had minimal impact on the CO reaction as the combustor was able to maintain efficiencies above 99%. At the coldest inlet temperature of 490F, emissions were acquired as a function of residence time beyond the quench air addition to provide further diagnostics of this CO oxidation behavior. As shown by the low CO emissions and low sensitivity to residence time in Figure VI - 25, the CO oxidation reaction to CO<sub>2</sub> is nearly complete prior to the air exiting the confined region of the quench zone with only minimal oxidation continuing in the exit transition region, even under these severe rich front end conditions with cold inlet temperatures.

## ***Discussion of Product Module Rig***

### ***Build 1 & 1A Test Results***

Results from build 1 and build 1A of the Product Module Rig for the 15% Thrust LTO descent condition are shown in Figure VI - 26 through Figure VI - 31. Figure VI - 26 shows the effect of the addition of the blockage ring on the rich zone equivalence ratio as a function of Set Point fuel/air ratio. Theoretically, for a fixed-geometry combustor, the stoichiometry of the rich zone must fall on a straight line that passes through the origin of the graph. Therefore, the curve fits shown on the graph have this behavior enforced on them. Figure VI - 27 shows the FARR ratio as a function of Set Point fuel/air ratio. FARR is defined as the ratio of the fuel/air ratio obtained from emissions sampling analysis relative to the fuel/air ratio input to the combustor as measured from venturis and fuel flow meters. With a FARR value of 1.0 implying perfect agreement between input and emissions-based fuel/air ratios, acceptable quality data is regarded as falling within +/- 10%. As shown on the graph, almost all of the data obtained showed adequate data quality. Figure VI - 28 shows the NO<sub>x</sub> behavior for the 15% Thrust LTO descent

condition. As expected, the  $\text{NO}_x$  increases as the rich zone approaches stoichiometric conditions and drops off significantly at higher fuel/air ratios, when the rich zone is well above stoichiometric conditions. There appears to be minimal impact on the  $\text{NO}_x$  emissions by the change in split (i.e. bulkhead effective flow area). On this, and all subsequent emissions plots, the nominal set point fuel/air ratio for the inlet condition specified is notated on the graph. For this 15% Thrust LTO descent condition, it is anticipated that the RQL would be operated in a fuel shifted mode with approximately 40% of the burner operating like the lean front end of the graph and approximately 60% of the combustor operating like the rich portion of the graph. Superposition of the two behaviors, presuming minimal interaction effects, may be used to predict emissions at the LTO nominal fuel/air ratio condition. From the graph, it is apparent that approximately  $\text{NO}_x$  emissions of approximately 4-5EI would result from the superposition of these two behaviors. Similarly, CO behavior is shown in Figure VI - 29. Again, CO increases for the near stoichiometric front end equivalence ratios as high front end temperatures cause dissociation of the  $\text{CO}_2$  combustion products, resulting in significant quantities of CO. At these relatively moderate power conditions, reduction in CO emissions occurs post quench air addition once the combustor exit flame temperatures are great enough to oxidize the CO molecules. Again, the fuel shifting technology applied at this condition would maintain CO emissions at very low levels. CO emissions did not appear to be impacted by the addition of the blockage ring on the swirler. Unburned hydrocarbon (UHC) emissions are shown in Figure VI - 30 and are very low, as one would expect from an RQL combustor, except at the very low fuel/air ratios as the combustor nears the lean blow out limit. The UHC emissions are higher from build 1 at higher fuel/air ratios. This may be a result of fuel-air mixedness of the injector at this condition. Other diagnostic techniques such as laser velocimetry and patternation would be necessary to fully comprehend the observed behavior. The CO and UHC behavior results in the combustor efficiencies as shown in Figure VI - 31. Excellent efficiency, greater than 99.5% were obtained for most fuel/air ratios tested.

## Build 2 Test Results

Results for the 5.8% Thrust LTO idle condition are shown in Figure VI - 32 through Figure VI - 37. As shown in the stoichiometry graph of Figure VI - 32, because of the lower than intended split associated with the build 2 hardware, operation at nominal idle fuel/air ratio would result in rich zone equivalence ratio of approximately 0.9, slightly higher than intended. Data quality (Figure VI - 33), as indicated by FARR, were excellent. As expected  $\text{NO}_x$  emissions are very low at this low inlet temperature condition as shown in Figure VI - 34. CO emissions at idle (Figure VI - 35) appear much higher than intended even for the lean front end conditions. The high CO emissions observed when the front end is operated above stoichiometric conditions, is a result of the inability to oxidize the CO because of the relatively cool combustor exit temperatures. The UHC emissions at idle, shown in Figure VI - 36, show rather large values and may be related to the particular flow field characteristics of this swirler/injector combination at the fuel-air momentum ratios associated with these conditions. The rather poor idle efficiencies that result from this CO and UHC behavior are shown in Figure VI - 37.

Results for the 15% Thrust LTO descent conditions are shown in Figure VI - 38 through Figure VI - 43 and are plotted along with the results from Build 1 and 1A. While the  $\text{NO}_x$  emissions show similar behavior, the distinct differences in behavior that were observed in the CO and UHC emissions further support the presumption that the flow field and fuel-air mixedness associated with the fuel injector/swirler used for build 2 was not optimal for low power performance.

Nominal subsonic cruise results are shown in Figure VI - 44 through Figure VI - 49. As shown in the stoichiometry graph in Figure VI - 44, at the nominal subsonic cruise fuel/air ratio, for the split associated with the build 2 fuel injector/swirler, the rich zone equivalence ratio would be 1.6. However, data was taken at richer conditions and much leaner conditions initially, for the purposes of estimating the emissions performance without subjecting the liner to the potential of high temperatures prior to acquiring emissions at the supersonic cruise condition, the prime goal of this series of tests. It was anticipated, that with additional time available after testing at the supersonic cruise condition, additional data could have been acquired at the exact nominal subsonic cruise fuel/air ratio. Data quality, as shown in Figure VI - 45 was acceptable. As anticipated, the  $\text{NO}_x$  behavior (Figure VI - 46) when the rich zone operates above stoichiometric conditions is fairly insensitive to fuel/air ratio where as the lean portion of the curve shows a much steeper dependency of  $\text{NO}_x$  as a function of fuel/air ratio. CO emissions were in

an acceptable range for this engine power condition as shown in Figure VI - 47 and UHC emissions were very small (Figure VI - 48), less than 1 EI. Combining the CO and UHC emissions behavior, the resultant combustor efficiency (Figure VI - 49) at the nominal supersonic cruise condition would be expected to be greater than the goal value of 99% required for cycle and economic performance of the HSCT aircraft.

Takeoff performance was assessed at a de-rated, reduced pressure condition, based on limitations of the facility that prevented operation of the combustor at inlet pressures above 150 psia. Time did not permit acquiring emissions as a function of inlet pressure at this condition. This data is usually acquired to determine the pressure dependency by which the data could be scaled to true combustor inlet pressure. However, previous experience with RQL combustors dictates that NO<sub>x</sub> emissions typically scales as a function of the square root of the pressure ratio scale factor. Data acquired on other reduced scale quench combustors, have shown pressure dependencies with scale factors as low as the pressure ratio raised to the 0.3 power. As shown in the stoichiometry curve of Figure VI - 50, because of the lower than intended split for build 2, the rich zone equivalence ratio would have been excessive at the nominal 100% Thrust LTO takeoff condition fuel/air ratio. However, the emissions behavior can be extrapolated from the data acquired. Data quality at this de-rated, low pressure takeoff condition was acceptable as shown in Figure VI - 51. NO<sub>x</sub> emissions shown in Figure VI - 52 highlight the behavior of an RQL combustor where NO<sub>x</sub> is fairly insensitive to changes in fuel/air ratio as most of the emissions are formed in the quench zone and are not impacted significantly by the combustor exit flame temperature. CO emissions (Figure VI - 53) are very low and UHC emissions are negligible (Figure VI - 54) as would be expected for these conditions, resulting in efficiencies greater than 99.9% (Figure VI - 55).

Supersonic cruise performance is shown on Figure VI - 56 through Figure VI - 61. Again, the stoichiometry curve (Figure VI - 56) shows the higher than desired rich zone equivalence ratio, 2.6 vs 2.0, at the nominal supersonic cruise fuel/air ratio. Data quality was excellent for this conditions as shown in Figure VI - 57. NO<sub>x</sub> emissions performance at supersonic cruise shows a slight increasing dependency as a function to fuel/air ratio as the inlet temperature and fuel/air ratio combine to result in a combustor exit flame temperature that is just on the border of inducing additional NO<sub>x</sub> production in the aft end of the combustor. However, this contribution is minimal compared to the NO<sub>x</sub> produced in the quench region of the combustor. A NO<sub>x</sub> EI of 8.5 was determined from the NO<sub>x</sub> data of Figure VI - 58 while a CO EI of 1.2 is shown in Figure VI - 59. Again, UHC emissions (Figure VI - 60) are negligible at this high inlet temperature condition, resulting in combustor efficiencies of 99.97% (Figure VI - 61).

### **Build 2a Test Results**

Based on the successful emissions performance observed from build 2, build 2A attempted to improve on this performance by correcting the split of the combustor to match the design intent, resulting in the more appropriate rich zone equivalence ratios as a function of overall fuel/air ratio. Data for build 2A was acquired, therefore, at the high power conditions, focusing on the 100% Thrust LTO takeoff and nominal supersonic cruise conditions.

The 100% Thrust LTO takeoff performance is shown on Figure VI - 50 through Figure VI - 55, which included the corresponding build 2 data for comparison purposes. The fuel air excursion was curtailed to a maximum fuel/air ratio of 0.032, slightly below the nominal fuel/air ratio for this LTO condition due to time constraints and the desire to proceed to the supersonic cruise condition. However, adequate data was acquired for comparison with build 2. Again, data quality was excellent (Figure VI - 51). The NO<sub>x</sub>, CO, UHC and efficiency performance of the build 2A combustor showed similar behavior to that observed in build 2 as shown in Figure VI - 52, Figure VI - 53, Figure VI - 54 and Figure VI - 55 respectively. The only difference observed is a slightly reduced sensitivity of NO<sub>x</sub> emissions at the higher end of the fuel/air ratios tested.

Similarly, the supersonic cruise performance of build 2A was comparable to that of build 2. The stoichiometry curve of Build 2A, shown in Figure VI - 56, highlights that the correct split was achieved for this configuration, resulting in a rich zone equivalence ratio of 2.1 at the nominal supersonic cruise fuel/air ratio. Data quality (Figure VI - 57), again, was excellent. The change in split for build 2A did not appear to impact the NO<sub>x</sub> emissions performance as shown in Figure VI - 58 which has similar

behavior to build 2. The cluster of data at the nominal supersonic cruise condition represent various ganged readings at different probe angles at the exit of the combustor, and one particular probe orientation provided a higher  $\text{NO}_x$  emissions index reading for the Build 2. This behavior, with the probe oriented at the 90 degree angular position, did not appear to exist for build 2 as it did for build 2A. Detailed diagnostic probe sampling and flow field evaluation would be necessary to provide further insight into this anomaly. CO emissions are slightly higher for this particular probe angular orientation as well as shown in Figure VI - 59 which may infer a unique flow field change associated with the particular swirl installed for build 2A. UHC emissions for build 2A were, of course, negligible for this condition, and combustor efficiency was still excellent as shown in Figure VI - 61.

## Section VII - Conclusions

The low emissions potential of a Rich-Quench-Lean (RQL) combustor for use in the High Speed Civil Transport (HSCT) application was demonstrated.

Specifically:

1. A Rich-Quench-Lean combustor, utilizing reduced scale quench technology implemented in a quench vane concept in a product-like configuration (Product Module Rig), demonstrated the capability of achieving an emissions index of nitrogen oxides ( $\text{NO}_x$  EI) of 8.5 gm/Kg fuel at the supersonic flight condition (relative to the program goal of 5 gm/Kg fuel).
2. Developmental parametric testing of various quench vane configurations in the more fundamental flametube, Single Module Rig Configuration, demonstrated  $\text{NO}_x$  EI as low as 5.2.
3. All configurations in both the Product Module Rig configuration and the Single Module Rig configuration demonstrated exceptional efficiencies, greater than 99.95%, relative to the program goal of 99.9% efficiency at supersonic cruise conditions.
4. For the rectangular quench orifices investigated, an aspect ratio (length/width) of approximately 2 was found to be near optimum.
5. An optimum for orifice spacing was found to exist at approximately 0.167 inches, resulting in 24 orifices per side of a quench vane, for the 0.435 inch quench zone channel height investigated in the Single Module Rig.
6. Smaller quench zone channel heights appeared to be beneficial in reducing emissions. However, benefits of reduced quench zone channel heights can be over-ridden by non-optimal quench orifice geometry.
7. Measurements obtained in the Single Module Rig configuration on the sensitivity of emissions to the critical combustor parameters of fuel/air ratio, pressure drop and residence time showed minimal sensitivity to these parameters.

## References

1. The Atmospheric Effects of Stratospheric Aircraft: A Fourth Program Report, NASA Reference Publication 1359, January 1995
2. Rosfjord, T. J. and Padget, F. C., Experimental Assessment of the Rich/Quench/Len Combustor for High Speed Civil Transport Aircraft Engines, Final Report on Task 3 of NASA Contract NAS3-25952, December 1995.
3. Siskind, K. S. et. al., Multi-Module Fuel Shifting Sector Test Complete - MT410255, Informal Test Report, NASA Contract NAS3-27235, March 1998
4. Lohmann, R. P., et. al., Variable Geometry Concepts for Rich-Quench-Len Combustors, Final Report on Task 22 of NASA Contract NAS3-26618.
5. Cohen, J. M. and Rosfjord, T.J., Influences on the Sprays Formed by High Shear Fuel Nozzle/Swirlers Assemblies, Journal of Propulsion and Power, AIAA, Vol. 9, No. 1, 1993.
6. Hautman, D., et. al., Transverse Gaseous Injection into Subsonic Airflows, AIAA Paper 91-576, Jan, 1991.
7. Chiappetta, L., et. al., Design Considerations for Aerodynamically Quenching Gas Sampling Probes, ASME 82-HT-39.
8. Spindt, R. S., Air-Fuel Ratios from Exhaust Gas Analysis, SAE Paer 650507, Jan, 1965.

## Section II Figures

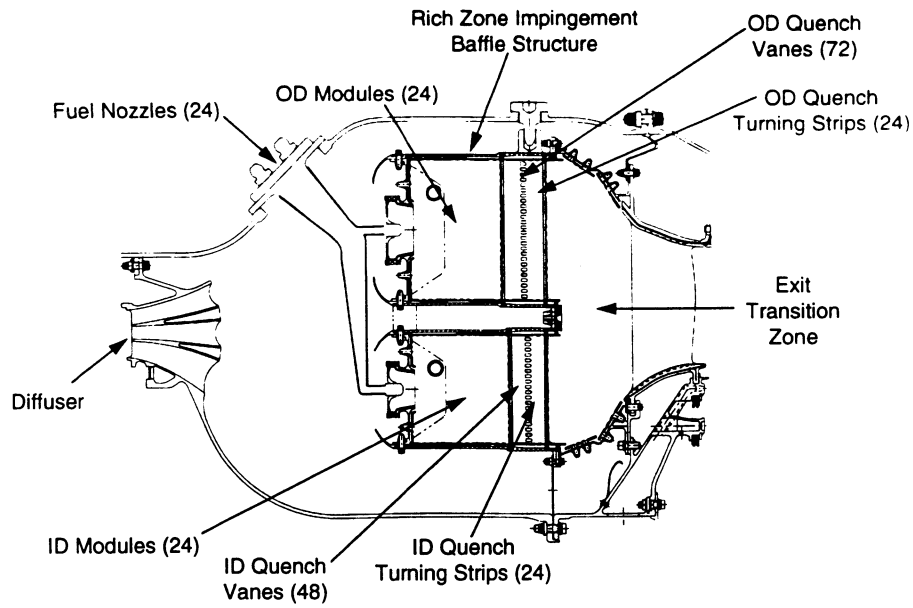


Figure II - 1 Multi-Modular Rich-Quench-Lean Combustor with Reduced Scale Quench Vanes

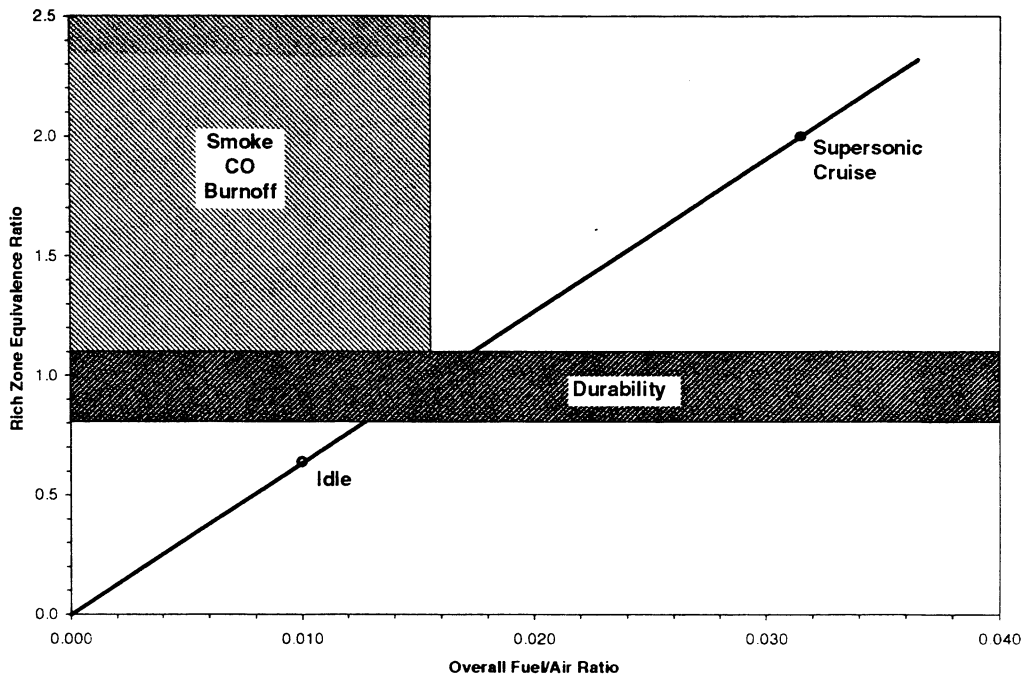


Figure II - 2 Rich Zone Stoichiometry of a Fixed Geometry RQL Combustor (22% rich zone, 73% quench zone, 5% lean zone cooling)

# Section IV Figures

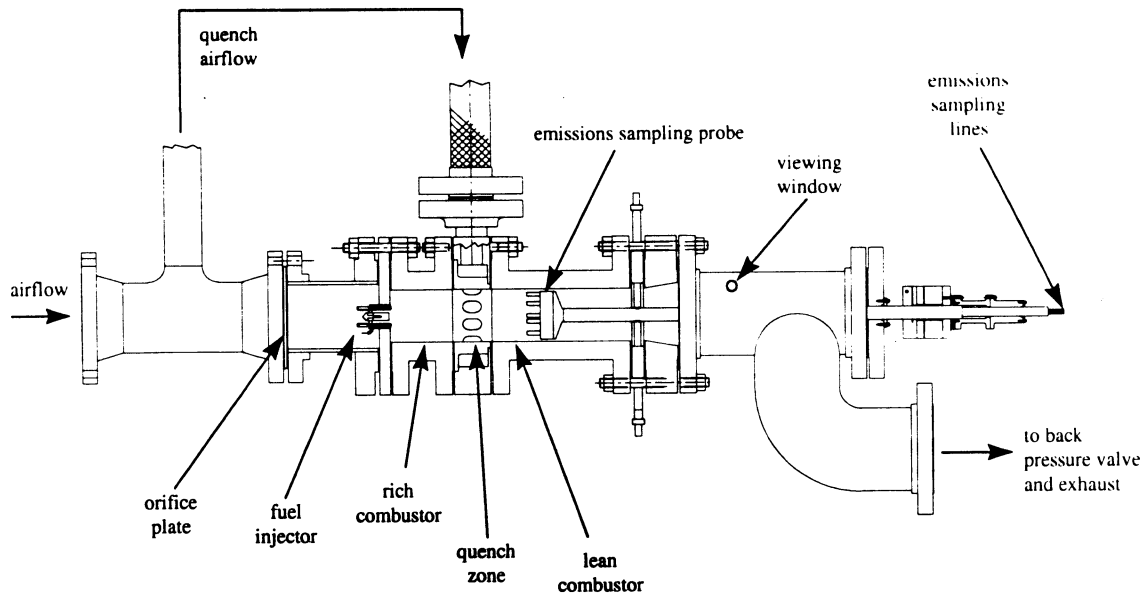


Figure IV - 1 RQL Single Module Rig Configuration used for Investigating Quench Vane Parametrics

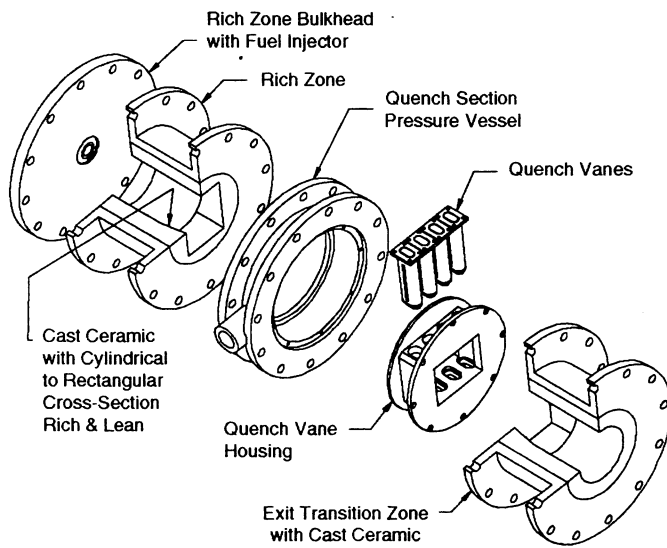
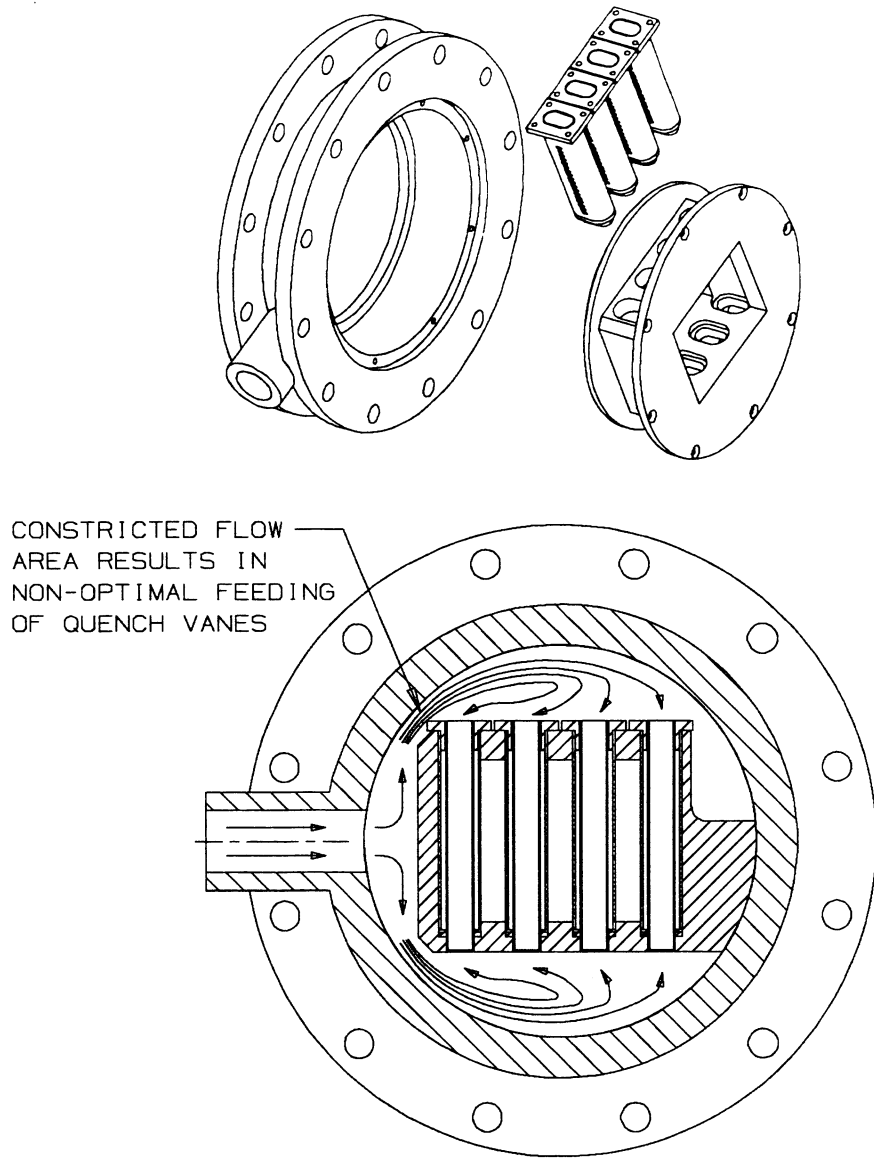


Figure IV - 2 Exploded View of Single Module Rig Configuration



*Figure IV - 3 Flowpath Feeding Quench Vanes in Single Module Rig Configuration*

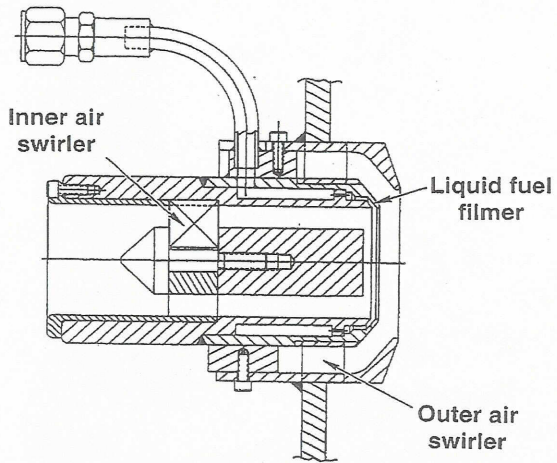


Figure IV - 4 Airblast Fuel Injector Design for Single Module Rig Configuration

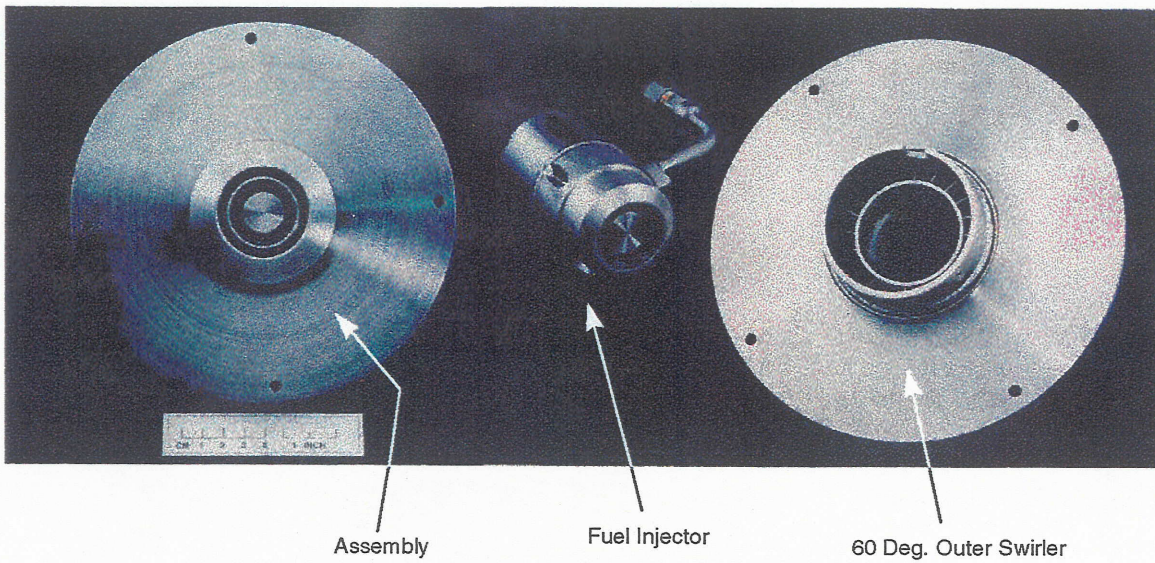


Figure IV - 5 Airblast Fuel Injector used in Single Module Rig Configuration

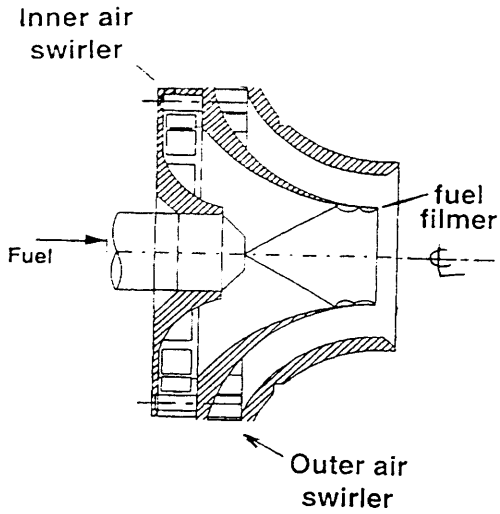


Figure IV - 6 Schematic of Radial Inflow Swirler/Fuel Injector Concept

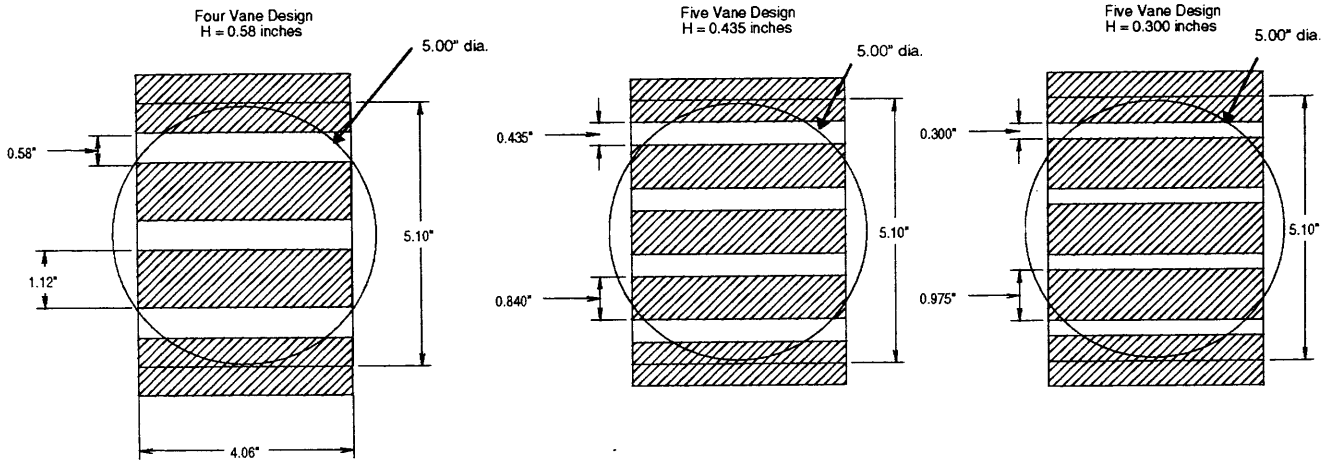


Figure IV - 7 Relationship of Quench Channel Geometries to Quench and Lean Zone Flow Areas - Single Module Rig

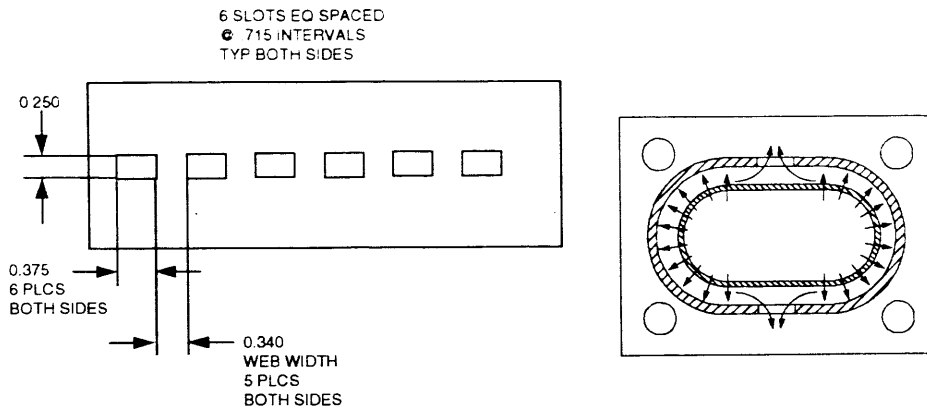


Figure IV - 8 Vane Geometry #1

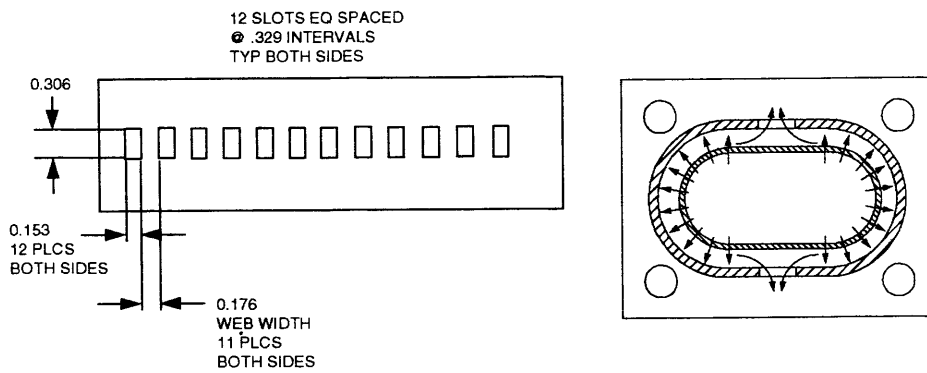


Figure IV - 9 Vane Geometry #2

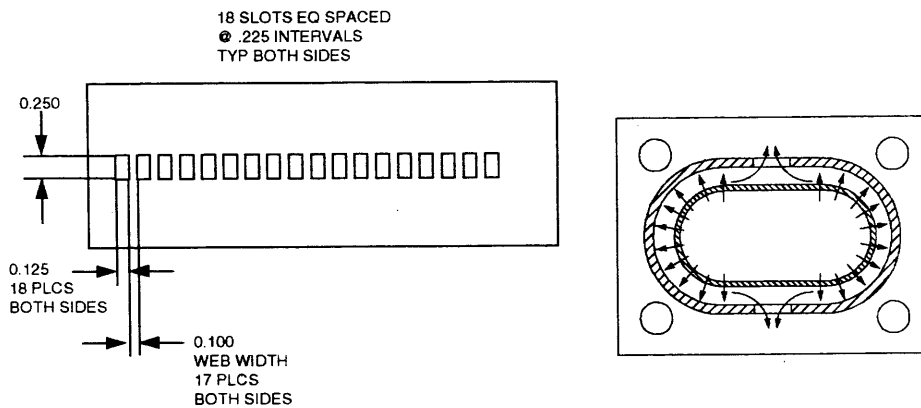


Figure IV - 10 Vane Geometry #3

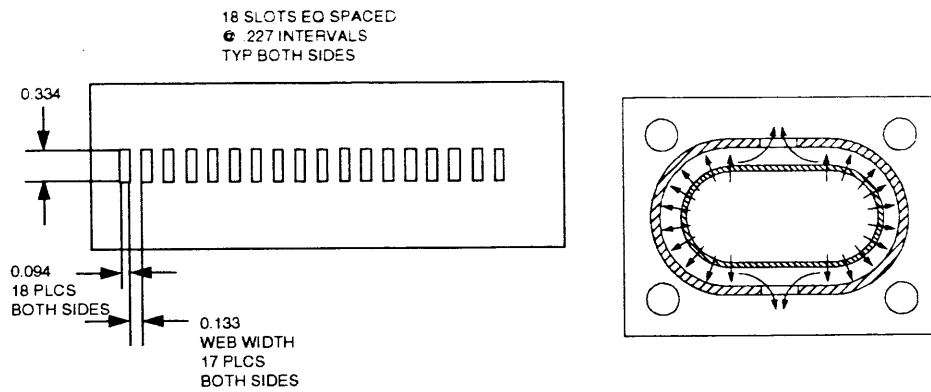


Figure IV - 11 Vane Geometry #4

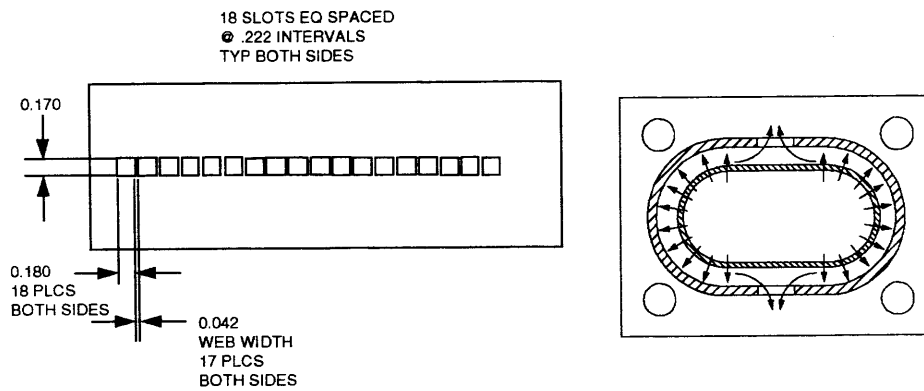


Figure IV - 12 Vane Geometry #5

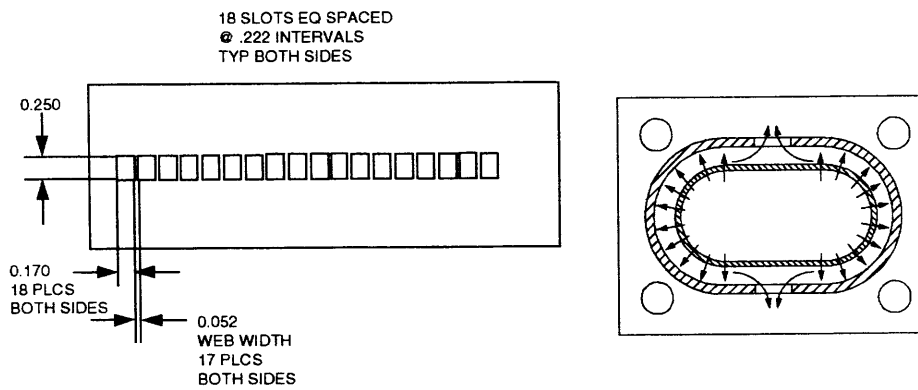


Figure IV - 13 Vane Geometry #6

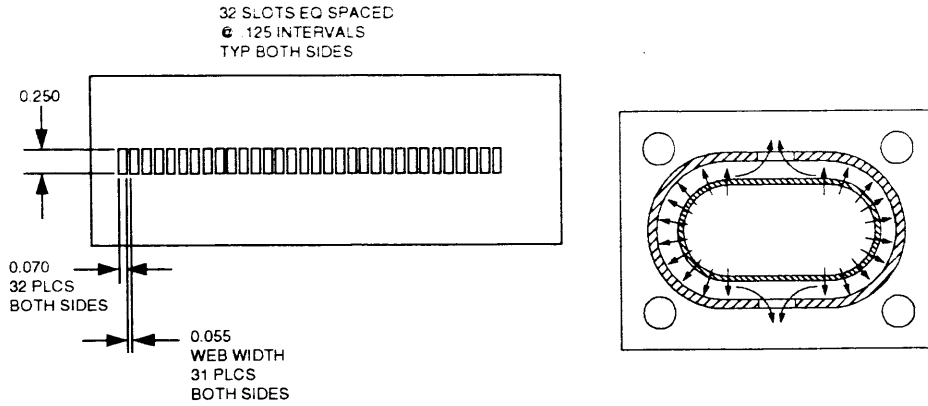


Figure IV - 14 Vane Geometry #7

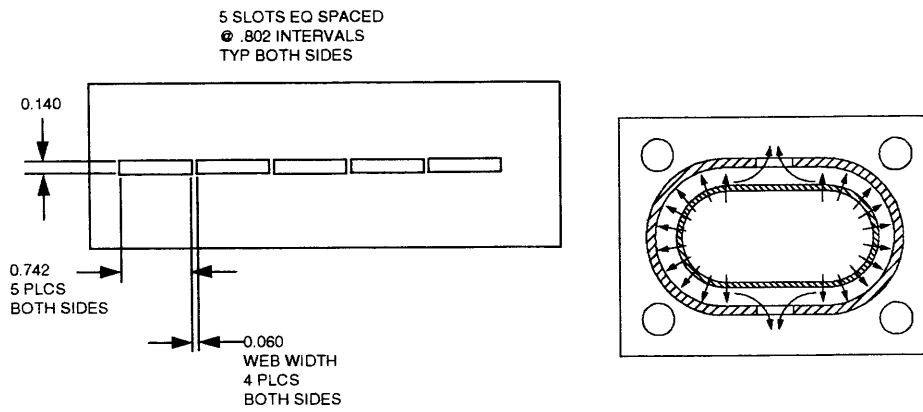


Figure IV - 15 Vane Geometry #8

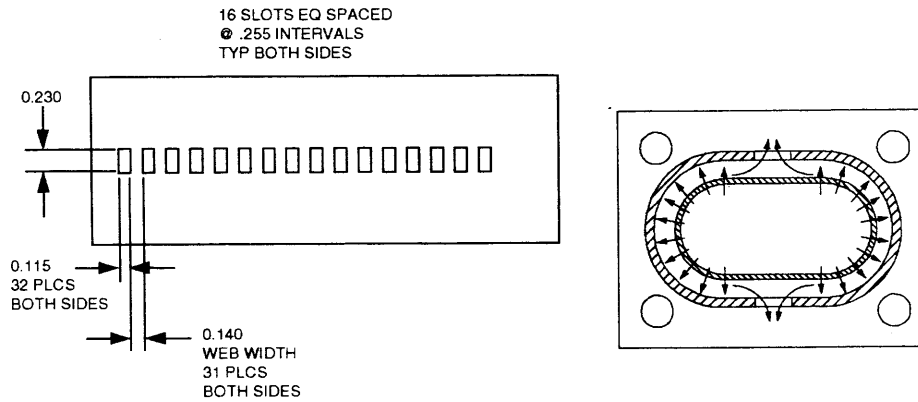


Figure IV - 16 Vane Geometry #9

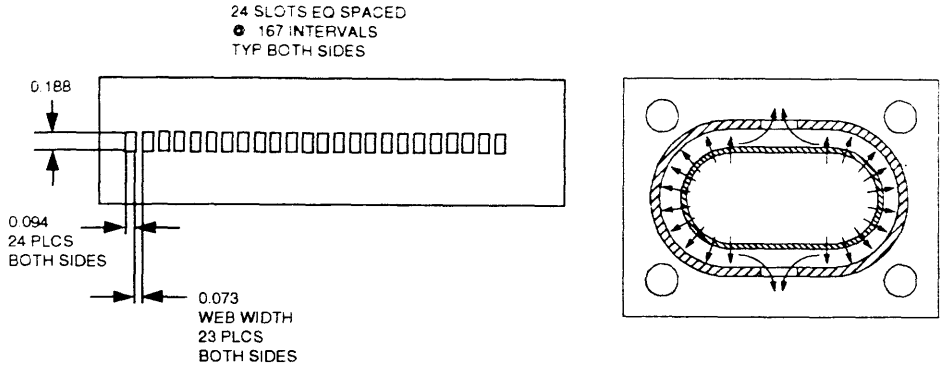


Figure IV - 17 Vane Geometry #10

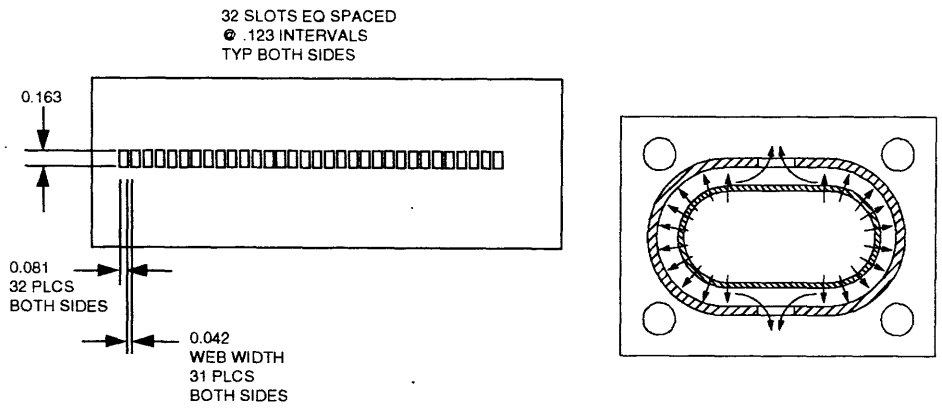


Figure IV - 18 Vane Geometry #11

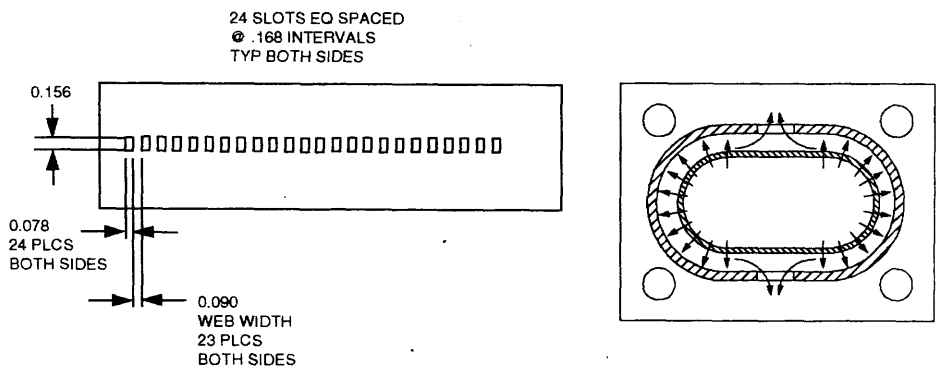


Figure IV - 19 Vane Geometry #12

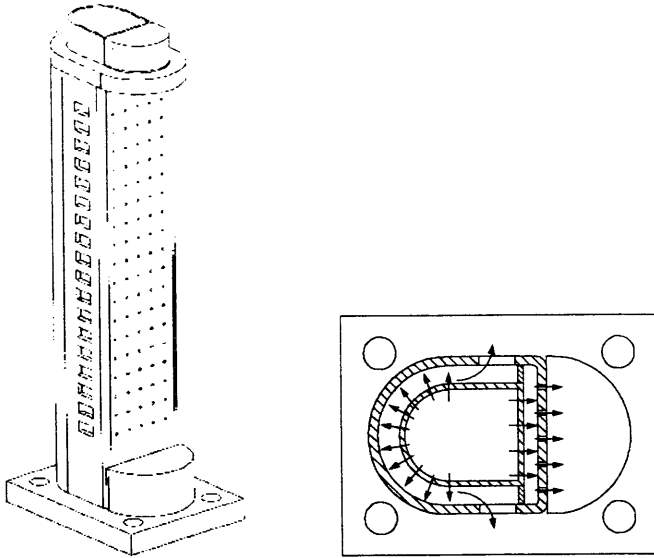


Figure IV - 20 Truncated Trailing Edge Quench Vane Geometry

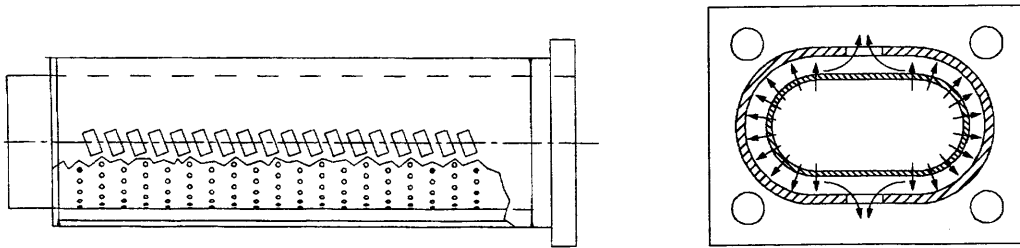


Figure IV - 21 Slanted Slot Quench Vane Geometry

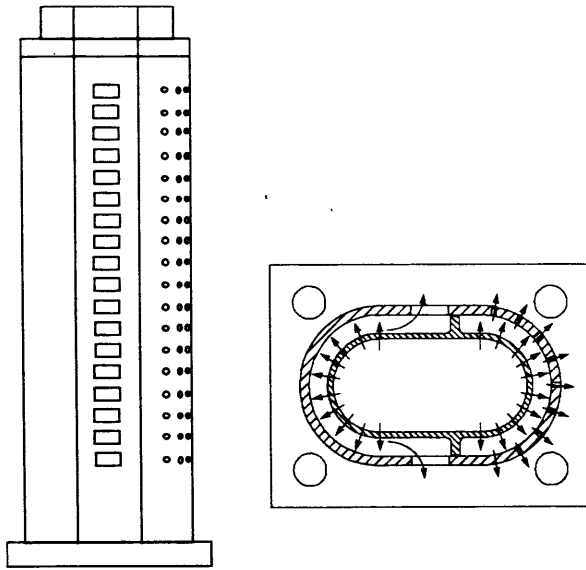


Figure IV - 22 Single Direction Feed Quench Vane Geometry

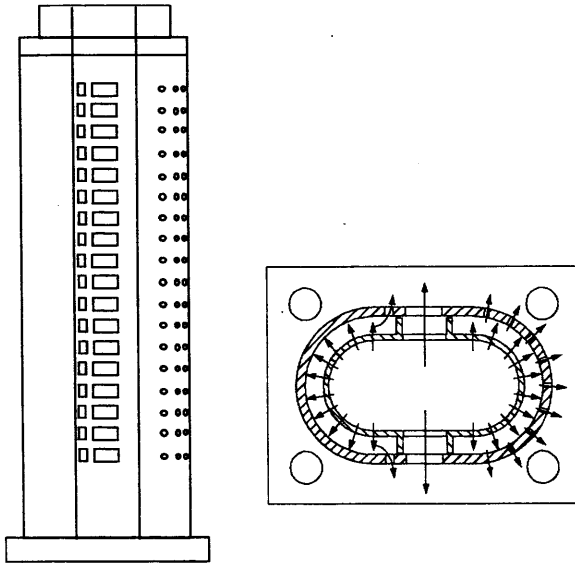


Figure IV - 23 Parallel Path Vane Geometry with Effusively Cooled Trailing Edge

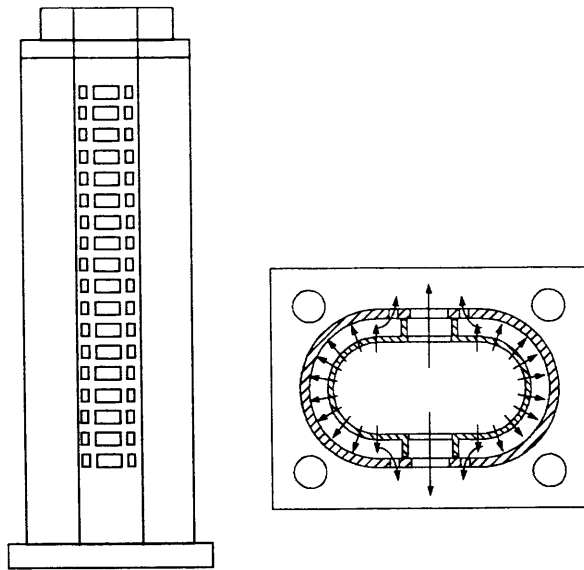


Figure IV - 24 Parallel Path Vane Geometry with Non-Effusively Cooled Trailing Edge

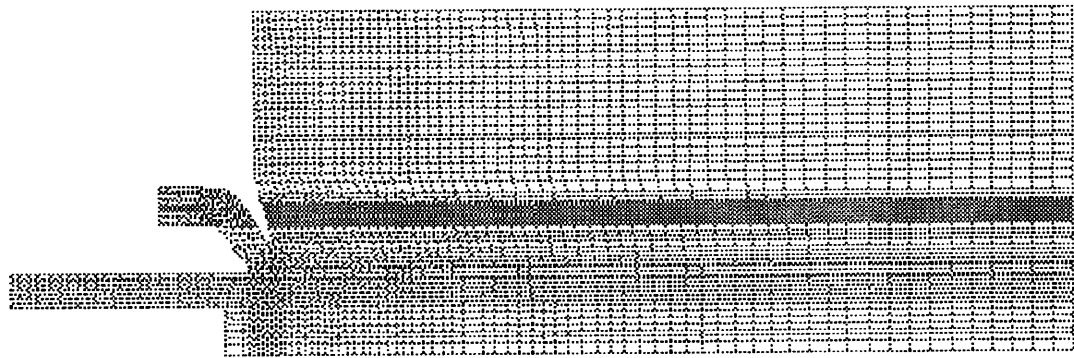


Figure IV - 25 Axisymmetric Grid of Rich Zone for Determining Inlet Boundary Conditions for Quench Vane CFD Analyses

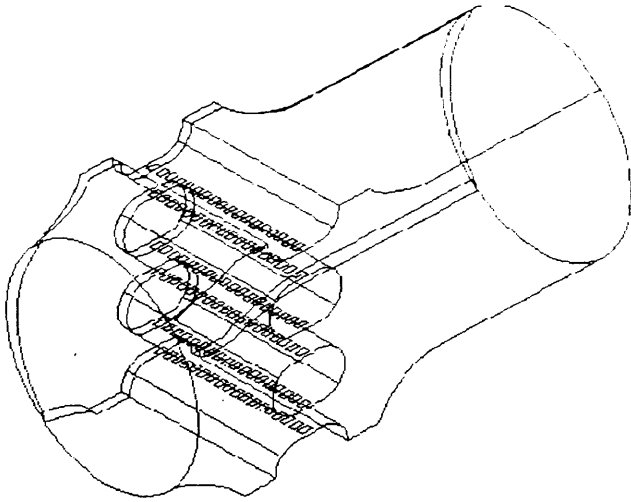


Figure IV - 26 Full Domain for CFD Analyses of Quench Vane Geometries

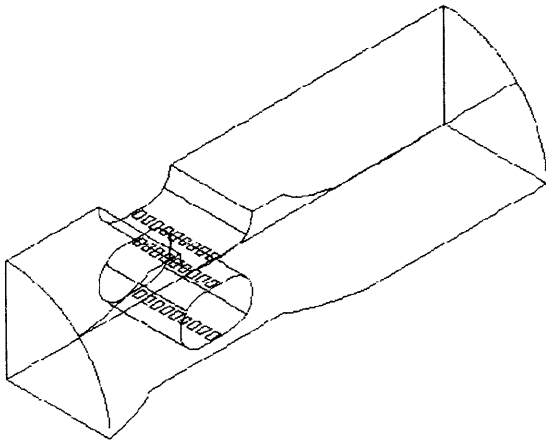


Figure IV - 27 Quarter Symmetry Domain for CFD Analyses of Quench Vane Geometries

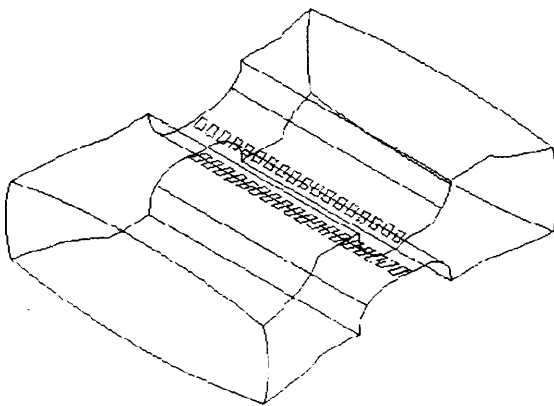


Figure IV - 28 Strut-to-Strut Domain for CFD Analyses of Quench Vane Geometries

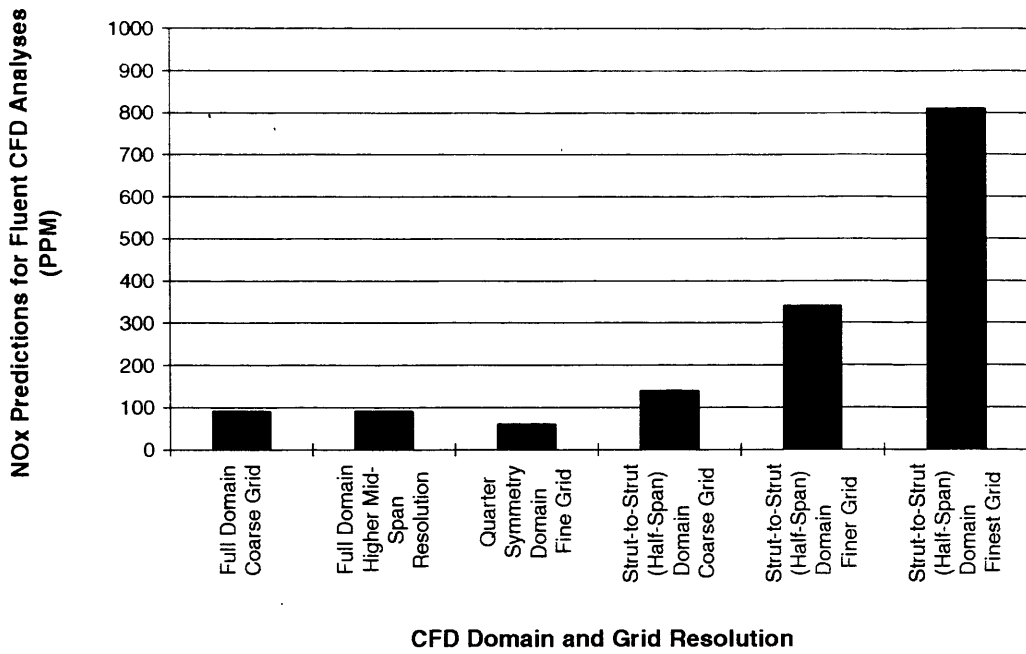


Figure IV - 29 NOx Calculation Sensitivity to Grid Density

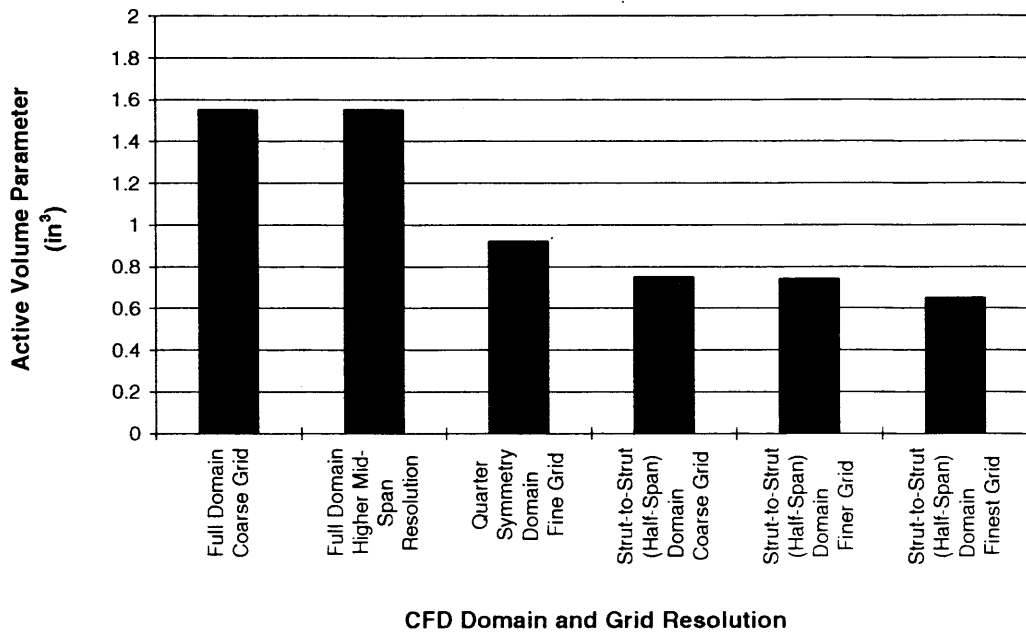


Figure IV - 30 Active Volume Parameter Insensitivity to Grid Density

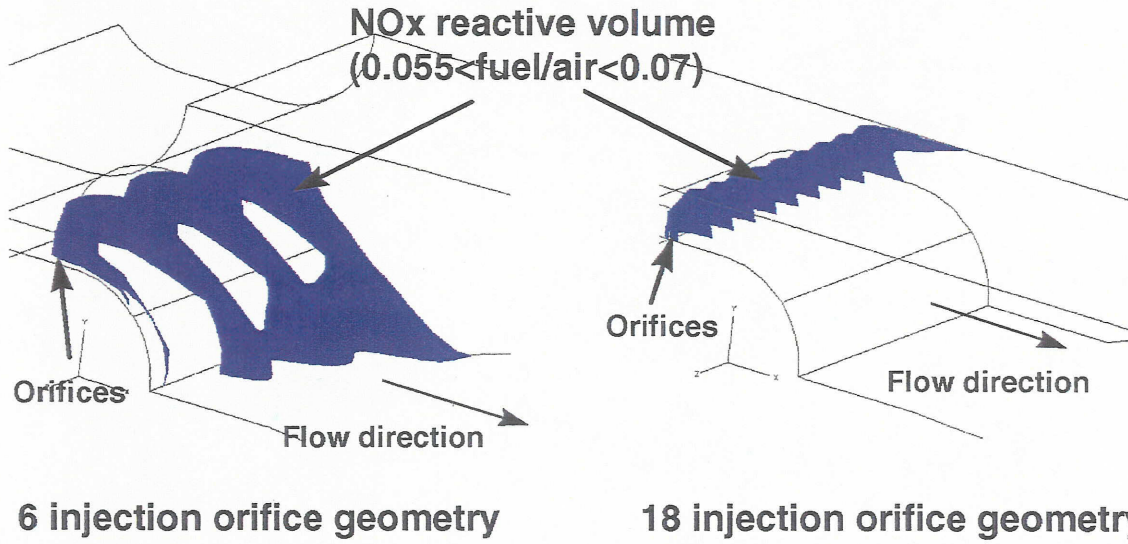


Figure IV - 31 Active Volume Controlled by Quench Orifice Size and Spacing  
(Left: Quench Vane Geometry #1; Right: Quench Vane Geometry #3)

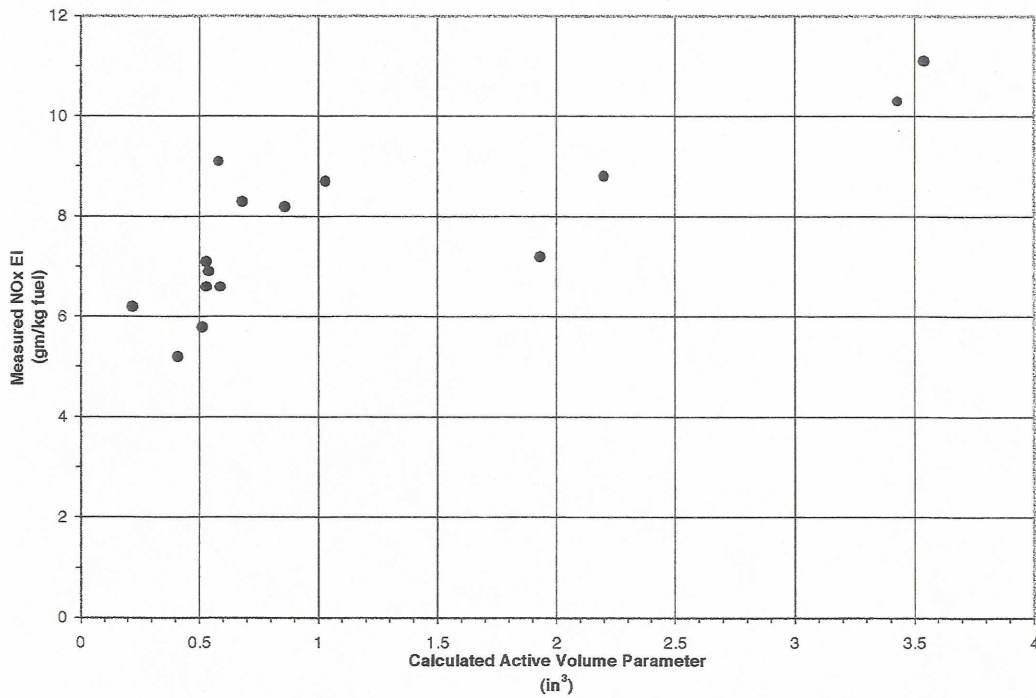


Figure IV - 32 Calculated Active Volume Parameter Correlated Against Measured NOx Emissions

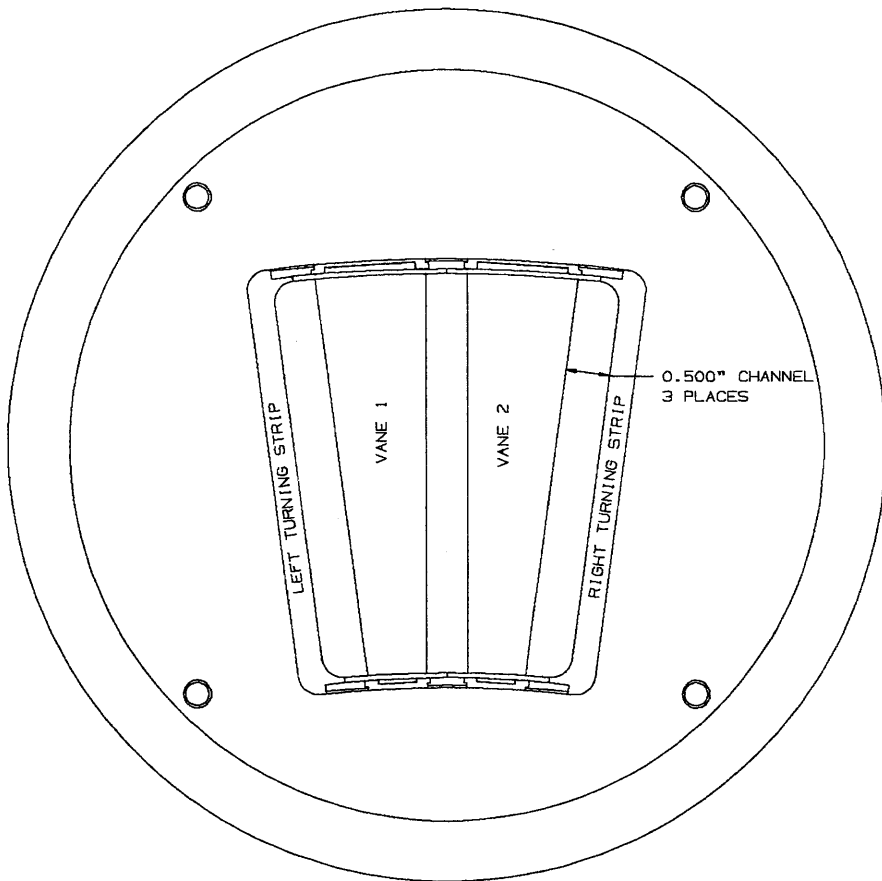


Figure IV - 33 Aft-Looking Forward View of Product Module Rig Build 1

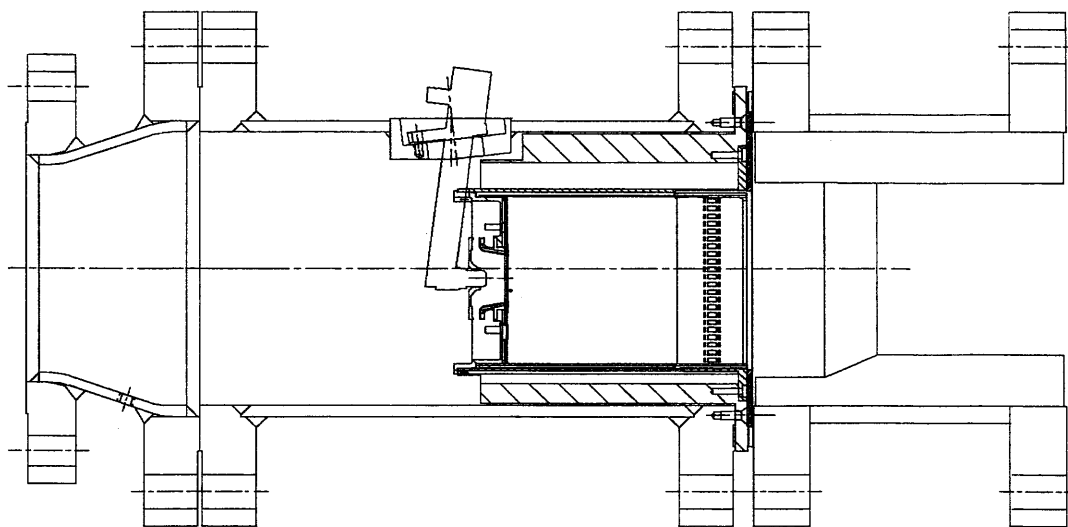


Figure IV - 34 Cross Section of Product Module Rig Build 1

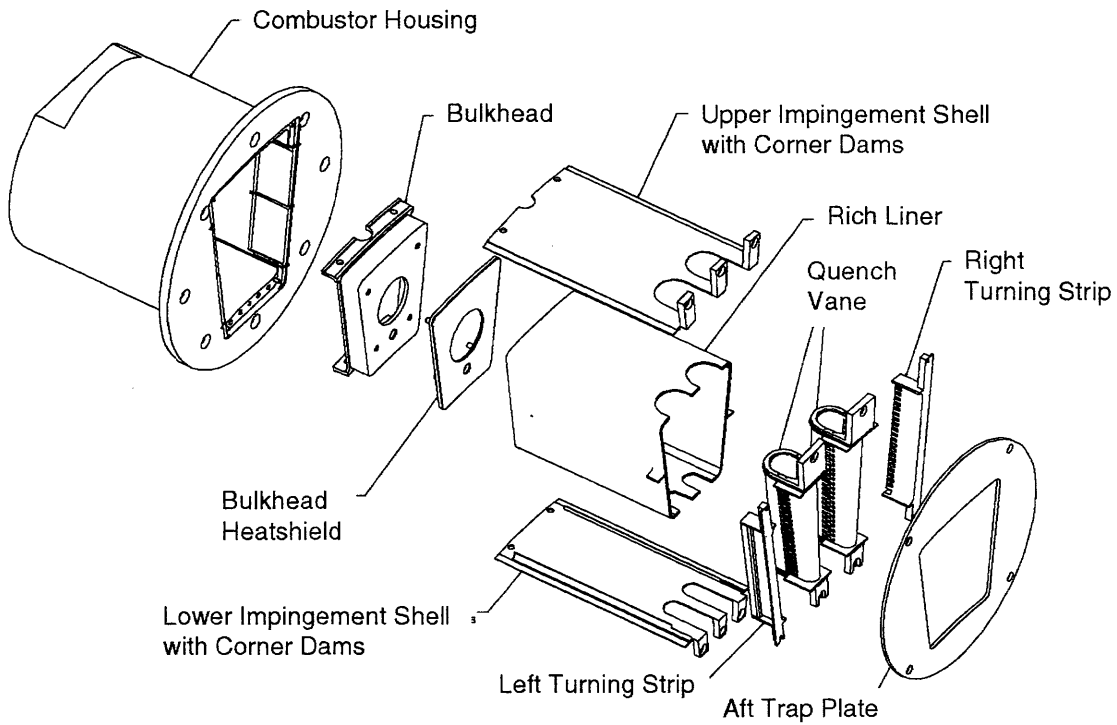


Figure IV - 35 Exploded View of Product Module Rig Build 1

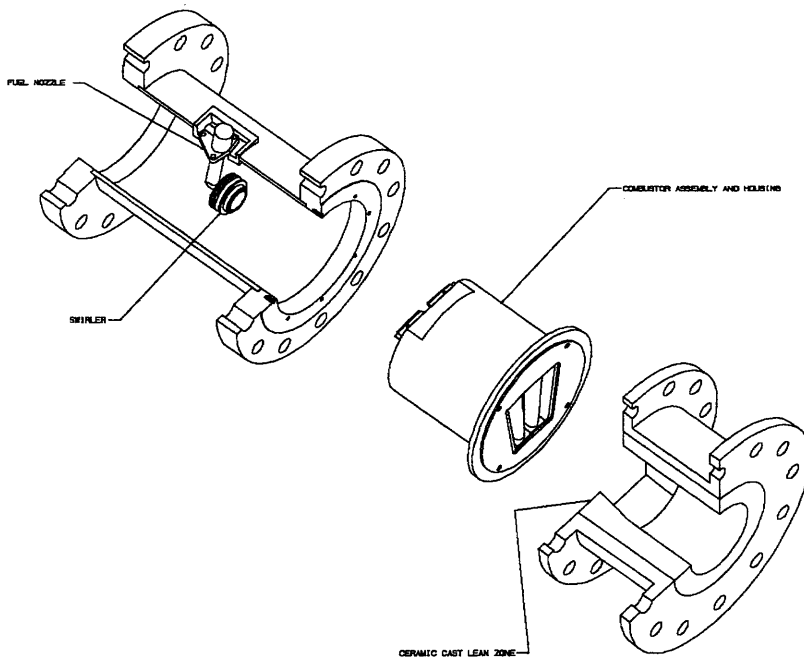
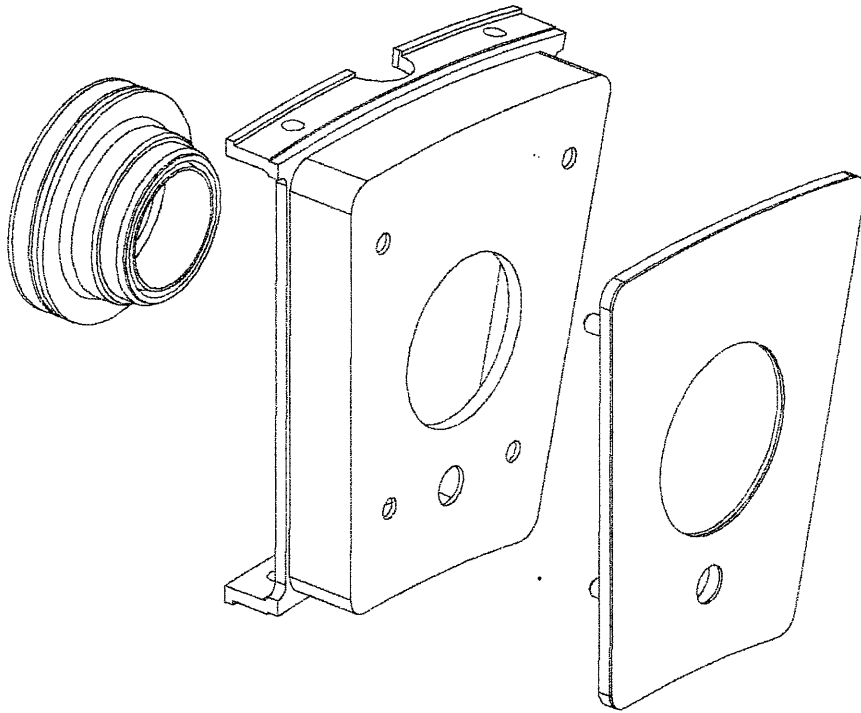


Figure IV - 36 Exploded View of Product Module Rig Combustor Assembly



*Figure IV - 37 Product Module Rig Bulkhead Assembly*

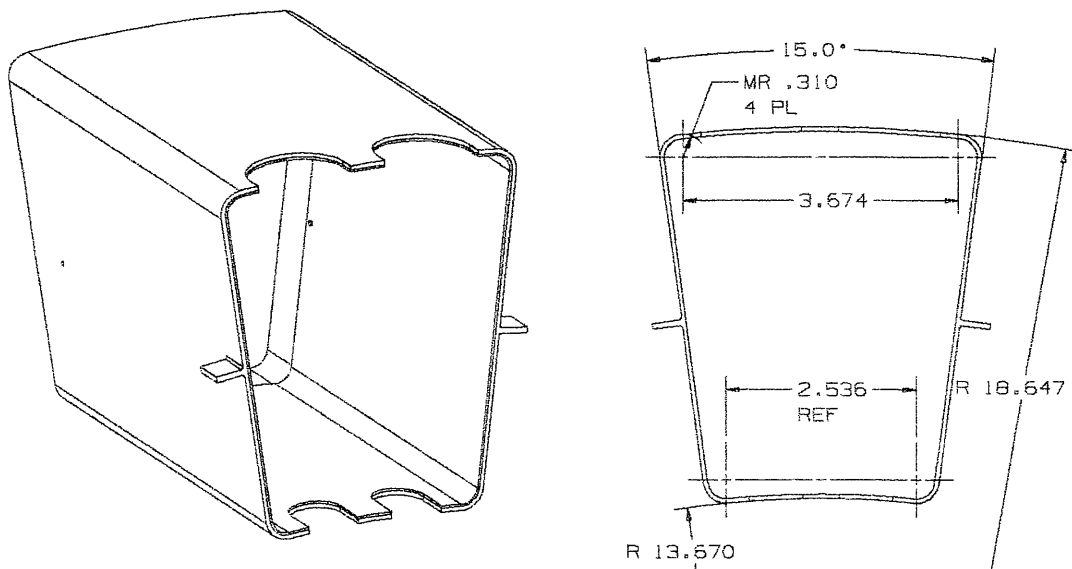


Figure IV - 38 Rich Zone Liner for Product Module Rig Build 1

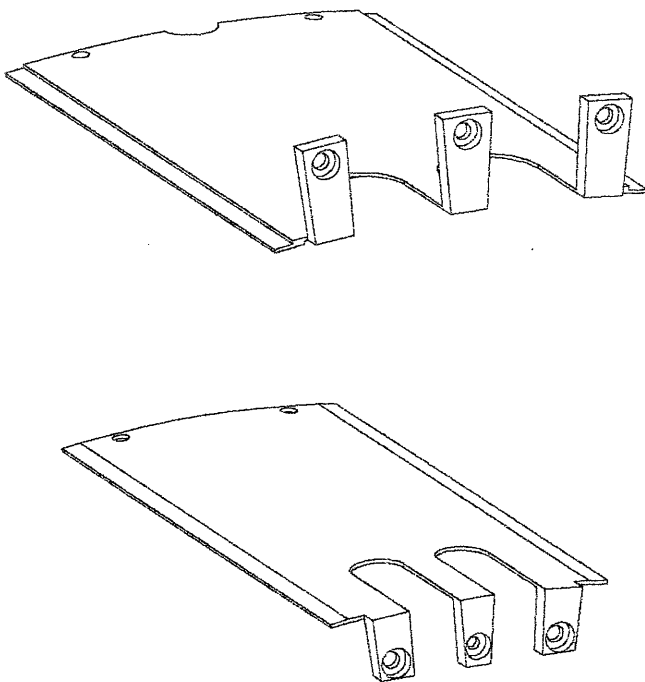


Figure IV - 39 Upper & Lower Impingement Shells of Product Module Rig Build 1

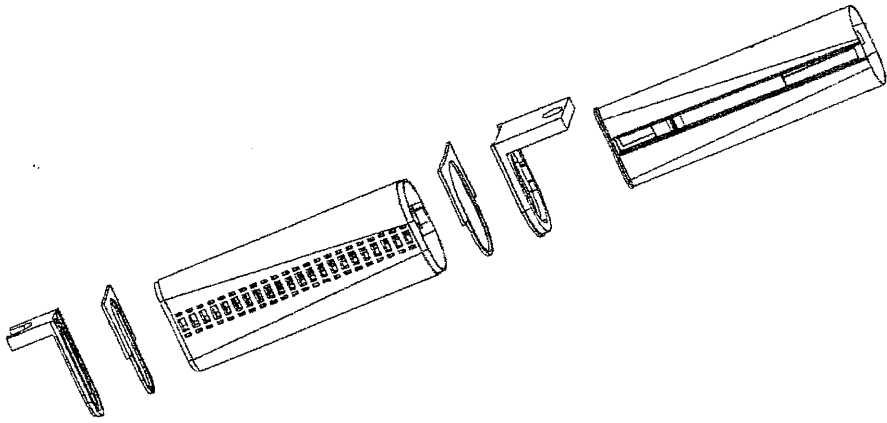


Figure IV - 40 Quench Vane Assembly for Product Module Rig Build 1

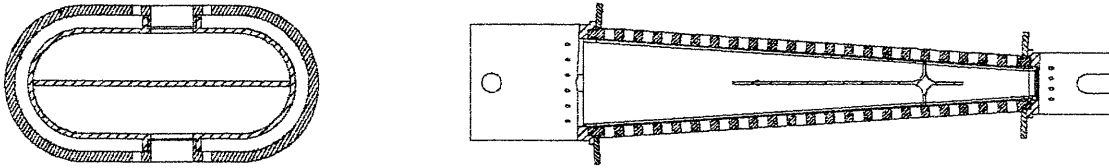


Figure IV - 41 Product Module Rig Build 1 Quench Vane FlowPath Views

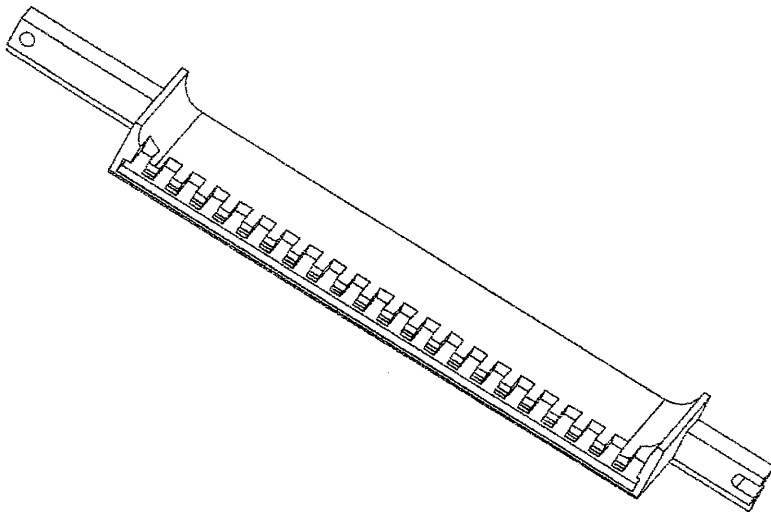


Figure IV - 42 Product Module Rig Build 1 Turning Strip. Forward-Looking-Aft Trimetric View.

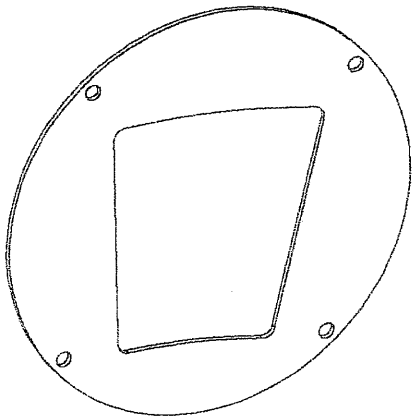
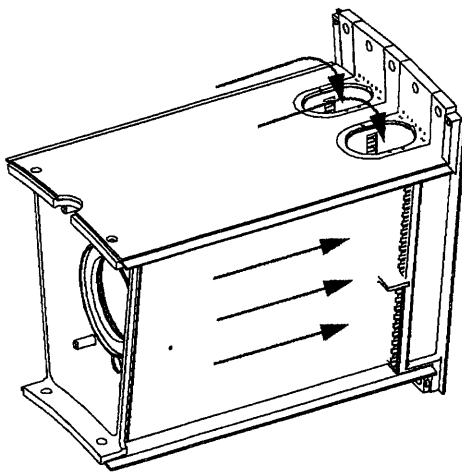
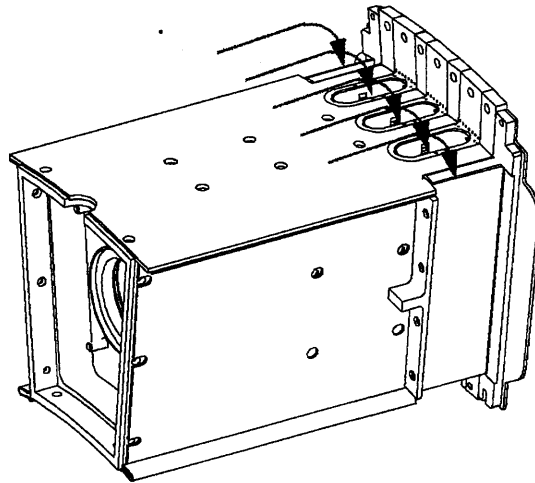


Figure IV - 43 Aft Trap Plate for Product Module Rig Build 1



**Build 1**

- Air convectively cools liner side walls and is then turned into the combustor at the quench plane
- Liner ID & OD surfaces are impingement cooled



**Build 2**

- Sidewall vanes are fed from ID & OD shrouds (identical to center vanes)
- All liner surfaces are impingement cooled

Figure IV - 44 Comparison of Airflow Paths for Product Module Rig Build 1 versus 2

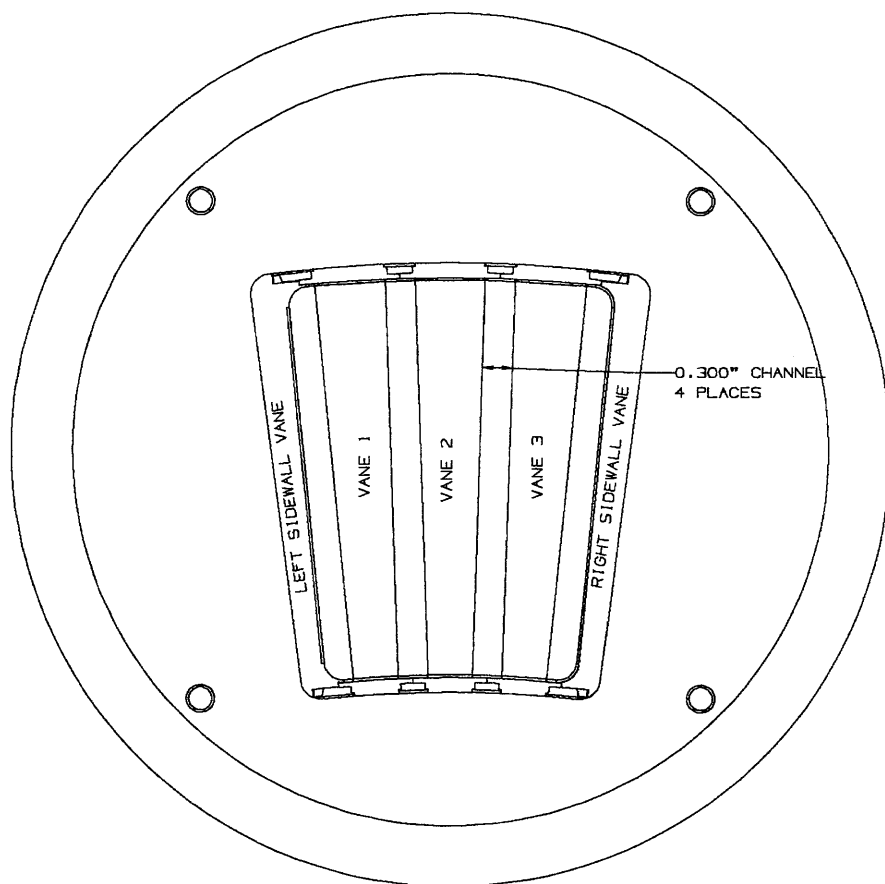


*Figure IV - 45 Aft-Looking-Forward View of Product Module Rig Build 2*

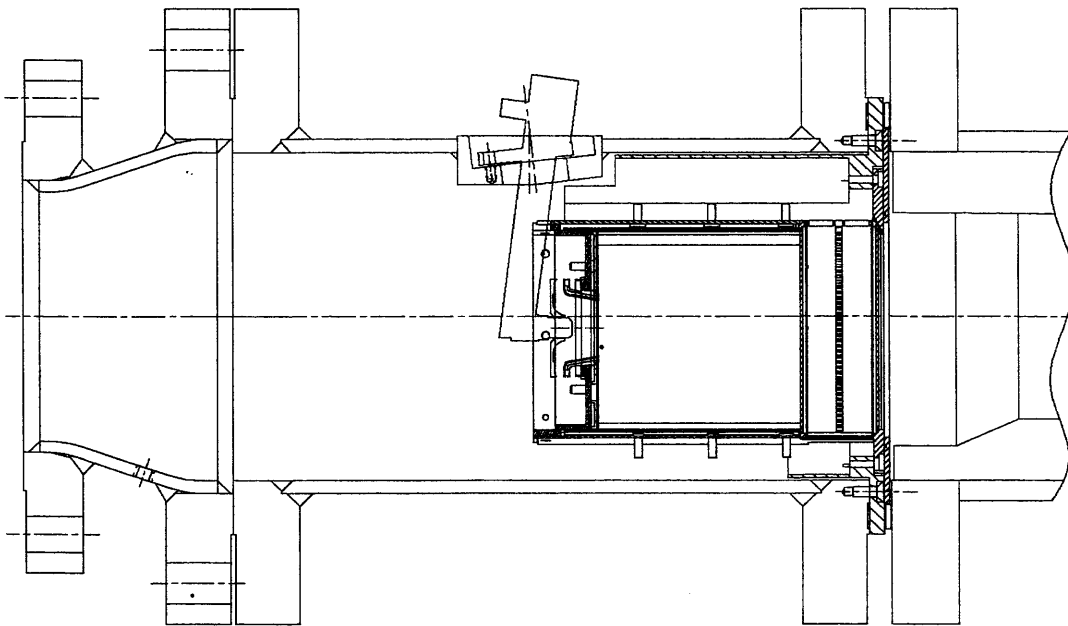


Figure IV - 46 Cross-Section of Product Module Rig Build 2

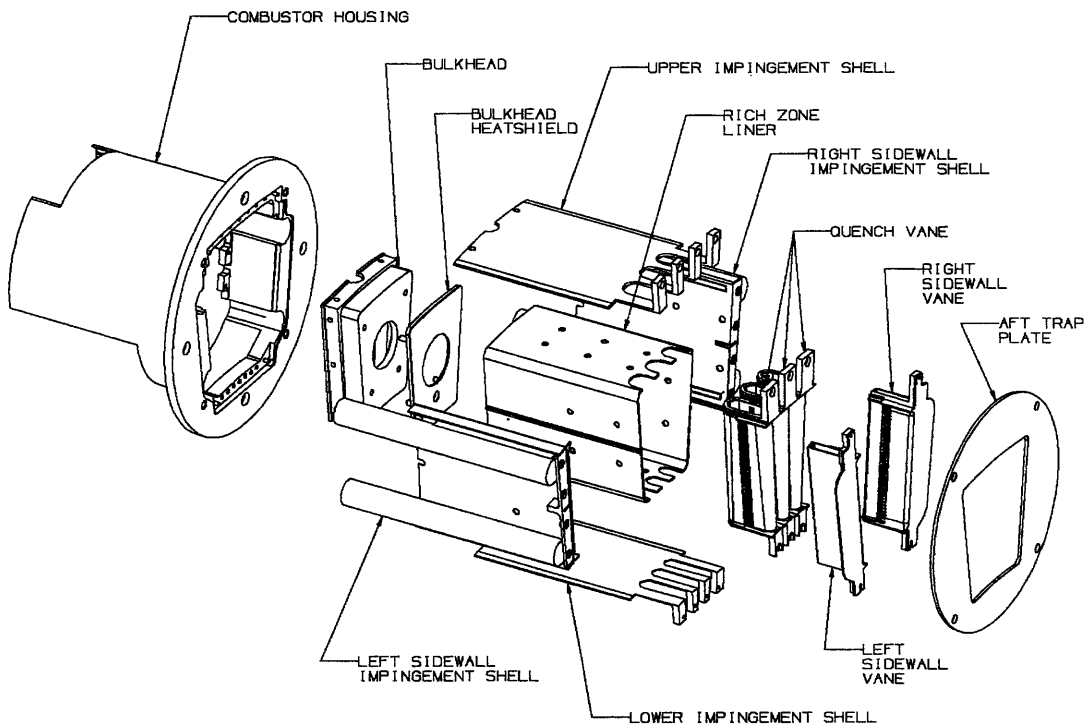


Figure IV - 47 Exploded View of Product Module Rig Build 2

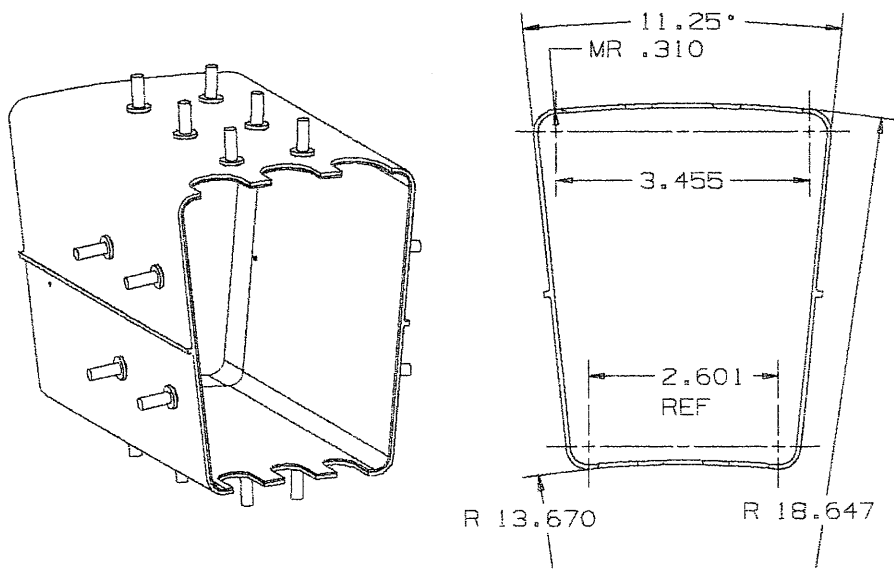


Figure IV - 48 Rich Zone Liner for Product Module Rig Build 2

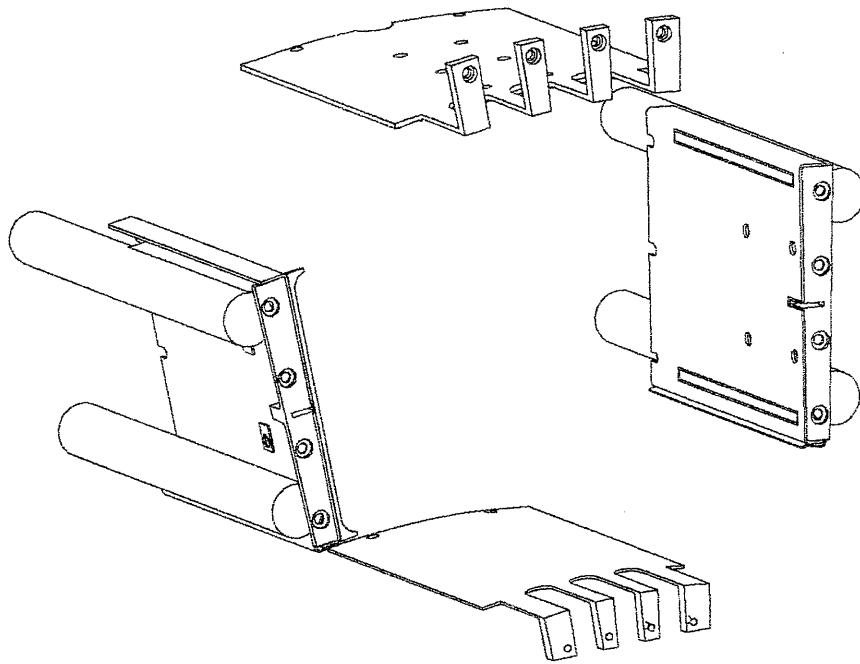
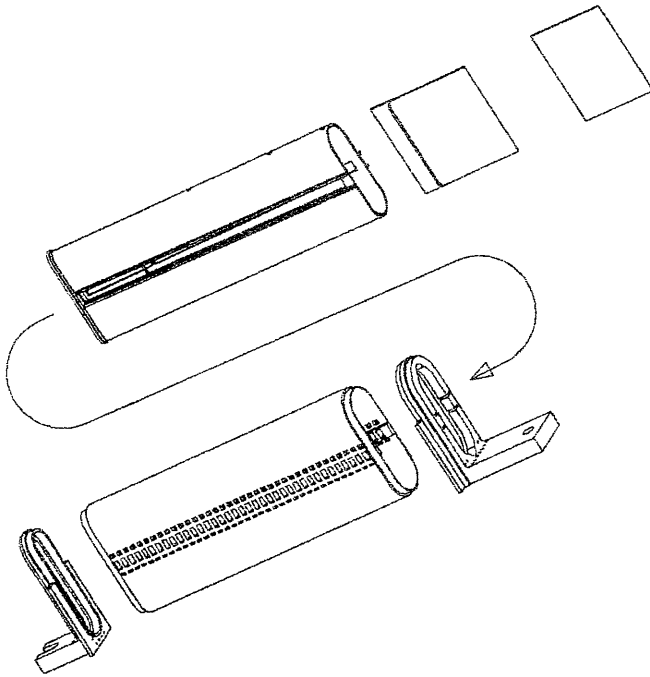
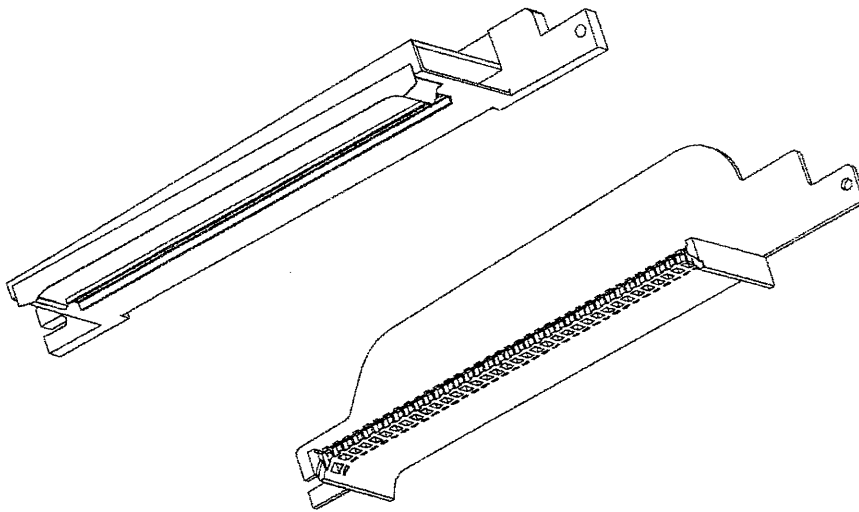


Figure IV - 49 Impingement Shells for Product Module Rig Build 2



*Figure IV - 50 Quench Vane Assembly for Product Module Rig Build 2*



*Figure IV - 51 Sidewall Vane Assembly for Product Module Rig Build 2*

# Section V Figures

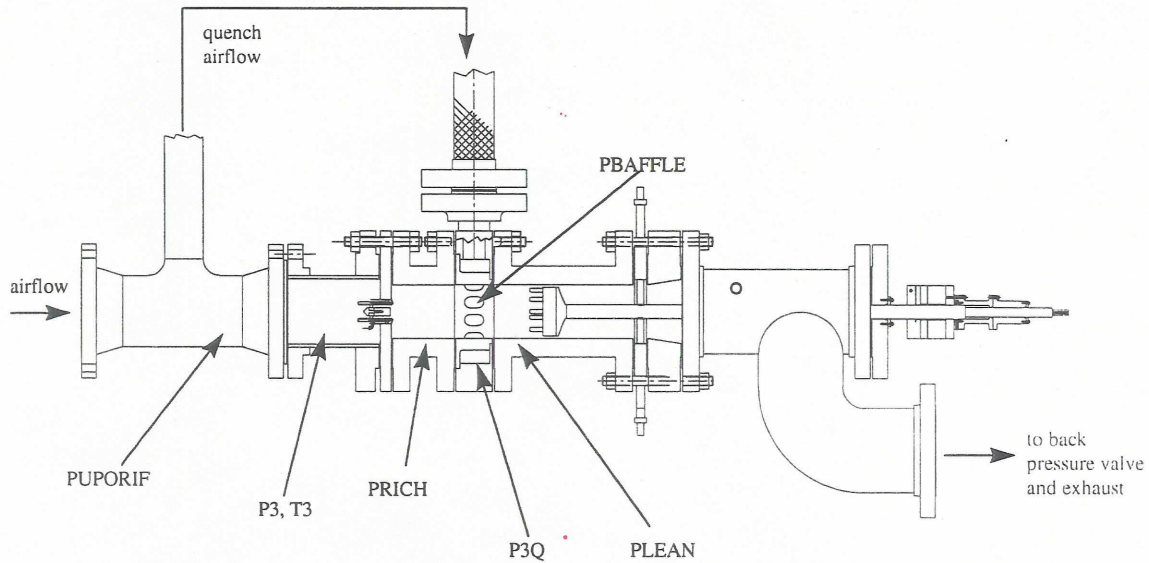


Figure V - 1 Single Module Rig Instrumentation

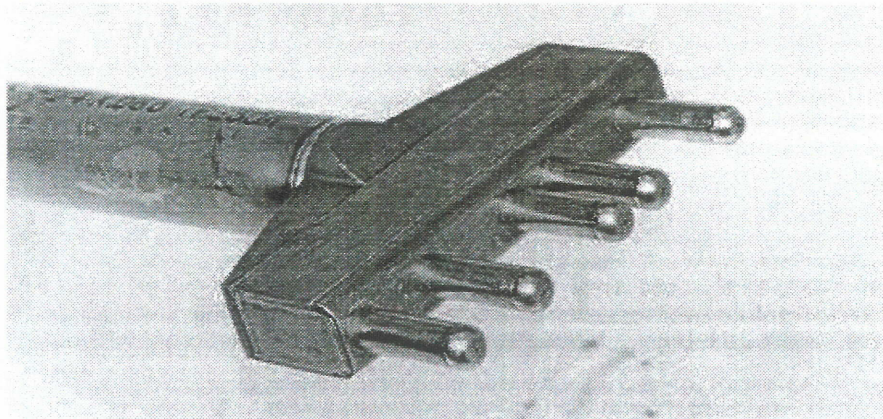
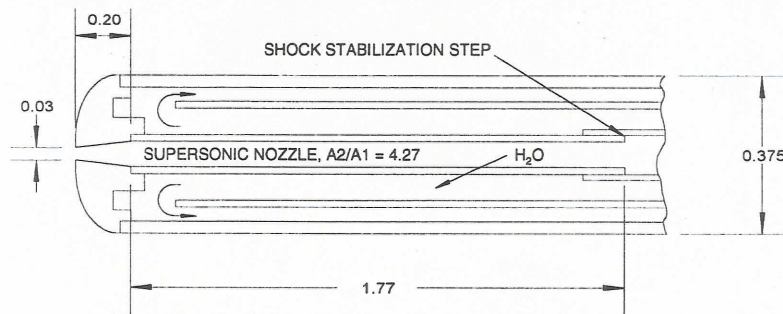


Figure V - 2 Emissions Sampling Probe System used in Single Module Rig and Product Module Rig Tests



NOTE: ALL DIMENSIONS IN INCHES

Figure V - 3 Aerodynamic Quenching Emissions Probe Tip Design

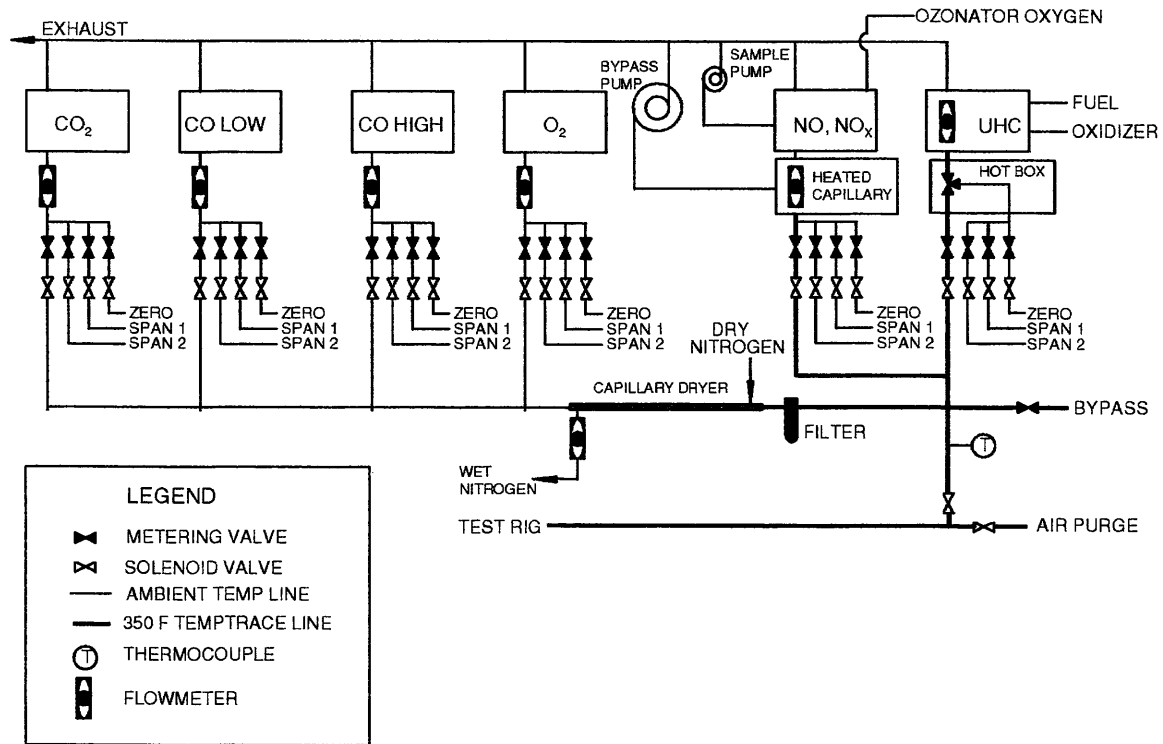
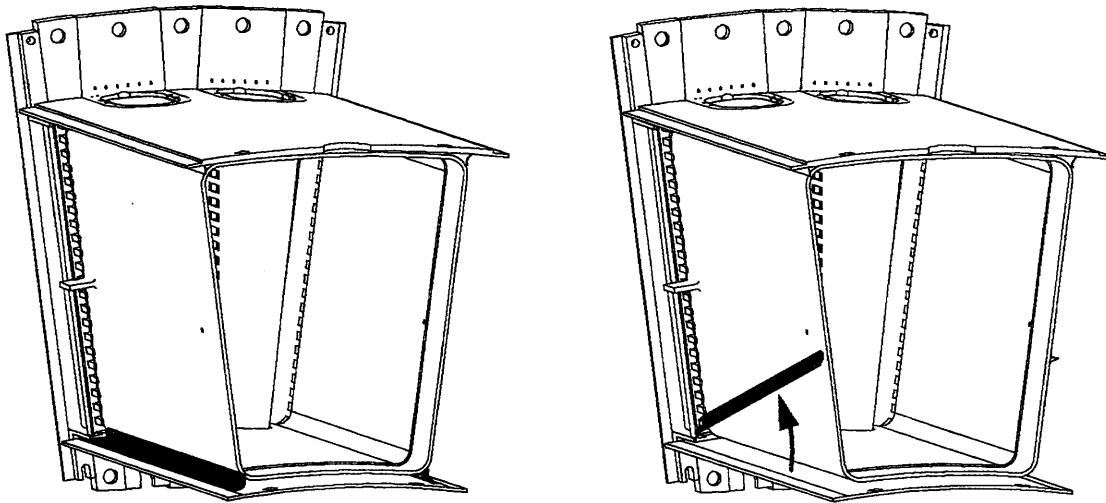


Figure V - 4 Emissions Analysis System Schematic

## Section VI Figures



Corner Dam Detached:

- Blocked sidewall convective air
- Crosstalk between convective air and spent impingement cooling air

*Figure VI - 1 Forward-Looking-Aft View of Product Module Rig Build 1 Combustor Showing Corner Dam Weld Failure and Impact*

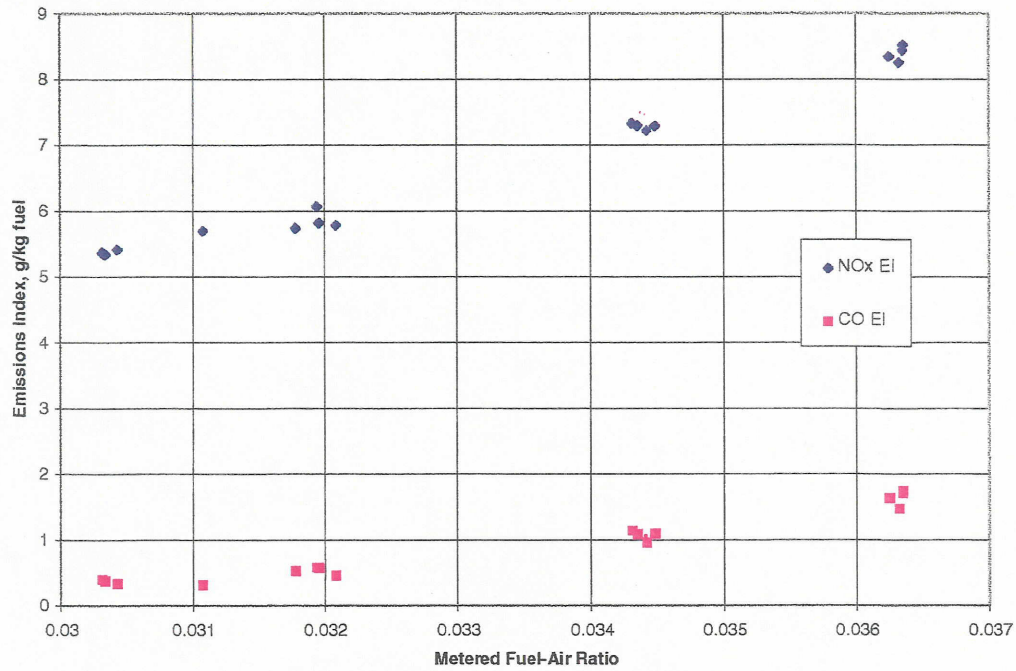


Figure VI - 2 Emissions as a Function of Fuel/Air Ratio for Vane Geometry #3

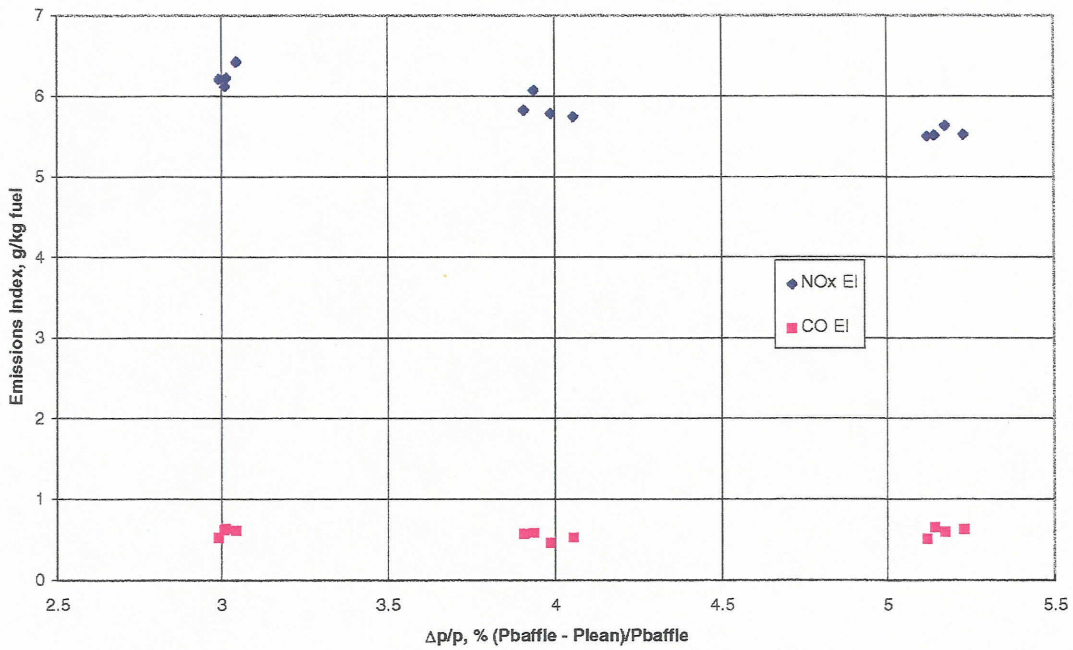


Figure VI - 3 Emissions as a Function of Pressure Drop for Vane Geometry #3

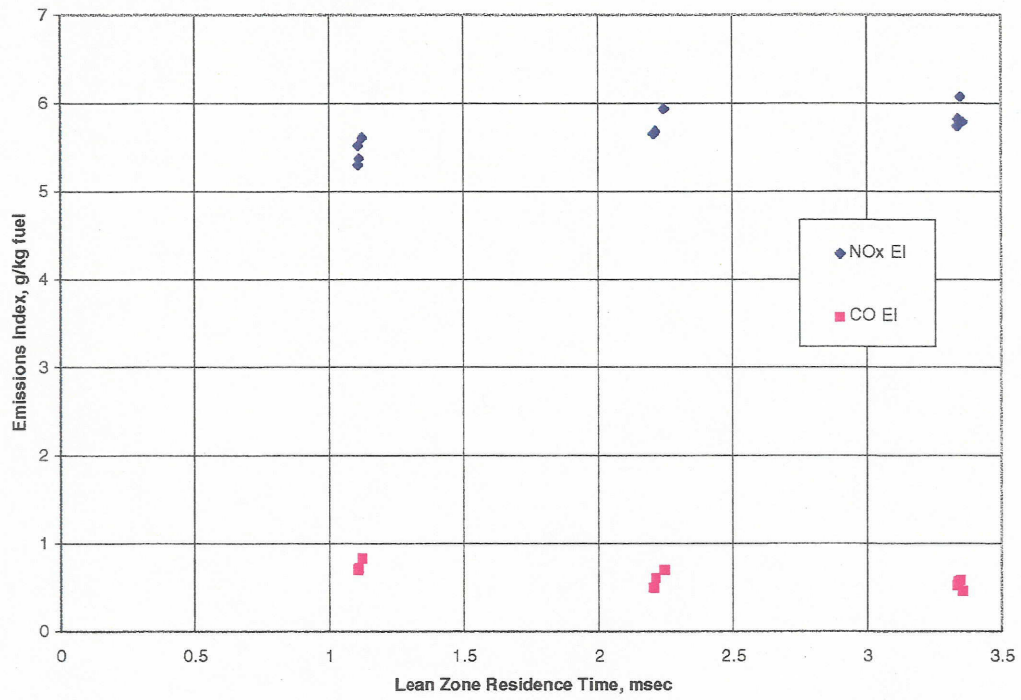


Figure VI - 4 Emissions as a Function of Lean Zone Residence Time for Vane Geometry #3

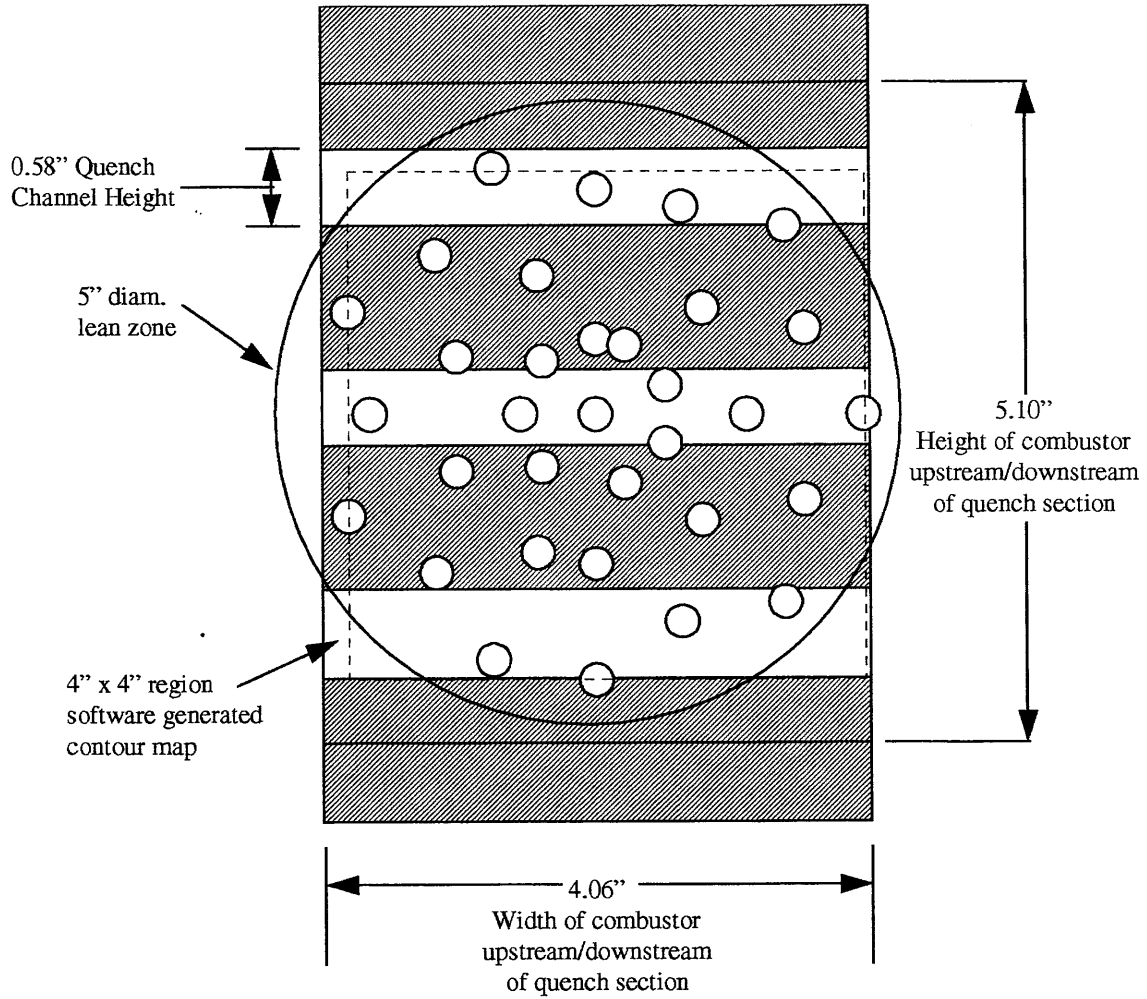


Figure VI - 5 Map of Sampling Locations for Single Module Rig Diagnostic Emissions Contours

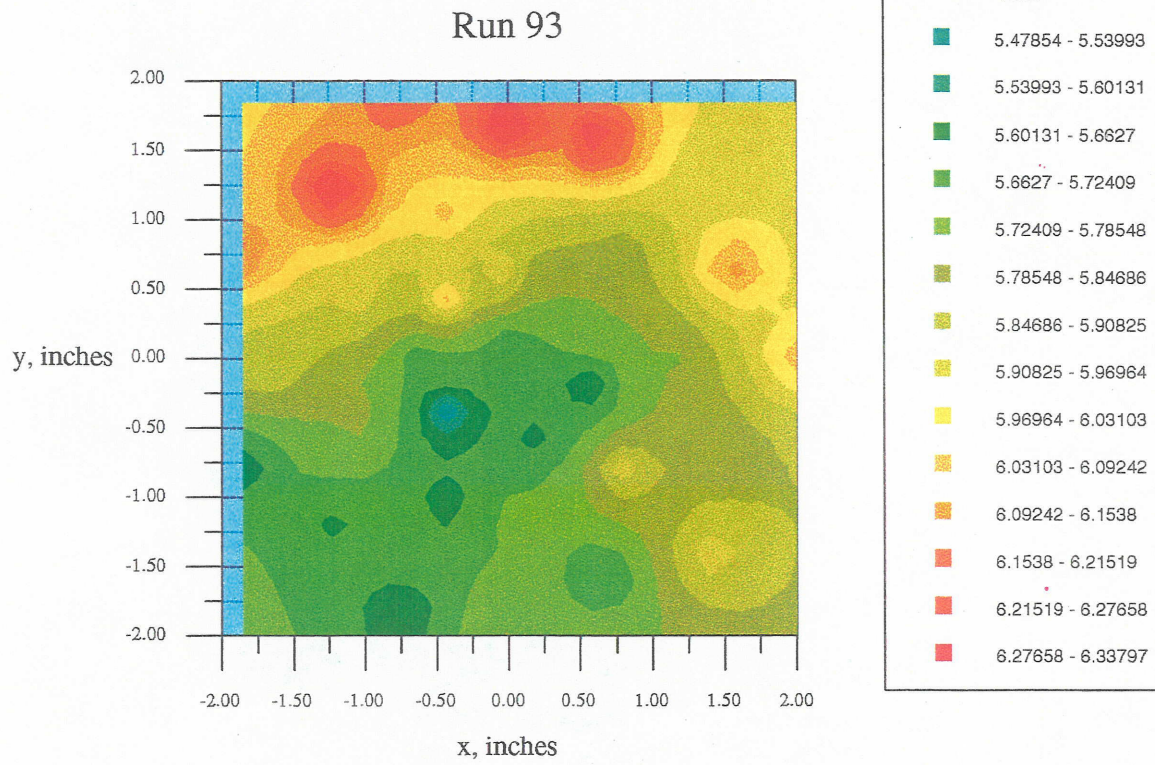


Figure VI - 6 NOx Emissions Index Contours for Vane Geometry #3

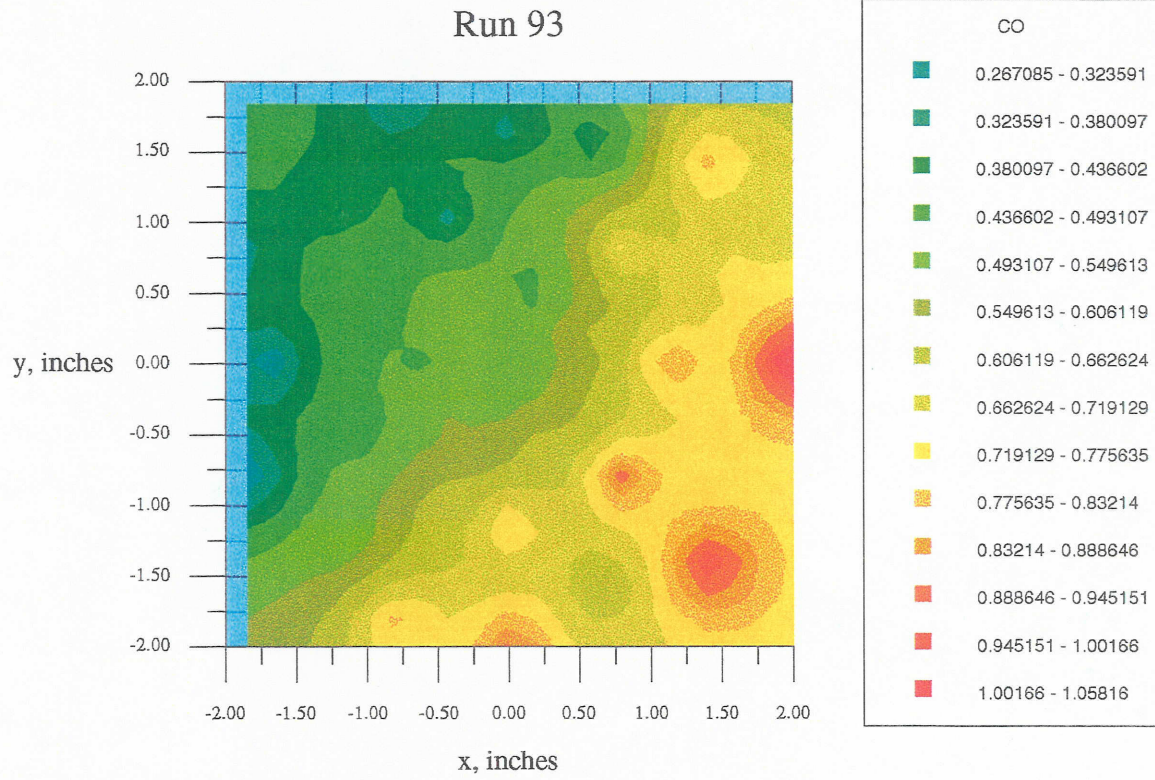


Figure VI - 7 CO Emissions Index Contours for Vane Geometry #3

# Run 93

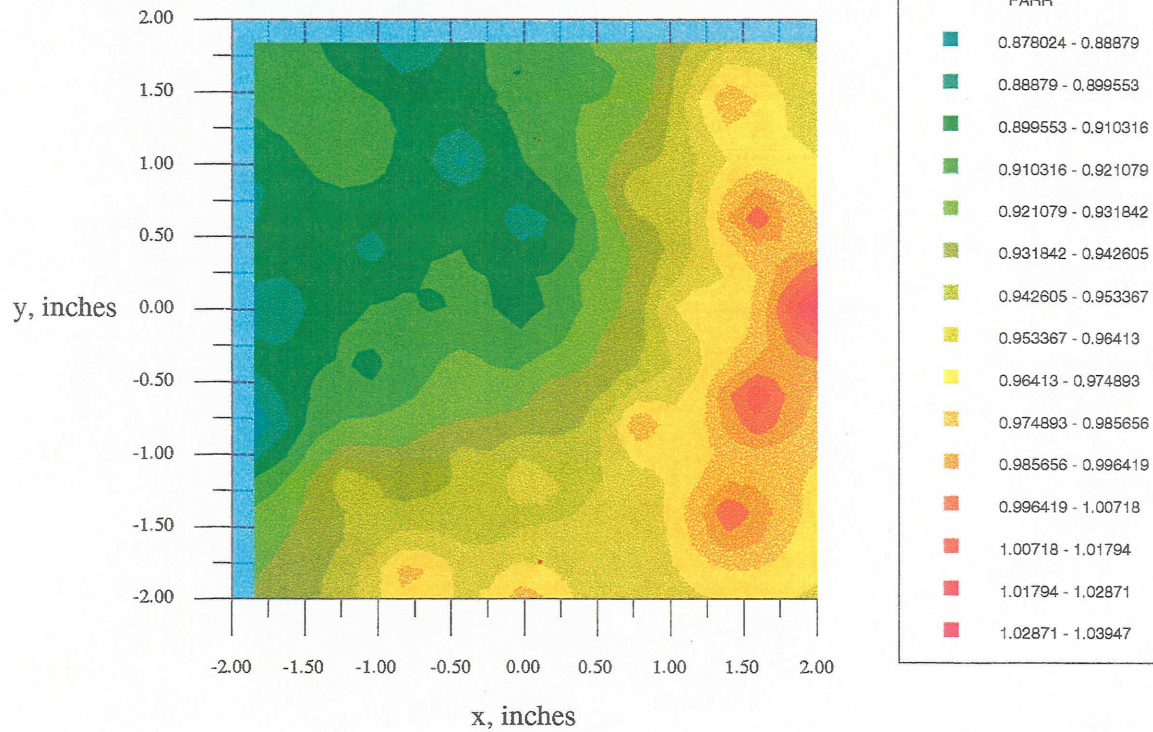


Figure VI - 8 Contours of the Ratio of Emissions-based Fuel/Air Relative to Metered Fuel/Air for Vane Geometry #3

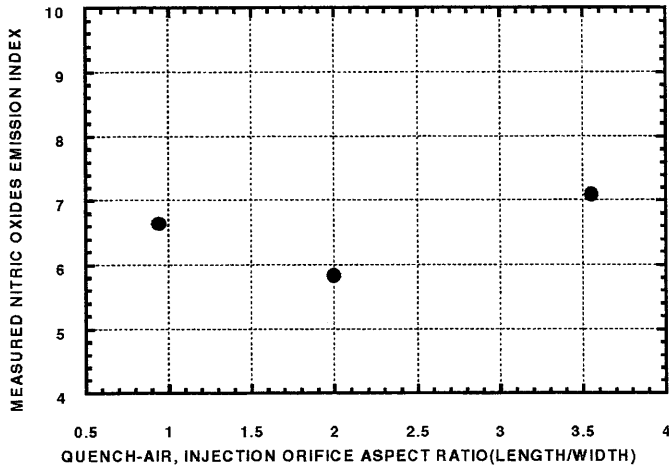


Figure VI - 9 NOx Emissions as a Function of Orifice Aspect Ratio

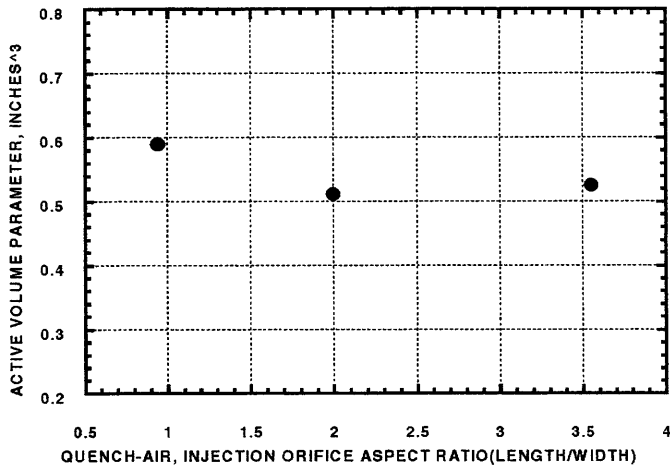


Figure VI - 10 Active Volume Parameter as a Function of Orifice Aspect Ratio

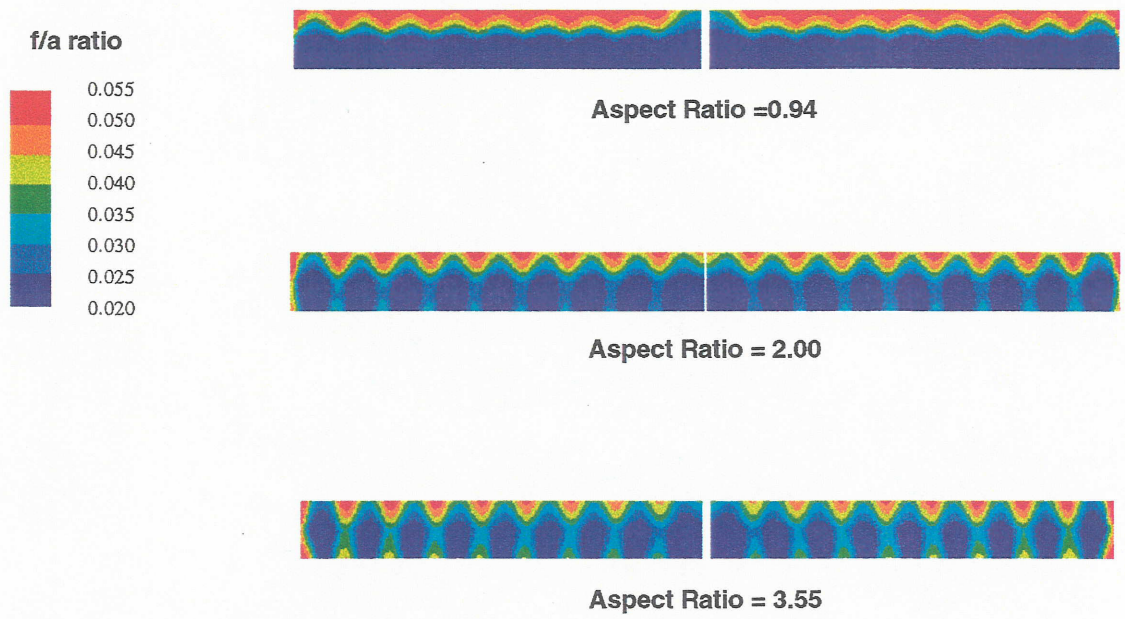


Figure VI - 11 CFD Calculated Fuel/Air Ratio Contours as a Function of Orifice Aspect Ratio

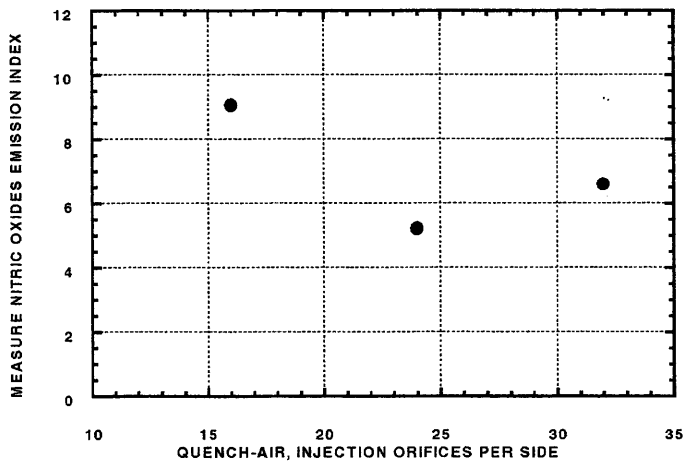


Figure VI - 12 NO<sub>x</sub> Emissions as a Function of Orifice Spacing

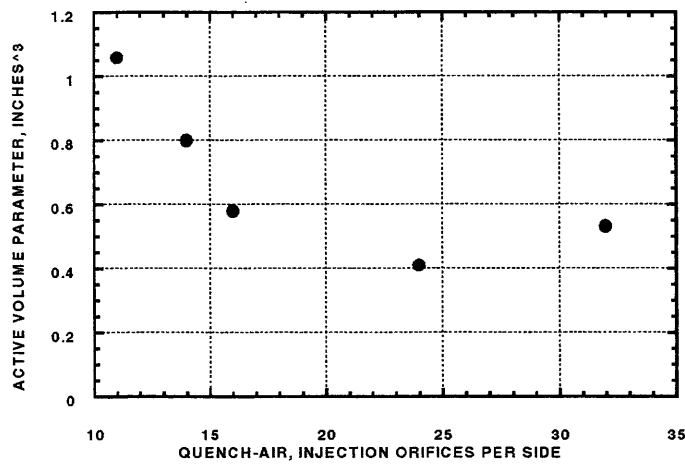


Figure VI - 13 Active Volume Parameter as a Function of Orifice Spacing

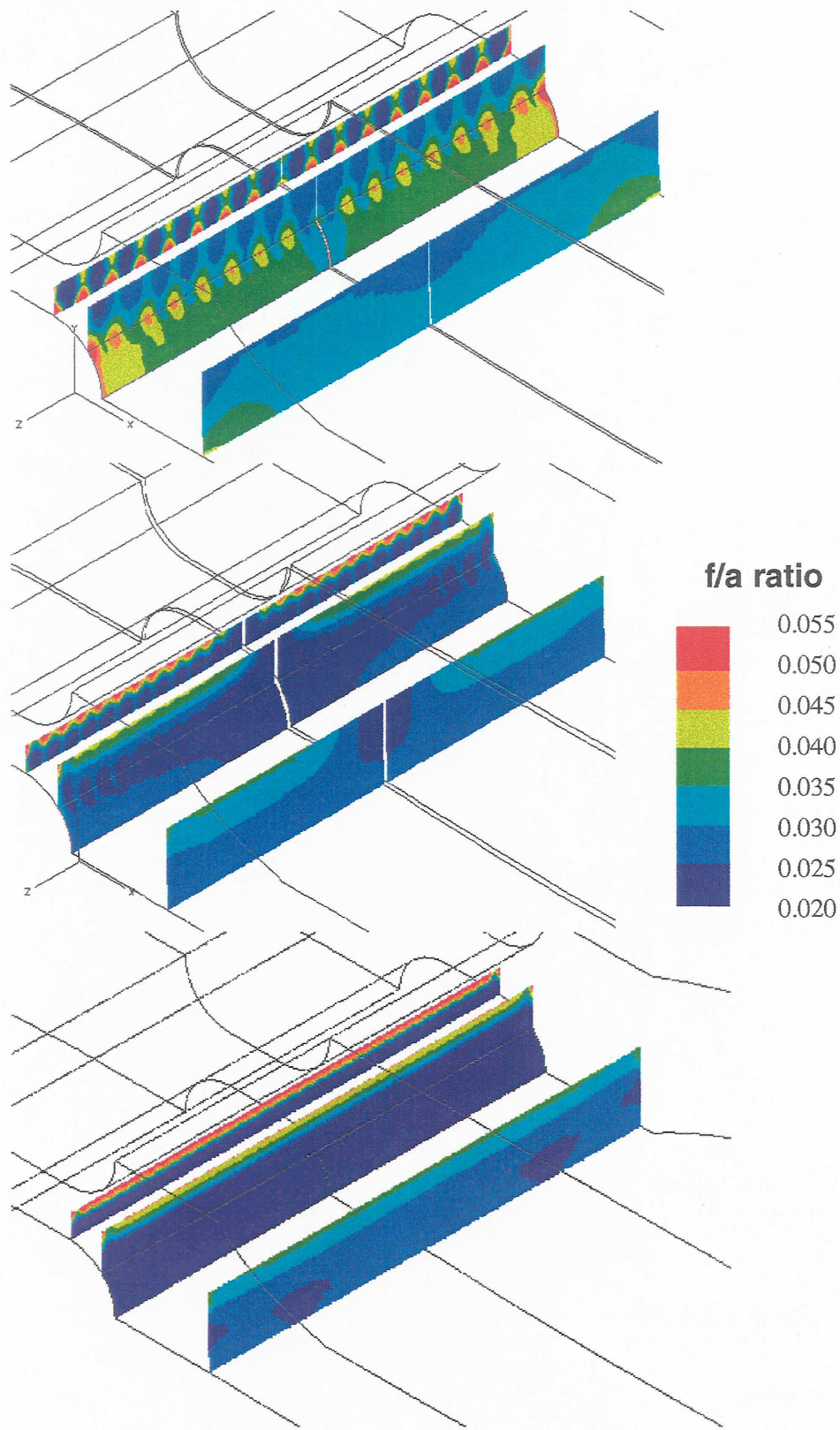


Figure VI - 14 CFD Calculated Contours of Fuel/Air Ratio as a Function of Orifice Spacing (Top: 16 Orifices per Side; Middle: 24 Orifices per Side; Bottom: 32 Orifices per Side)

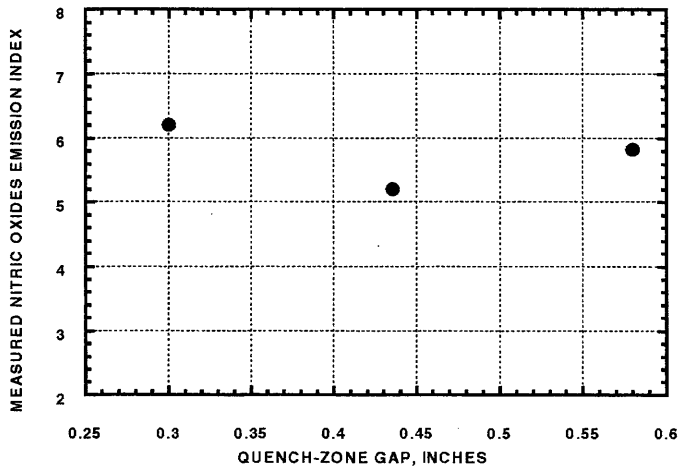


Figure VI - 15 NO<sub>x</sub> Emissions as a Function of Quench Zone Channel Height

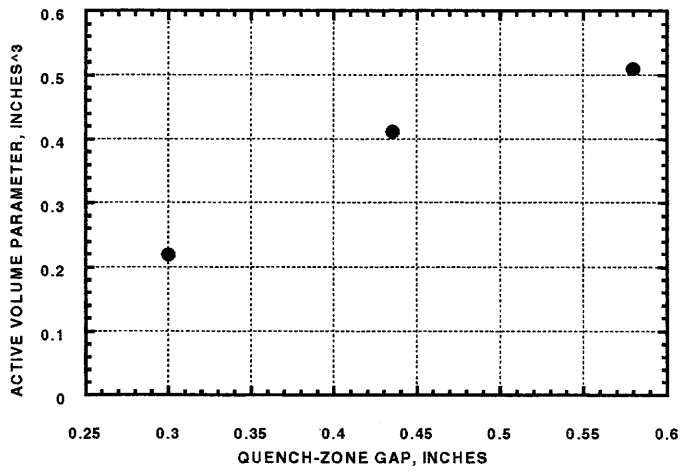


Figure VI - 16 Active Volume Parameter as a Function of Quench Zone Channel Height

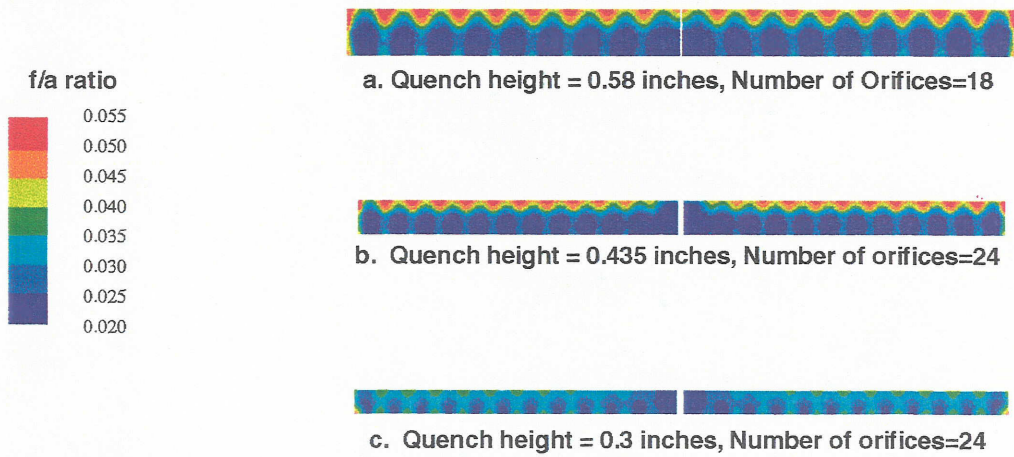


Figure VI - 17 CFD Calculated Fuel/Air Ratio Contours as a Function of Quench Zone Channel Height

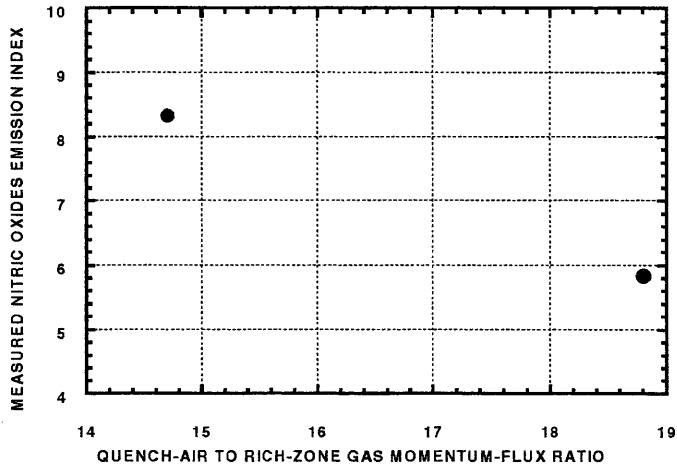


Figure VI - 18 NO<sub>x</sub> Emissions as a Function of Momentum Flux Ratio

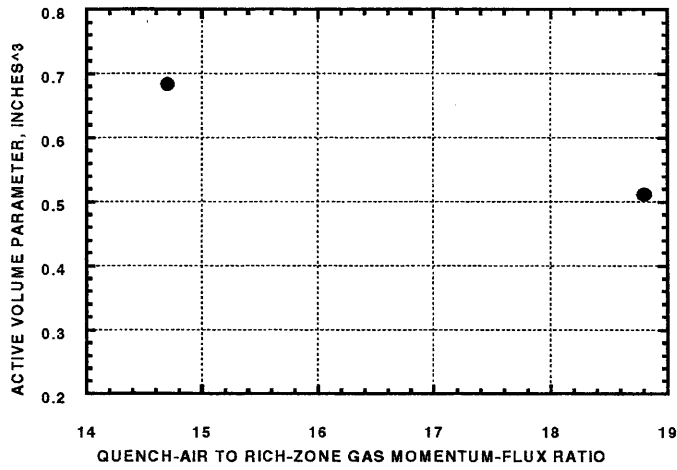
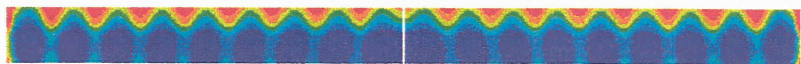
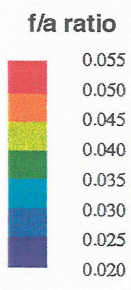


Figure VI - 19 Active Volume Parameter as a Function of Momentum Flux Ratio



**a. Momentum flux ratio = 15.5**



**b. Momentum flux ratio = 8**

*Figure VI - 20 CFD Calculated Fuel/Air Ratio Contours as a Function of Momentum Flux Ratio*

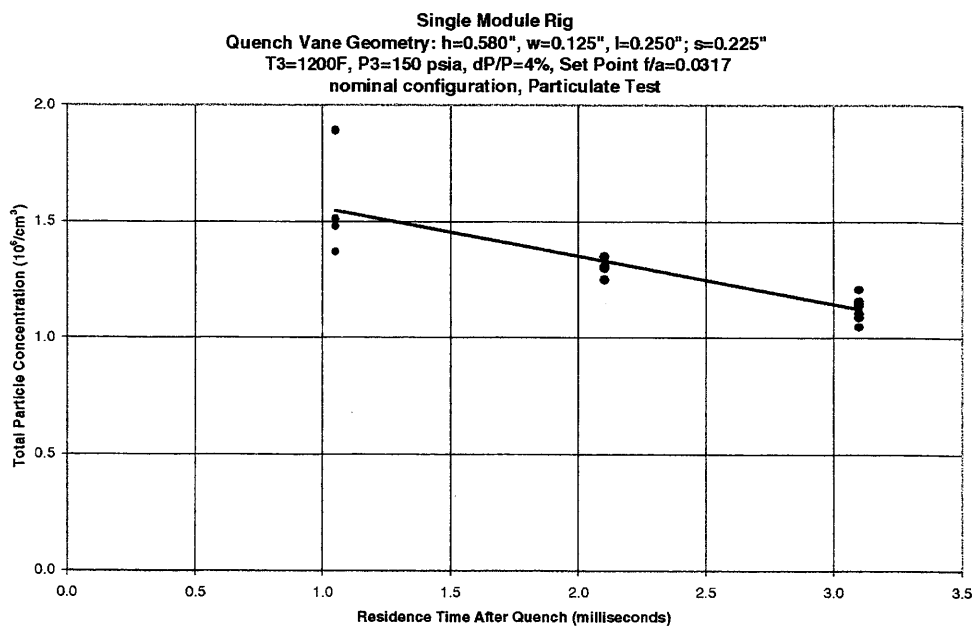


Figure VI - 21 Particle Concentration Measurements at Nominal Supersonic Cruise Condition for Vane Geometry #3 as a Function of Residence Time after Quench

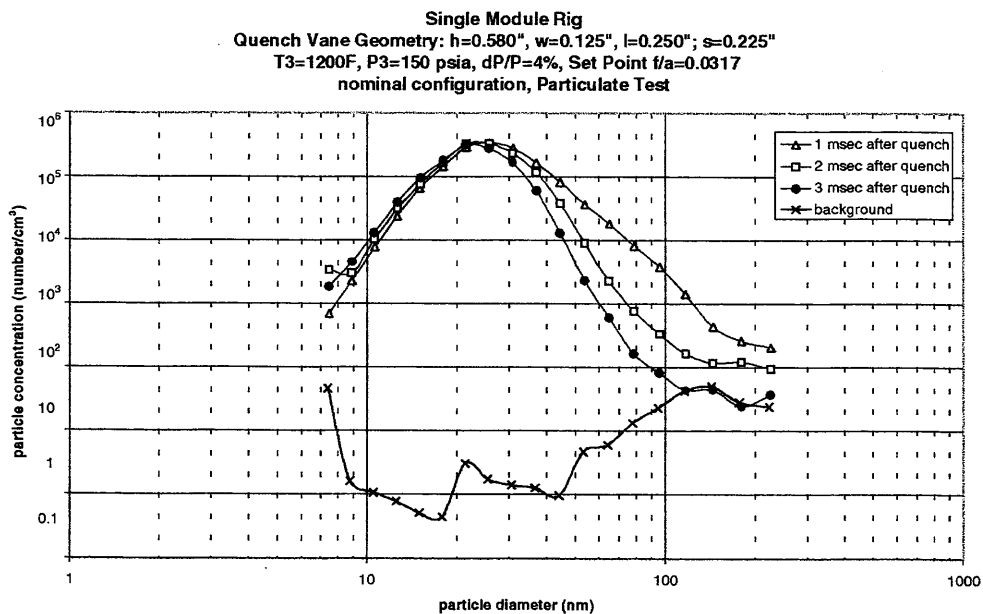
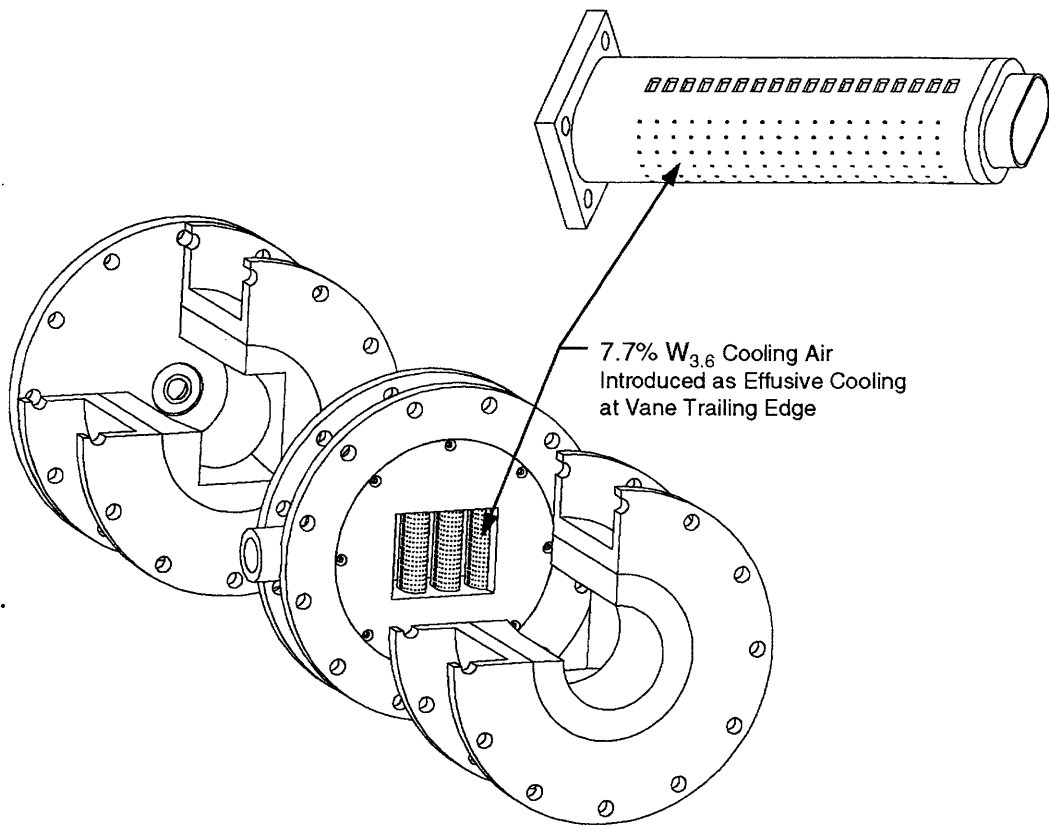


Figure VI - 22 Particle Concentration Distributions at Nominal Supersonic Cruise Condition for Vane Geometry #3 as a Function of Residence Time after Quench



*Figure VI - 23 Effect of Cooling Air Assessed in Single Module Rig with Effusively Cooled Single Direction Feed Vane*

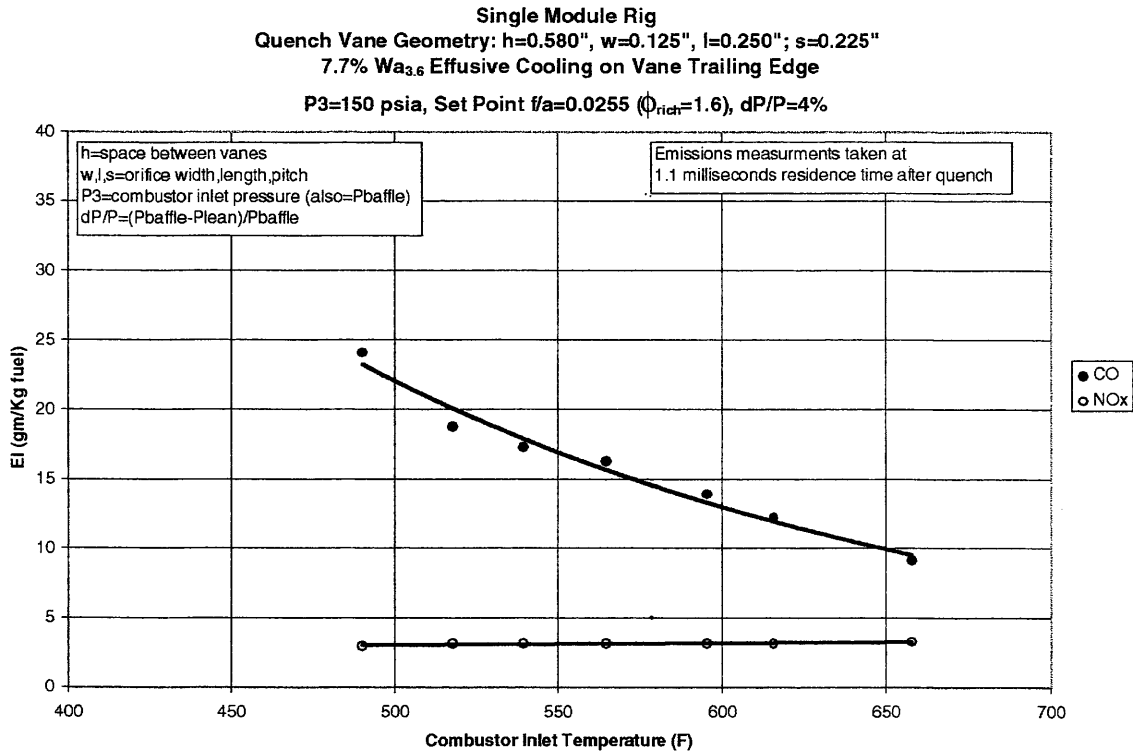


Figure VI - 24 Emissions as a Function of Combustor Inlet Temperature for Assessment of Cooling Air Impact

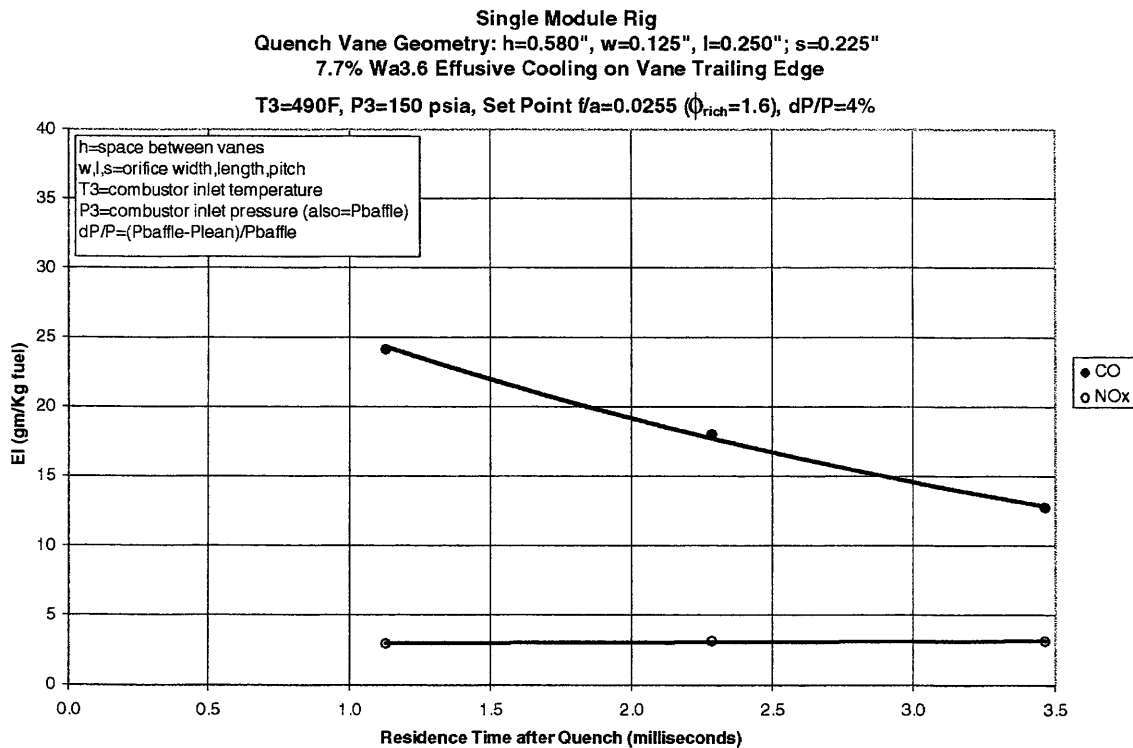


Figure VI - 25 Emissions as a Function of Residence Time for Assessment of Cooling Air Impact

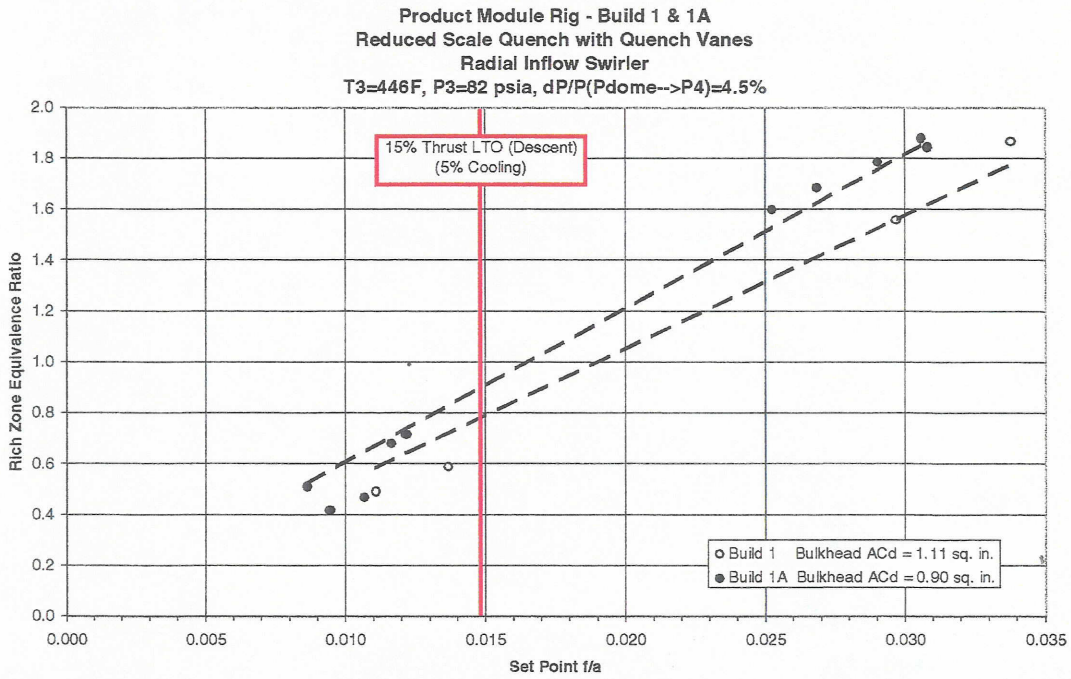


Figure VI - 26 Rich Zone Stoichiometry Comparison at 15% Thrust LTO (Descent) Condition for Product Module Rig Builds 1 & 1A

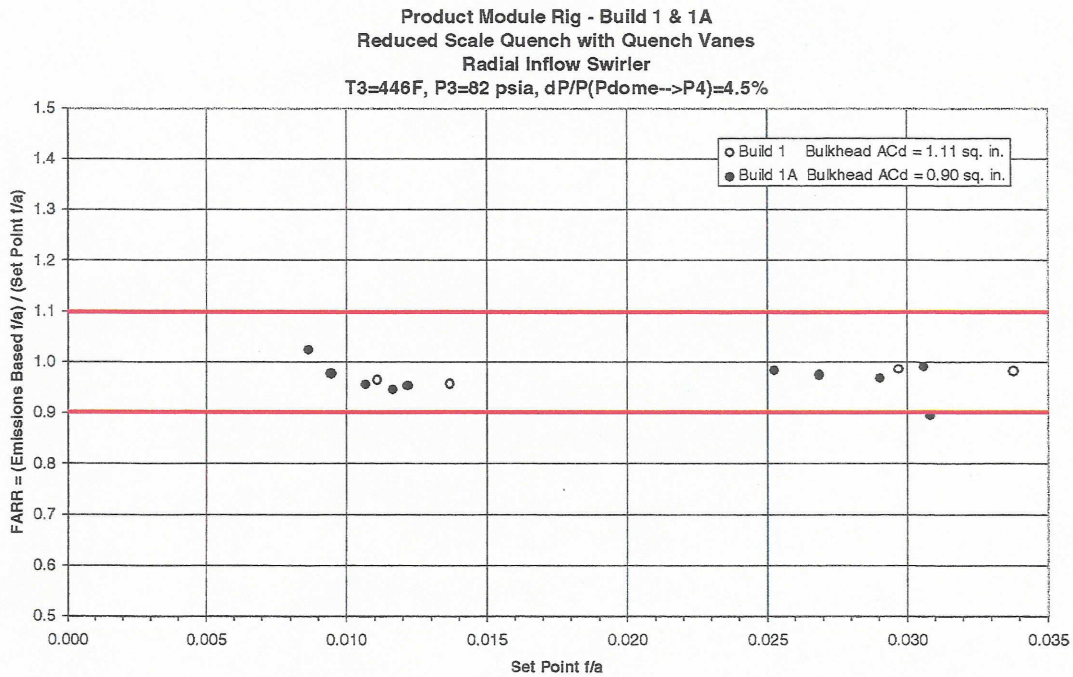


Figure VI - 27 Emissions Data Quality at 15% Thrust LTO (Descent) Condition for Product Module Rig Builds 1 & 1A

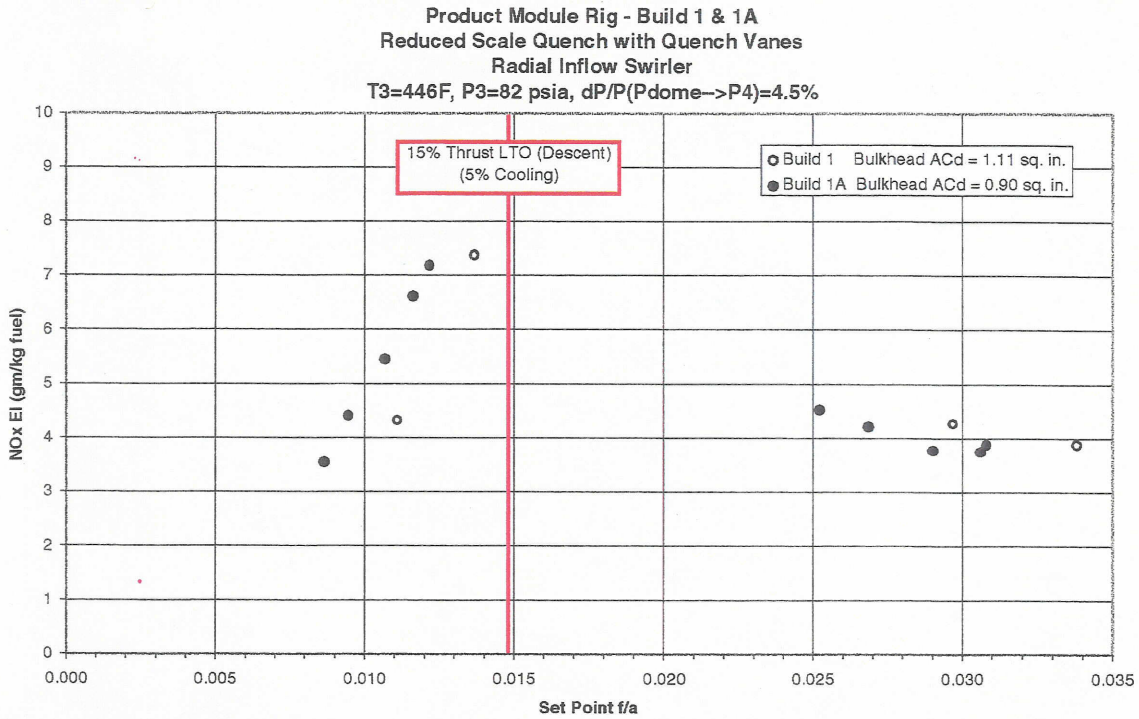


Figure VI - 28 NO<sub>x</sub> Emissions at 15% Thrust LTO (Descent) Condition for Product Module Rig Builds 1 & 1A

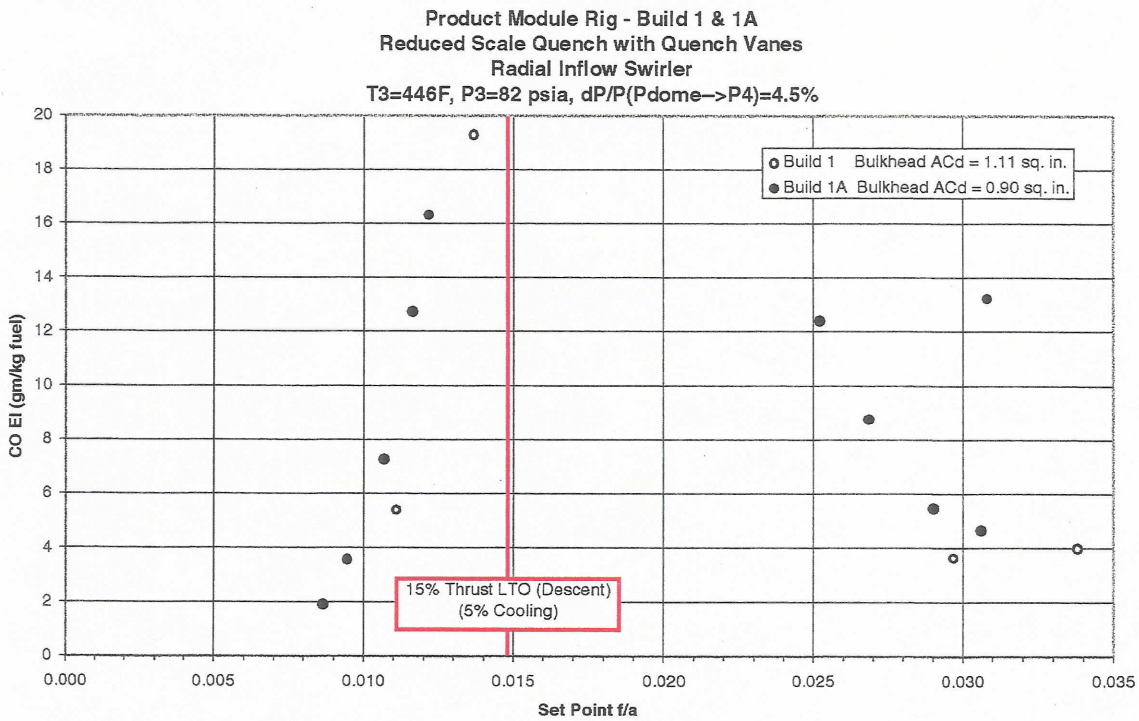


Figure VI - 29 CO Emissions at 15% Thrust LTO (Descent) Condition for Product Module Rig Builds 1 & 1A

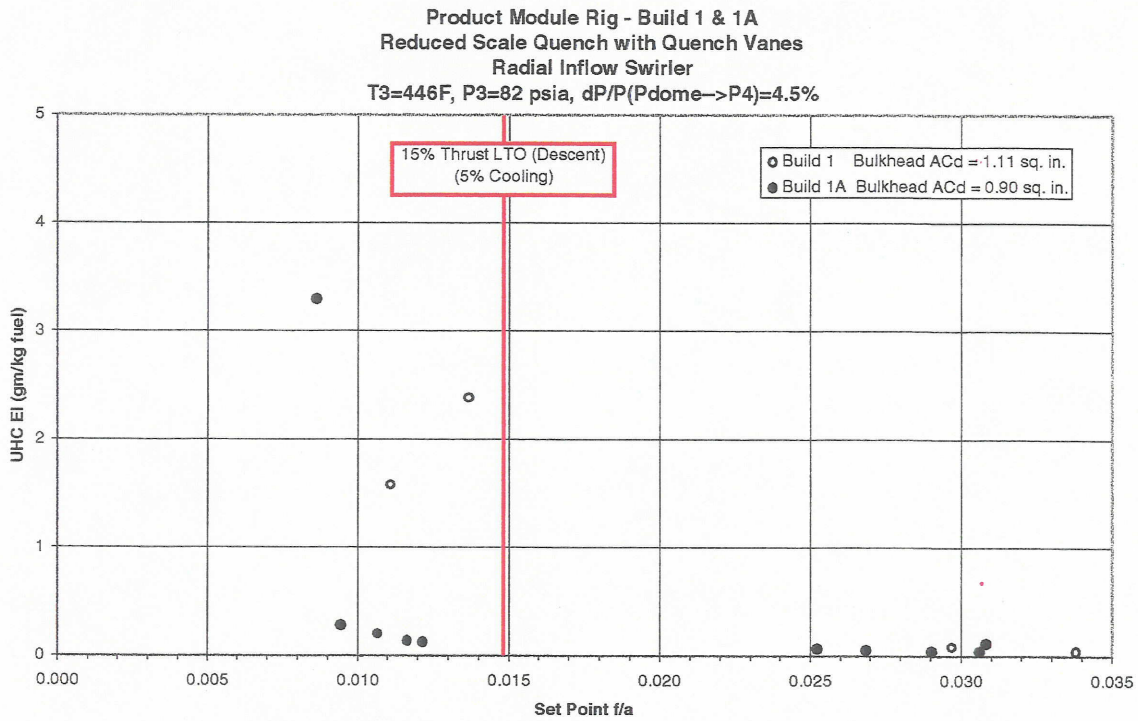


Figure VI - 30 UHC Emissions at 15% Thrust LTO (Descent) Condition for Product Module Rig Builds 1 & 1A

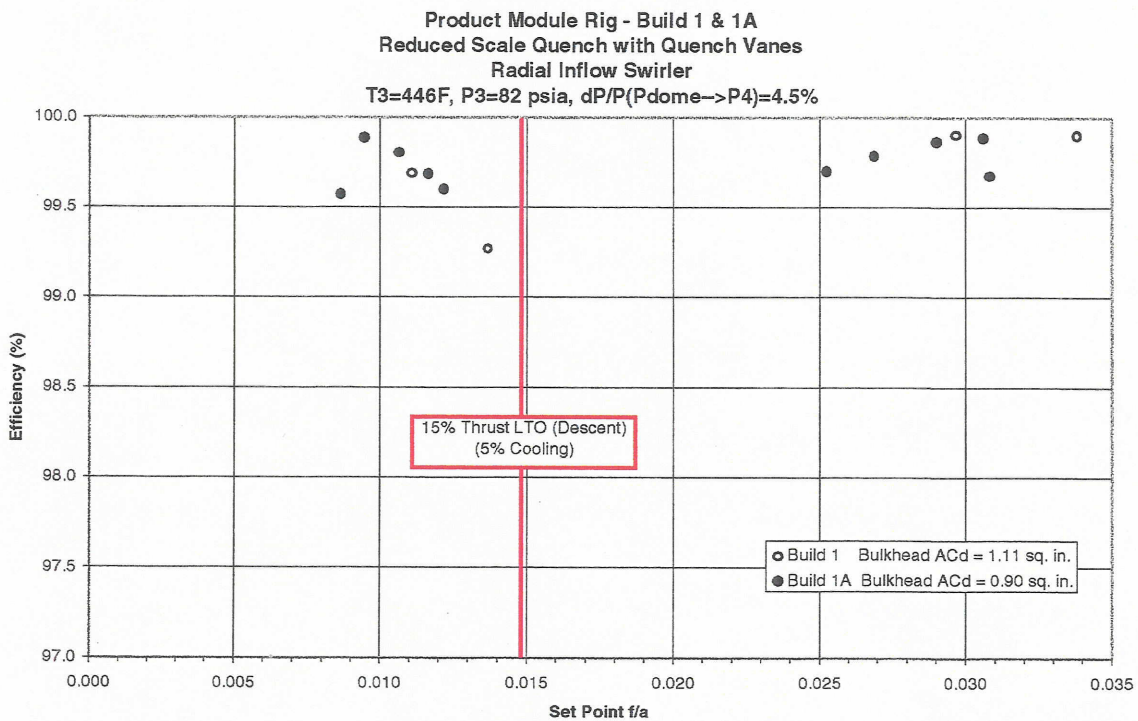


Figure VI - 31 Efficiency at 15% Thrust LTO (Descent) Condition for Product Module Rig Builds 1 & 1A

Product Module Rig - Build 2  
 Reduced Scale Quench with Quench Vanes  
 Radial Inflow Swirler  
 T3=295F, P3=45 psia, dP/P(Pdome→P4)=4.5%

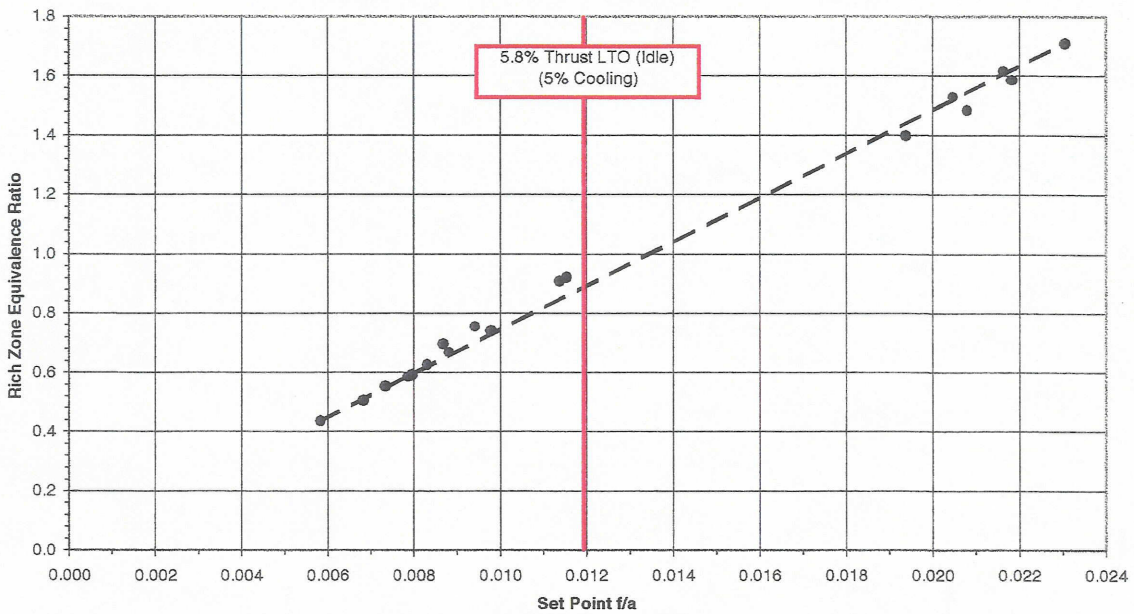


Figure VI - 32 Rich Zone Stoichiometry at 5.8% Thrust LTO (Idle) Condition for Product Module Rig Build 2

Product Module Rig - Build 2  
 Reduced Scale Quench with Quench Vanes  
 Radial Inflow Swirler  
 T3=295F, P3=45 psia, dP/P(Pdome→P4)=4.5%

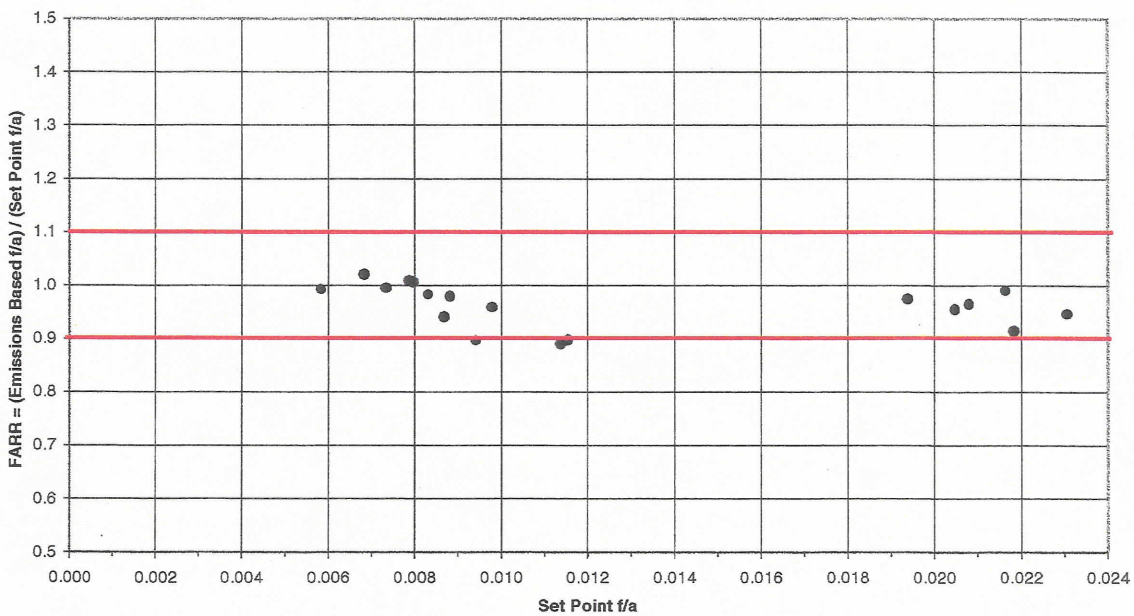


Figure VI - 33 Emissions Data Quality at 5.8% Thrust LTO (Idle) Condition for Product Module Rig Build 2

Product Module Rig - Build 2  
 Reduced Scale Quench with Quench Vanes  
 Radial Inflow Swirler  
 T3=295F, P3=45 psia, dP/P(Pdome→P4)=4.5%

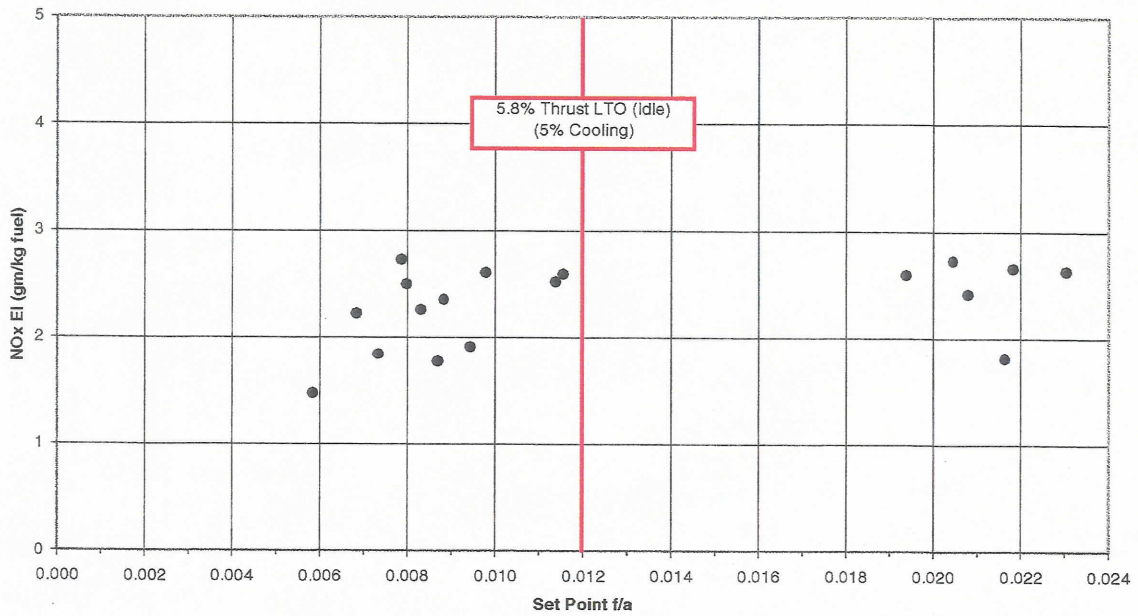


Figure VI - 34 NO<sub>x</sub> Emissions at 5.8% Thrust LTO (Idle) Condition for Product Module Rig Build 2

Product Module Rig - Build 2  
 Reduced Scale Quench with Quench Vanes  
 Radial Inflow Swirler  
 T3=295F, P3=45 psia, dP/P(Pdome→P4)=4.5%

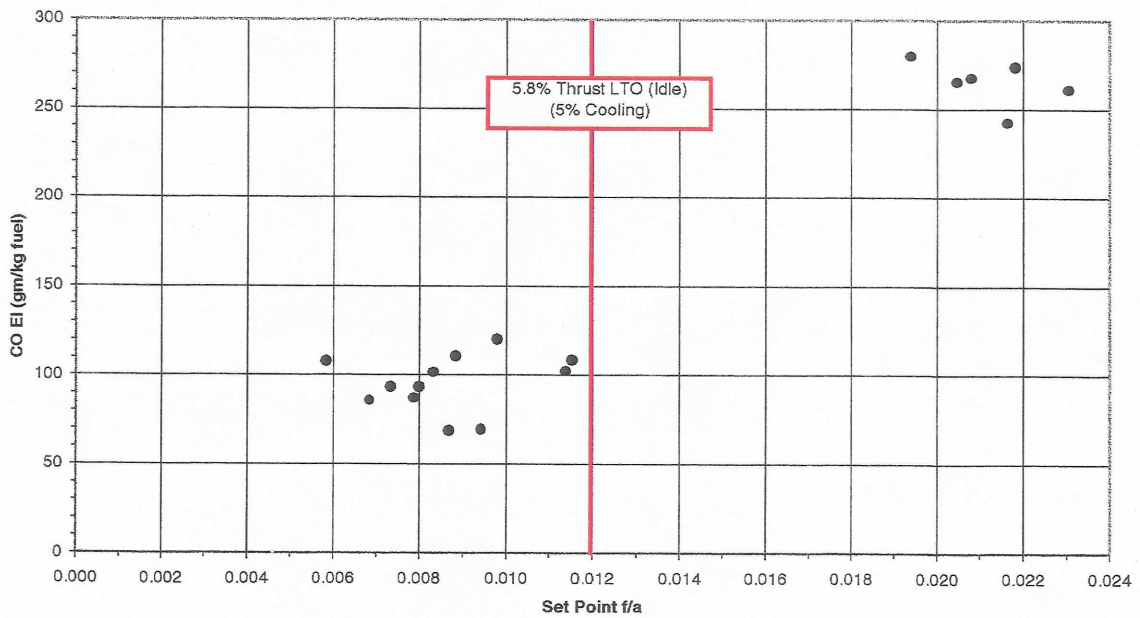


Figure VI - 35 CO Emissions at 5.8% Thrust LTO (Idle) Condition for Product Module Rig Build 2

Product Module Rig - Build 2  
 Reduced Scale Quench with Quench Vanes  
 Radial Inflow Swirler  
 T3=295F, P3=45 psia, dP/P(Pdome->P4)=4.5%

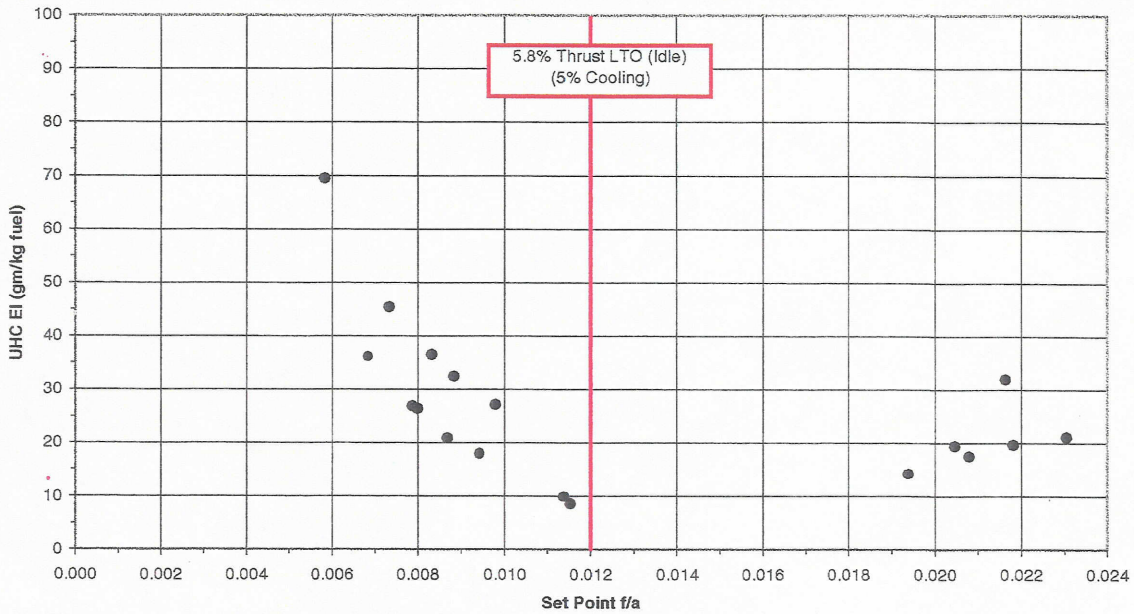


Figure VI - 36 UHC Emissions at 5.8% Thrust LTO (Idle) Condition for Product Module Rig Build 2

Product Module Rig - Build 2  
 Reduced Scale Quench with Quench Vanes  
 Radial Inflow Swirler  
 T3=295F, P3=45 psia, dP/P(Pdome->P4)=4.5%

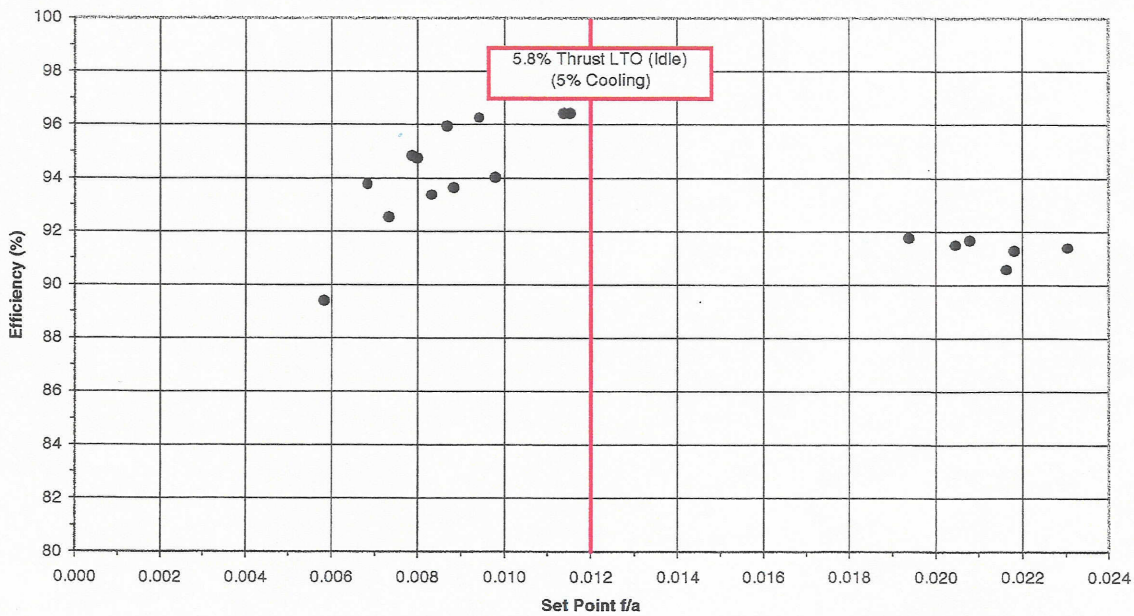


Figure VI - 37 Efficiency at 5.8% Thrust LTO (Idle) Condition for Product Module Rig Build 2

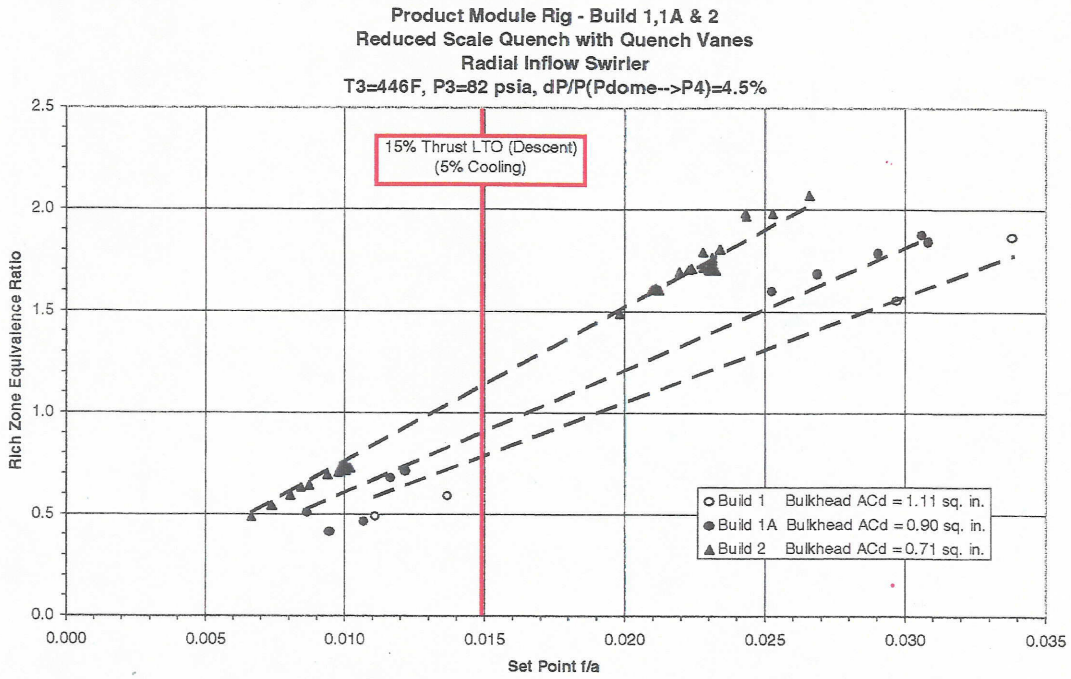


Figure VI - 38 Rich Zone Stoichiometry Comparison at 15% Thrust LTO (Descent) Condition for Product Module Rig Builds 1, 1A & 2

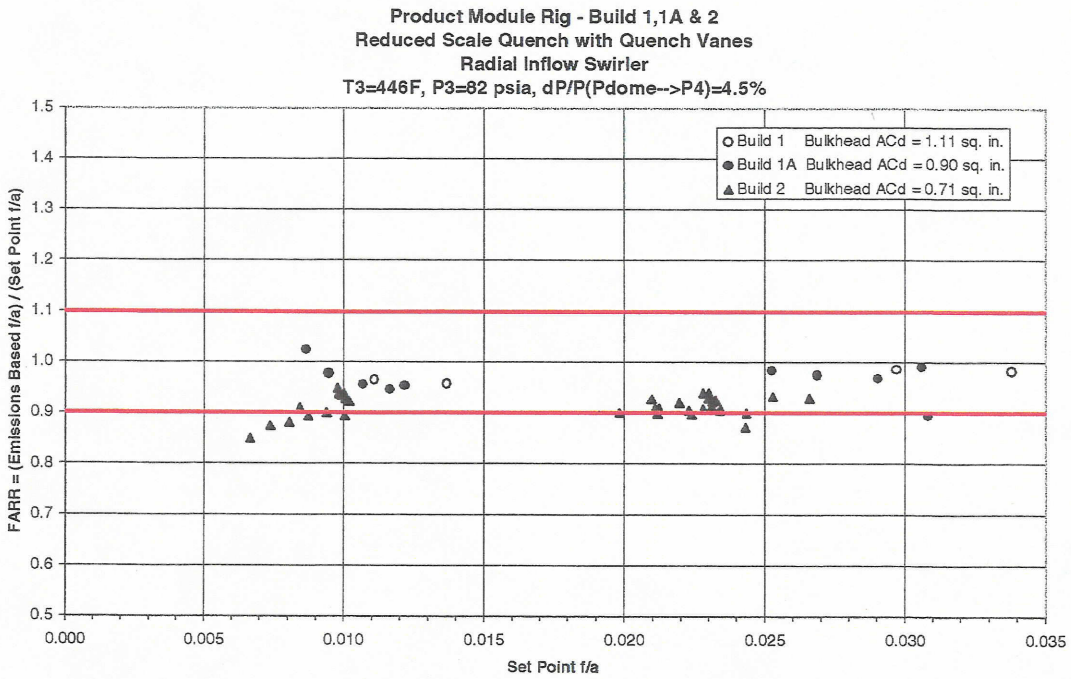


Figure VI - 39 Emissions Data Quality at 15% Thrust LTO (Descent) Condition for Product Module Rig Builds 1, 1A & 2

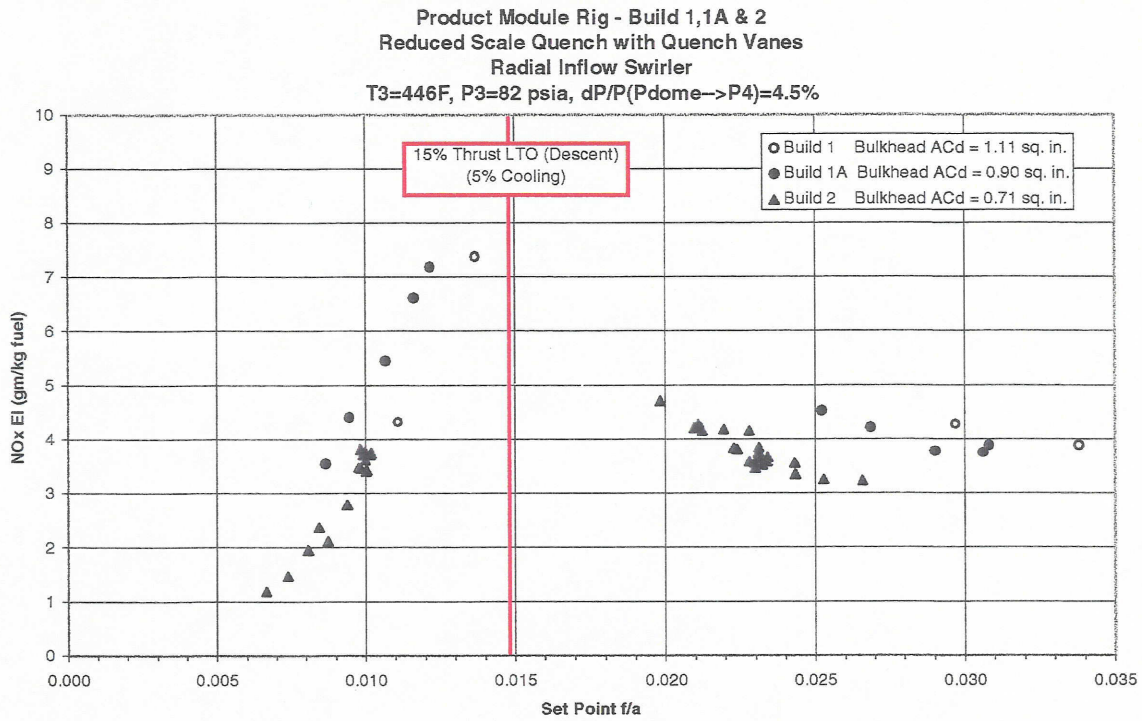


Figure VI - 40 NO<sub>x</sub> Emissions at 15% Thrust LTO (Descent) Condition for Product Module Rig Builds 1, 1A & 2

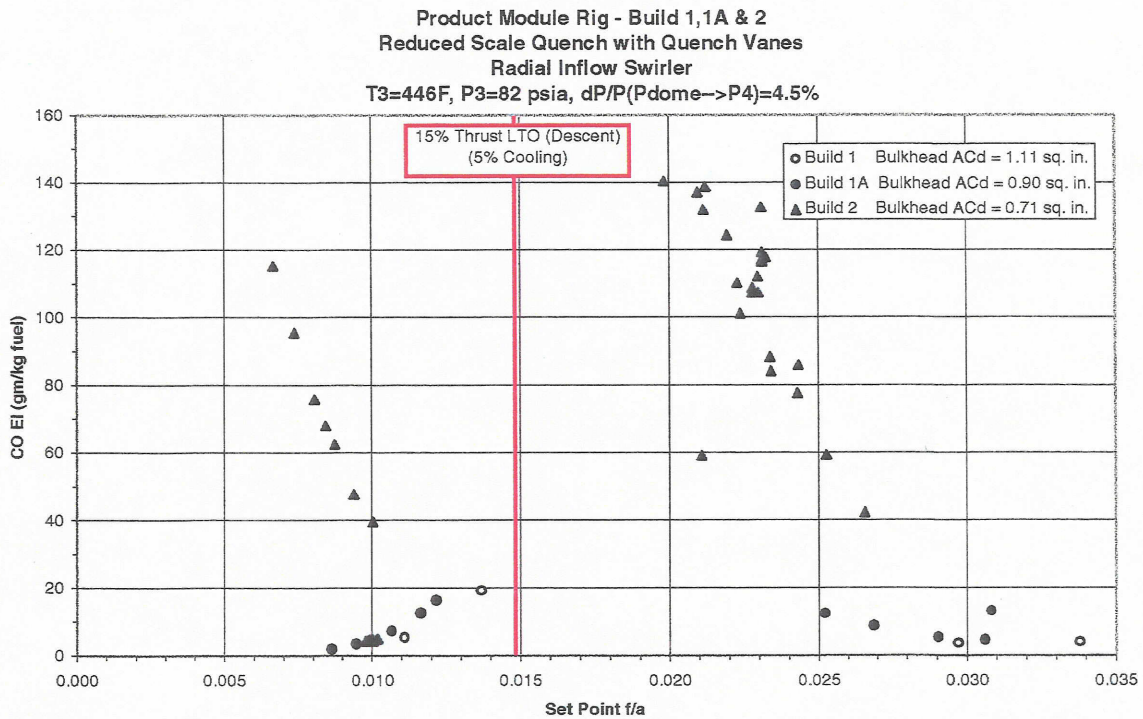


Figure VI - 41 CO Emissions at 15% Thrust LTO (Descent) Condition for Product Module Rig Builds 1, 1A & 2

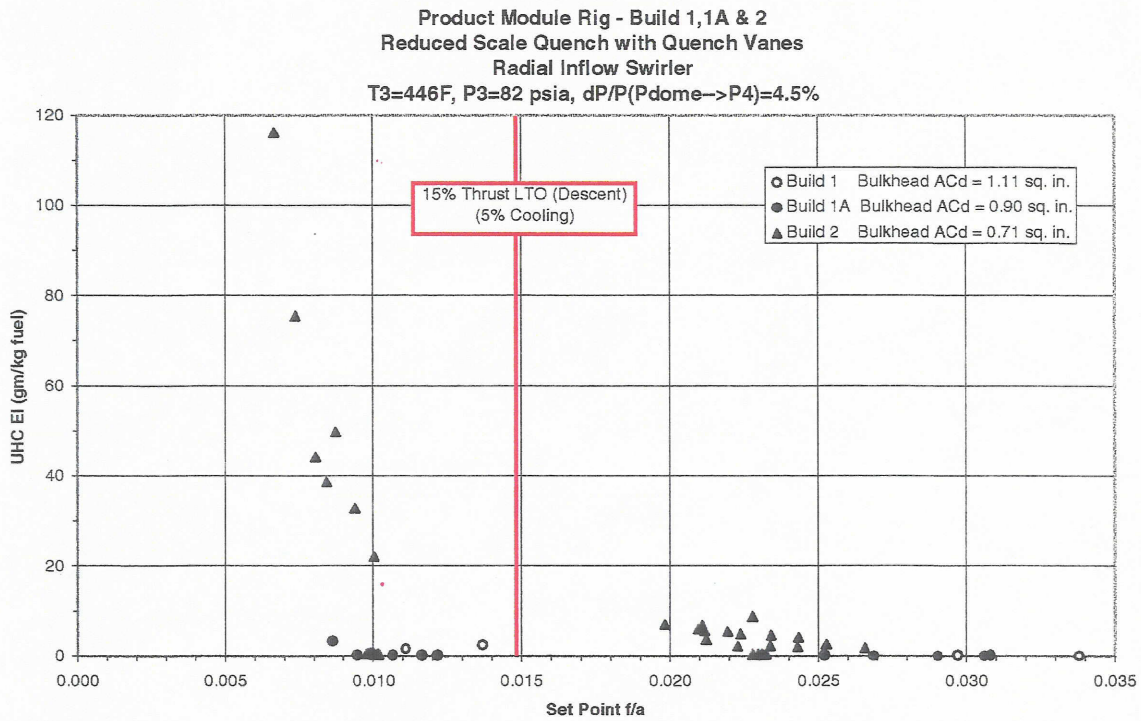


Figure VI - 42 UHC Emissions at 15% Thrust LTO (Descent) Condition for Product Module Rig Builds 1, 1A & 2

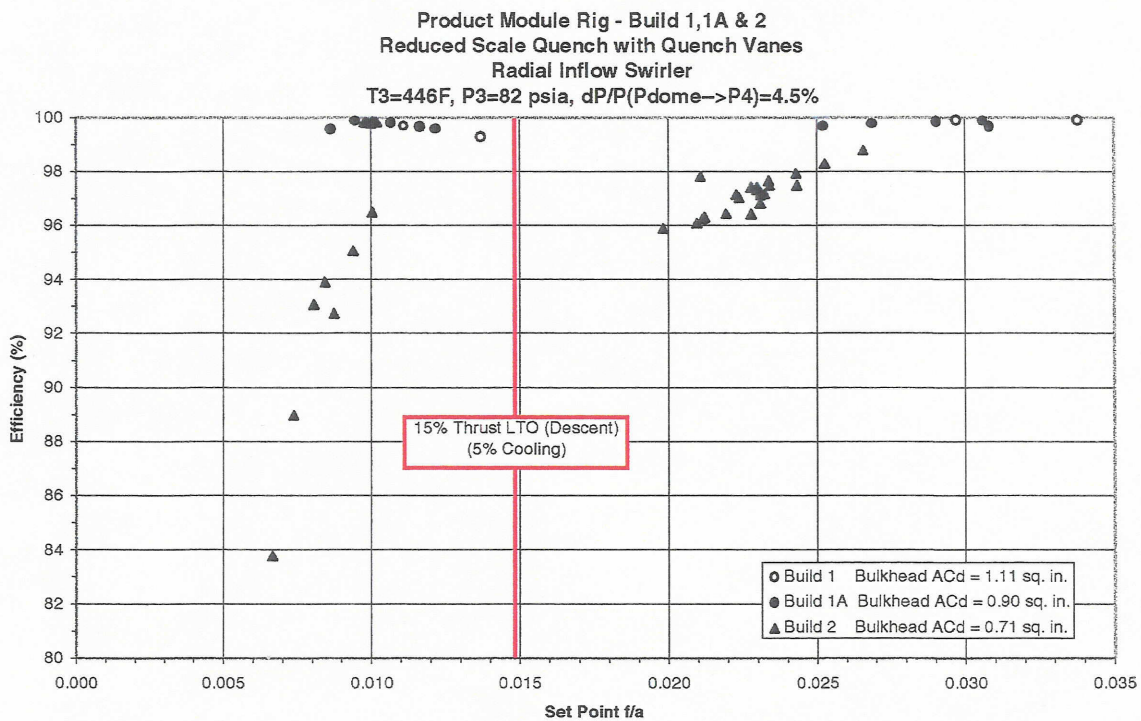


Figure VI - 43 Efficiency at 15% Thrust LTO (Descent) Condition for Product Module Rig Builds 1, 1A & 2

Product Module Rig - Build 2  
 Reduced Scale Quench with Quench Vanes  
 Radial Inflow Swirler  
 T3=650F, P3=80 psia, dP/P(Pdome→P4)=4.5%

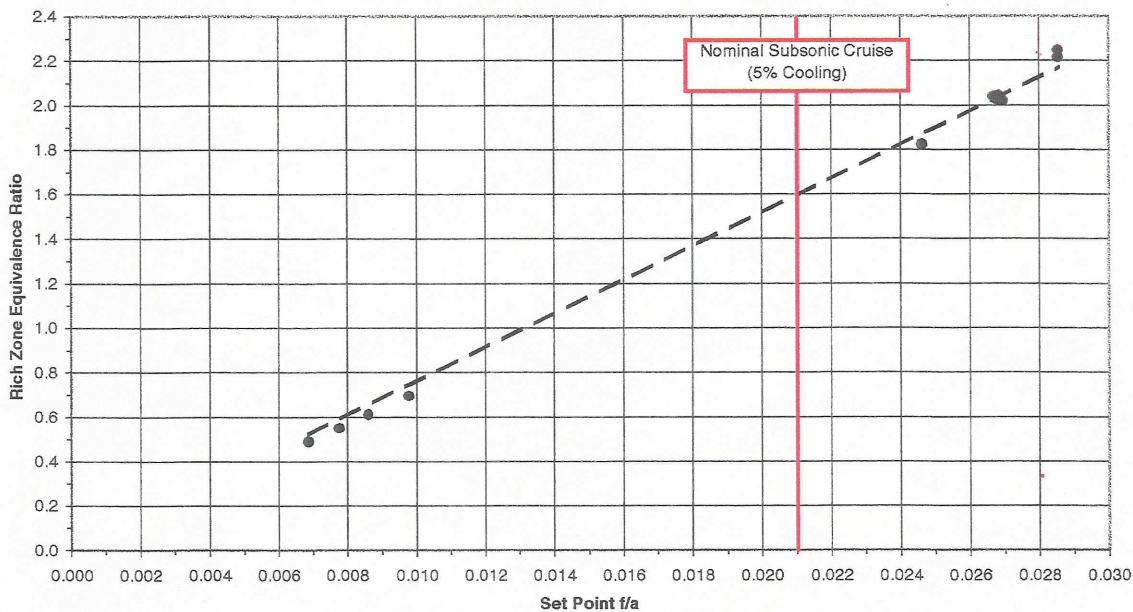


Figure VI - 44 Rich Zone Stoichiometry at Nominal Subsonic Cruise Condition for Product Module Rig Build 2

Product Module Rig - Build 2  
 Reduced Scale Quench with Quench Vanes  
 Radial Inflow Swirler  
 T3=650F, P3=80 psia, dP/P(Pdome→P4)=4.5%

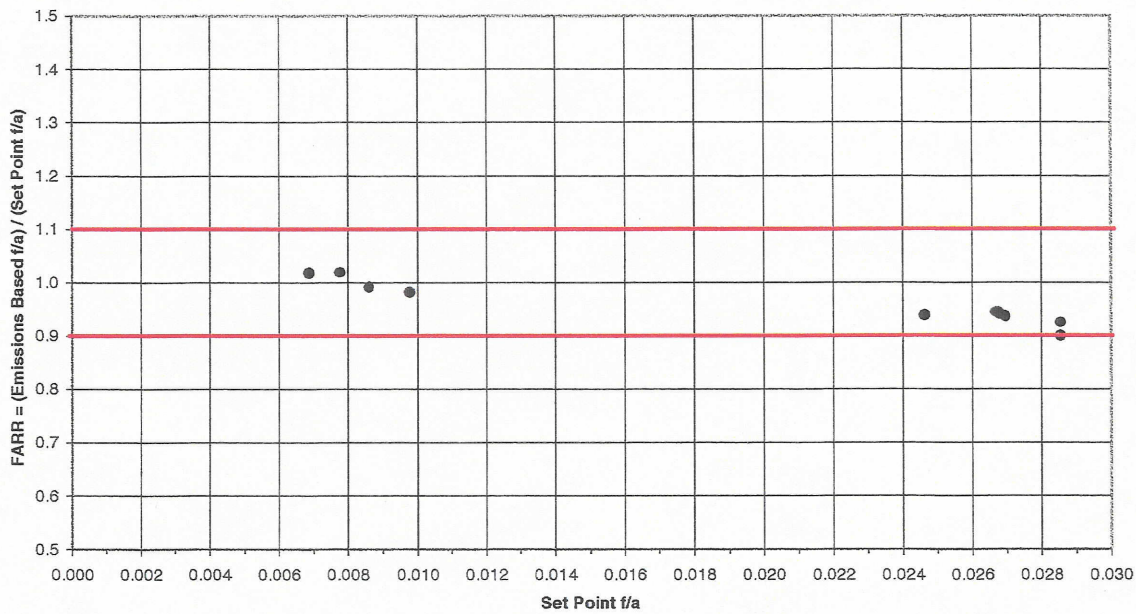


Figure VI - 45 Emissions Data Quality at Nominal Subsonic Cruise Condition for Product Module Rig Build 2

Product Module Rig - Build 2  
 Reduced Scale Quench with Quench Vanes  
 Radial Inflow Swirler  
 T3=650F, P3=80 psia, dP/P(Pdome→P4)=4.5%

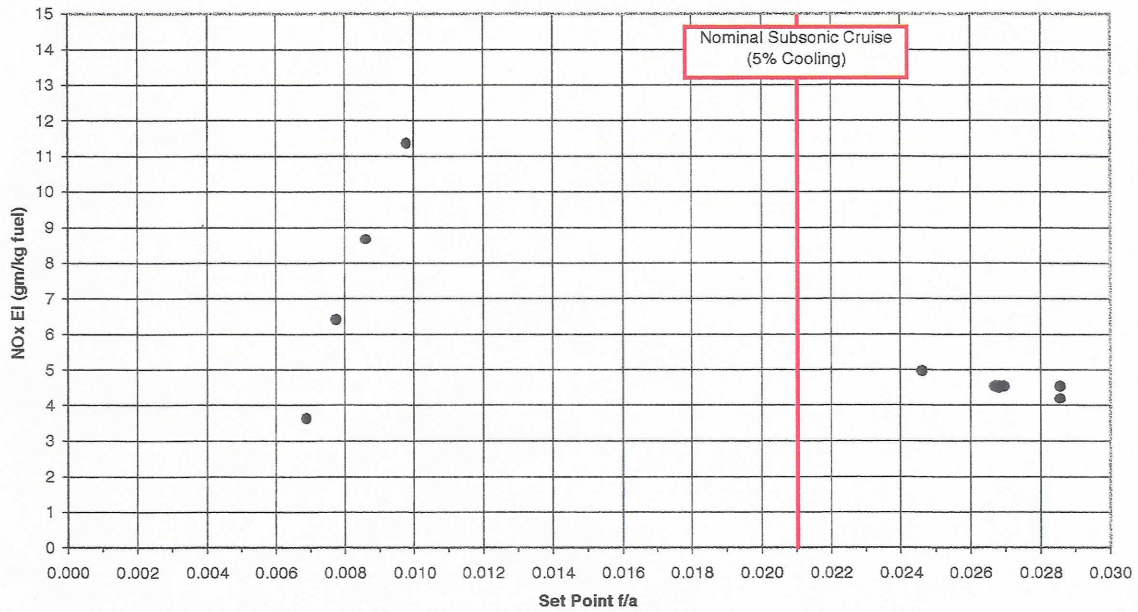


Figure VI - 46 NO<sub>x</sub> Emissions at Nominal Subsonic Cruise Condition for Product Module Rig Build 2

Product Module Rig - Build 2  
 Reduced Scale Quench with Quench Vanes  
 Radial Inflow Swirler  
 T3=650F, P3=80 psia, dP/P(Pdome→P4)=4.5%

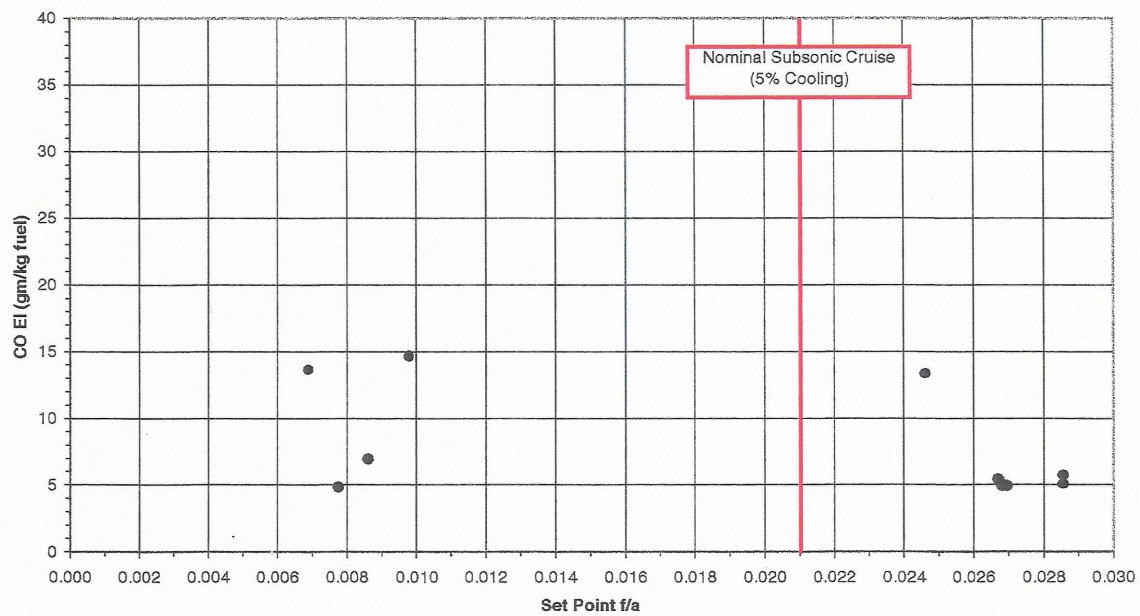


Figure VI - 47 CO Emissions at Nominal Subsonic Cruise Condition for Product Module Rig Build 2

Product Module Rig - Build 2  
 Reduced Scale Quench with Quench Vanes  
 Radial Inflow Swirler  
 T3=650F, P3=80 psia, dP/P(Pdome→P4)=4.5%

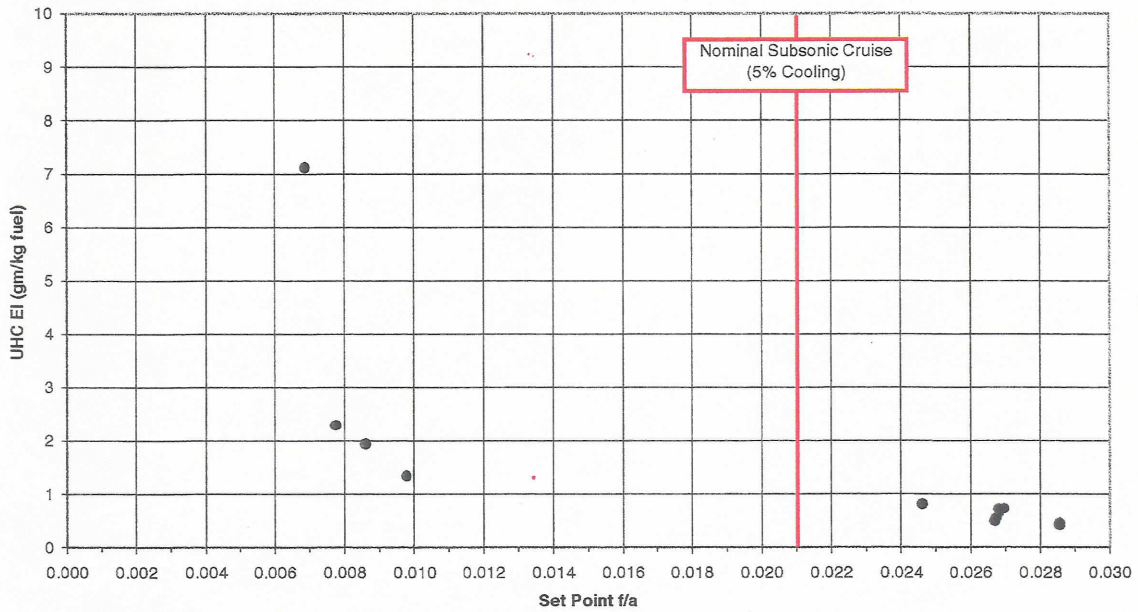


Figure VI - 48 UHC Emissions at Nominal Subsonic Cruise Condition for Product Module Rig Build 2

Product Module Rig - Build 2  
 Reduced Scale Quench with Quench Vanes  
 Radial Inflow Swirler  
 T3=650F, P3=80 psia, dP/P(Pdome→P4)=4.5%

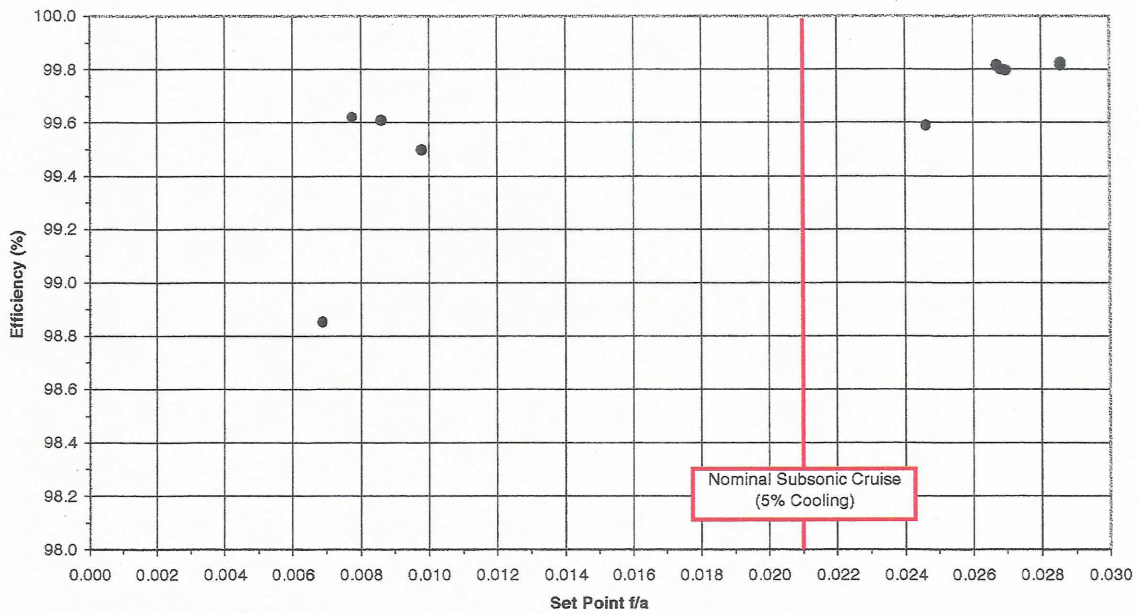


Figure VI - 49 Efficiency at Nominal Subsonic Cruise Condition for Product Module Rig Build 2

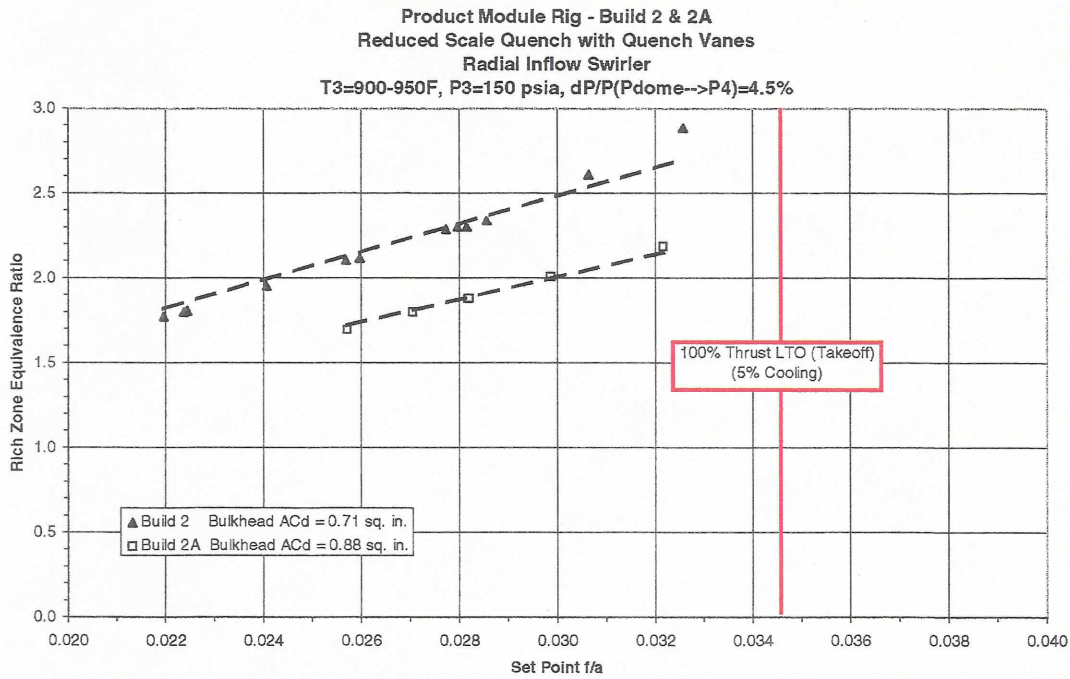


Figure VI - 50 Rich Zone Stoichiometry Comparison at De-rated, Reduced Pressure 100% Thrust LTO (Takeoff) Condition for Product Module Rig Builds 2 & 2A

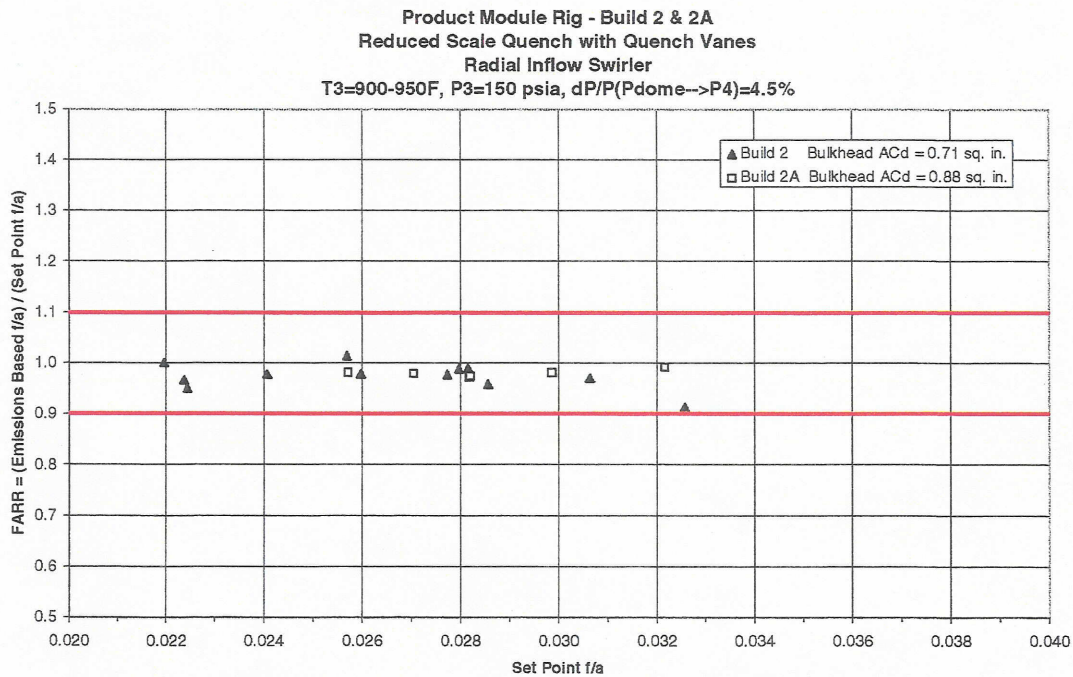


Figure VI - 51 Emissions Data Quality at De-rated, Reduced Pressure 100% Thrust LTO (Takeoff) Condition for Product Module Rig Builds 2 & 2A

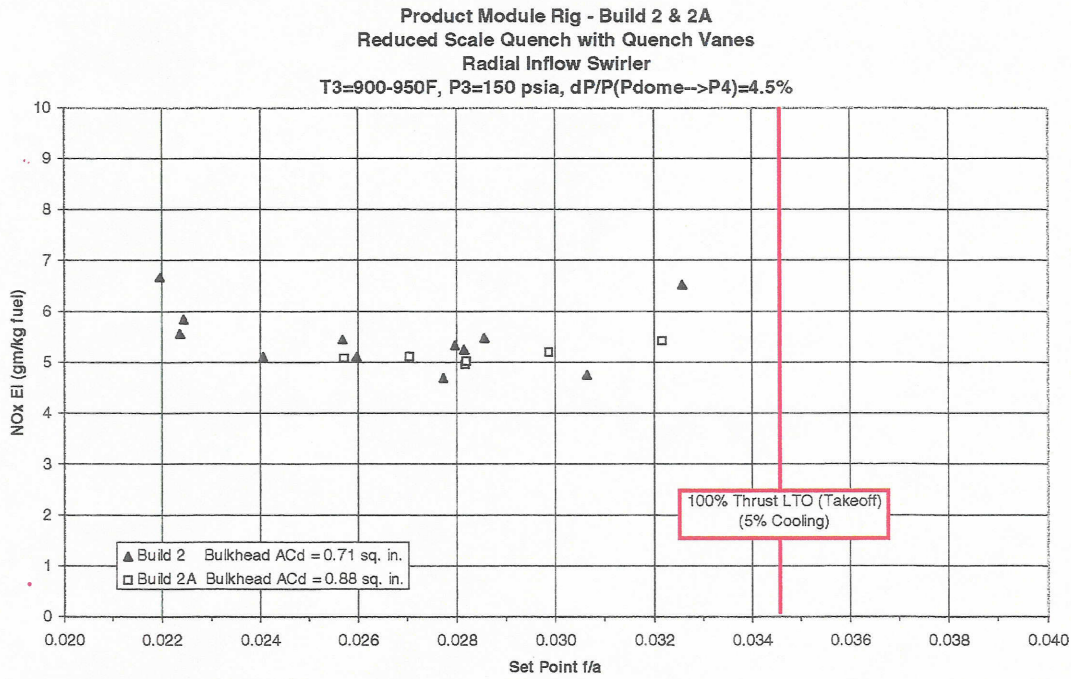


Figure VI - 52 NO<sub>x</sub> Emissions at De-rated, Reduced Pressure 100% Thrust LTO (Takeoff) Condition for Product Module Rig Builds 2 & 2A

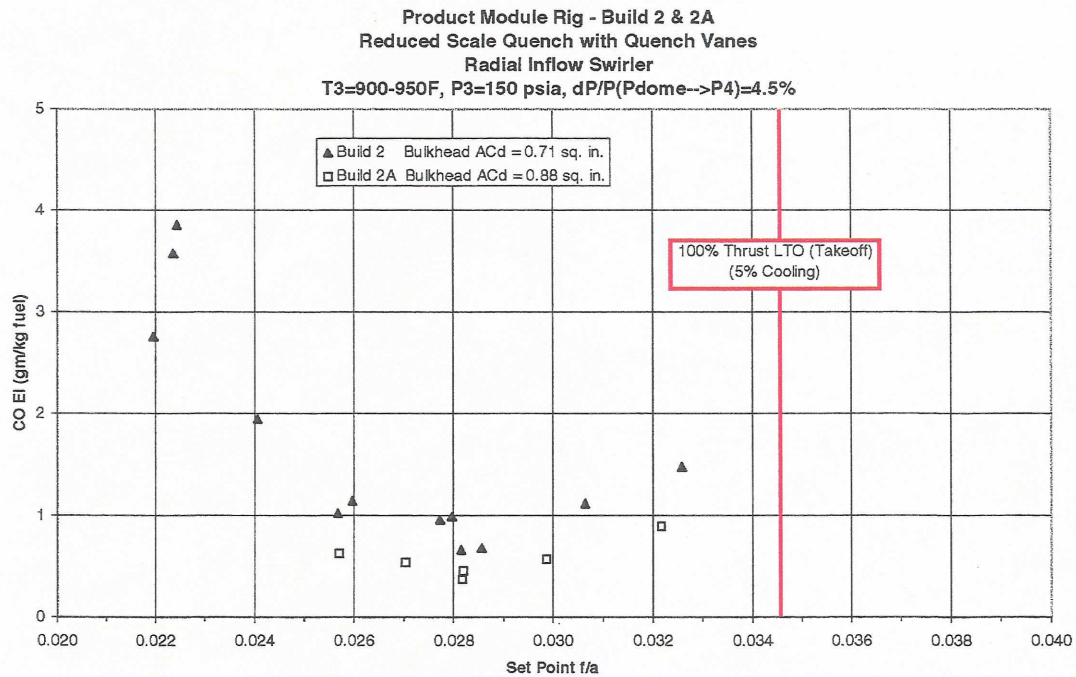


Figure VI - 53 CO Emissions at De-rated, Reduced Pressure 100% Thrust LTO (Takeoff) Condition for Product Module Rig Builds 2 & 2A

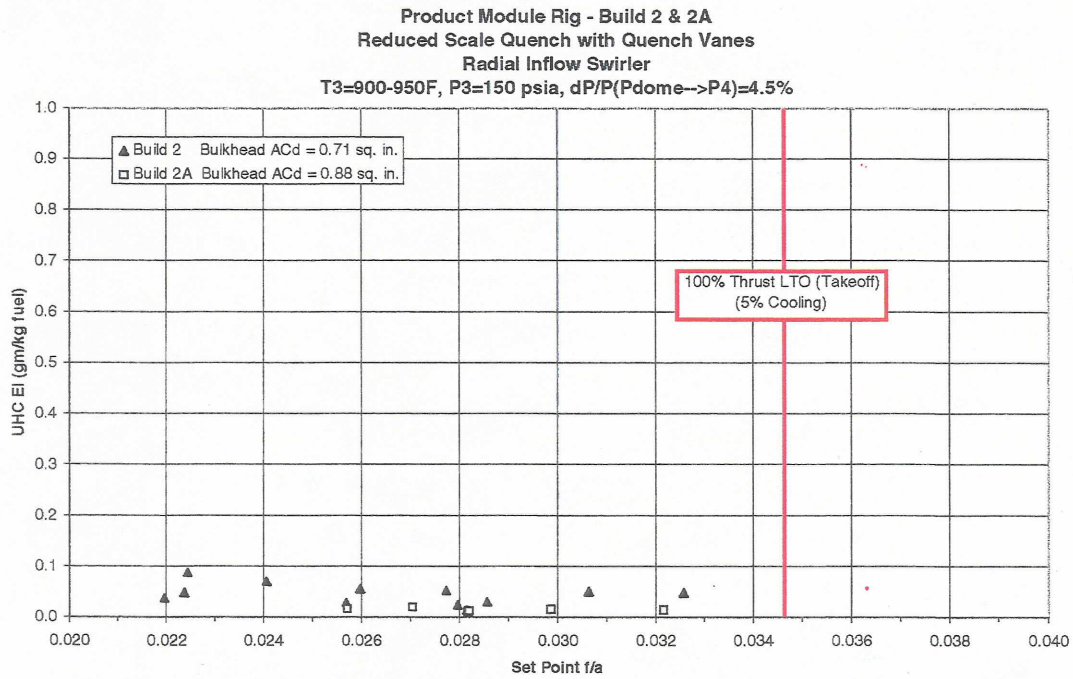


Figure VI - 54 UHC Emissions at De-rated, Reduced Pressure 100% Thrust LTO (Takeoff) Condition for Product Module Rig Builds 2 & 2A

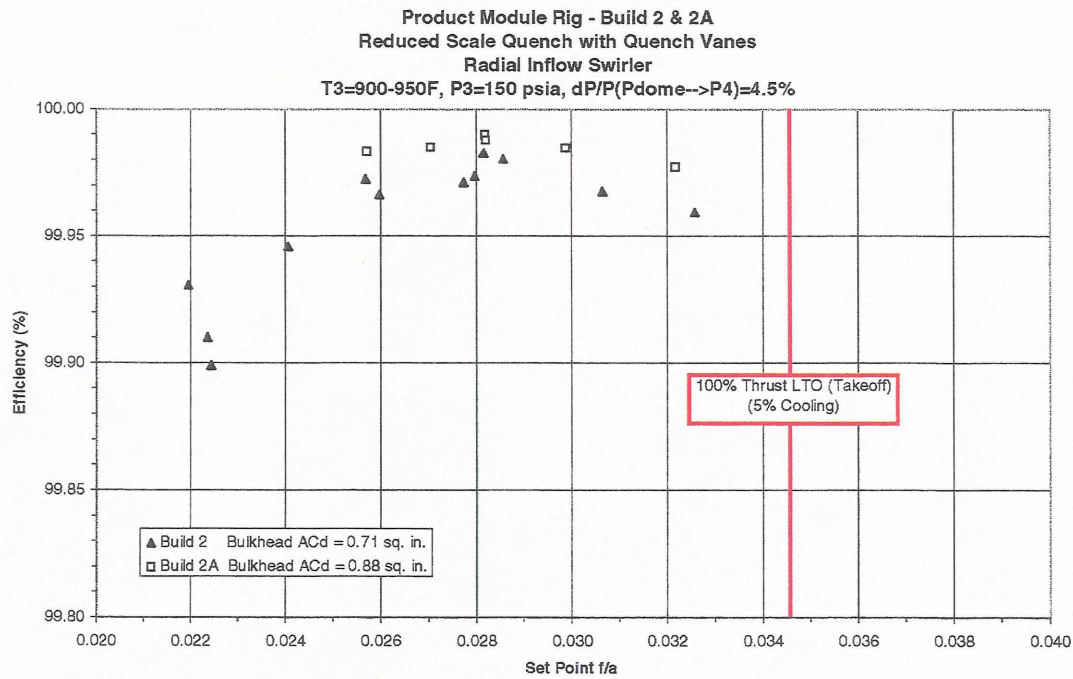


Figure VI - 55 Efficiency at De-rated, Reduced Pressure 100% Thrust LTO (Takeoff) Condition for Product Module Rig Builds 2 & 2A

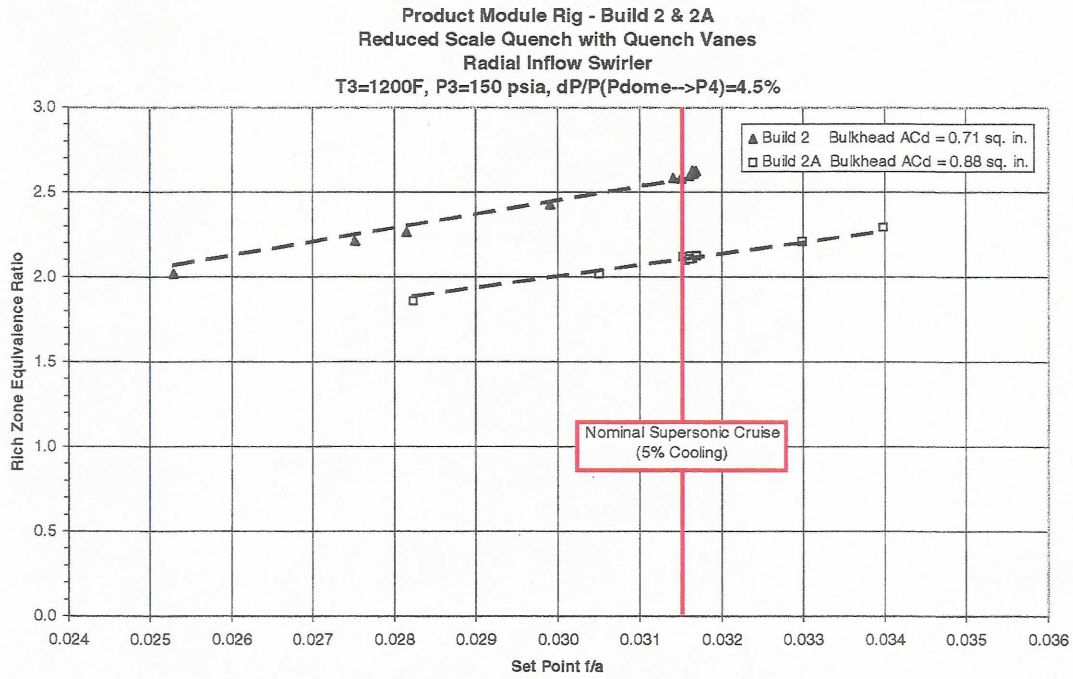


Figure VI - 56 Rich Zone Stoichiometry Comparison at Nominal Supersonic Cruise Condition for Product Module Rig Builds 2 & 2A

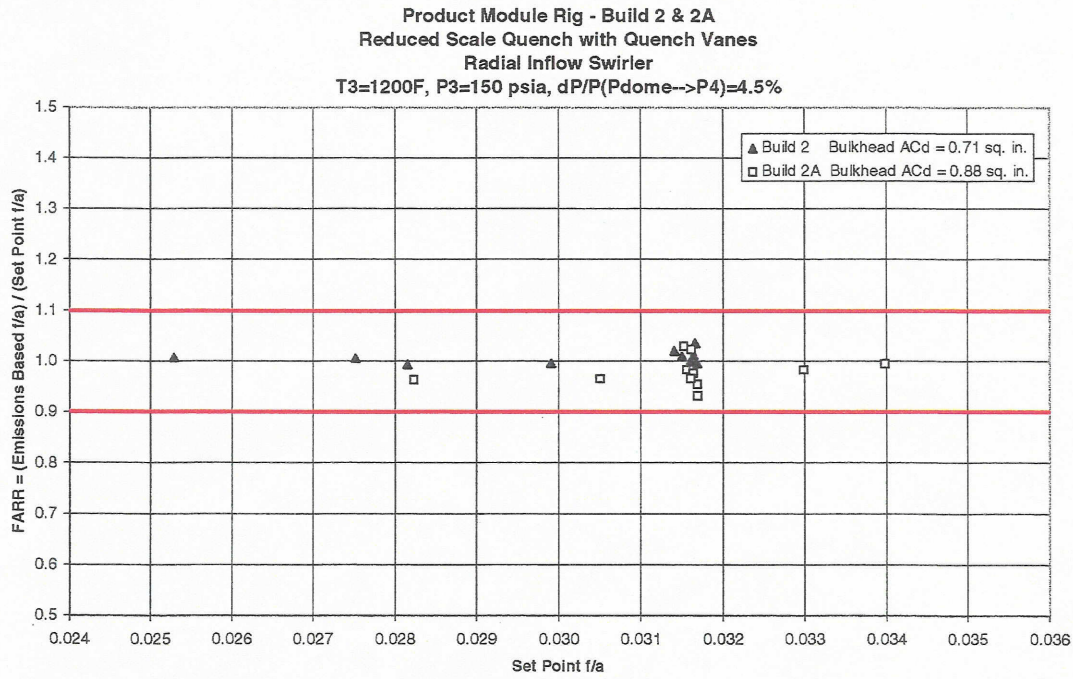


Figure VI - 57 Emissions Data Quality at Nominal Supersonic Cruise Condition for Product Module Rig Builds 2 & 2A

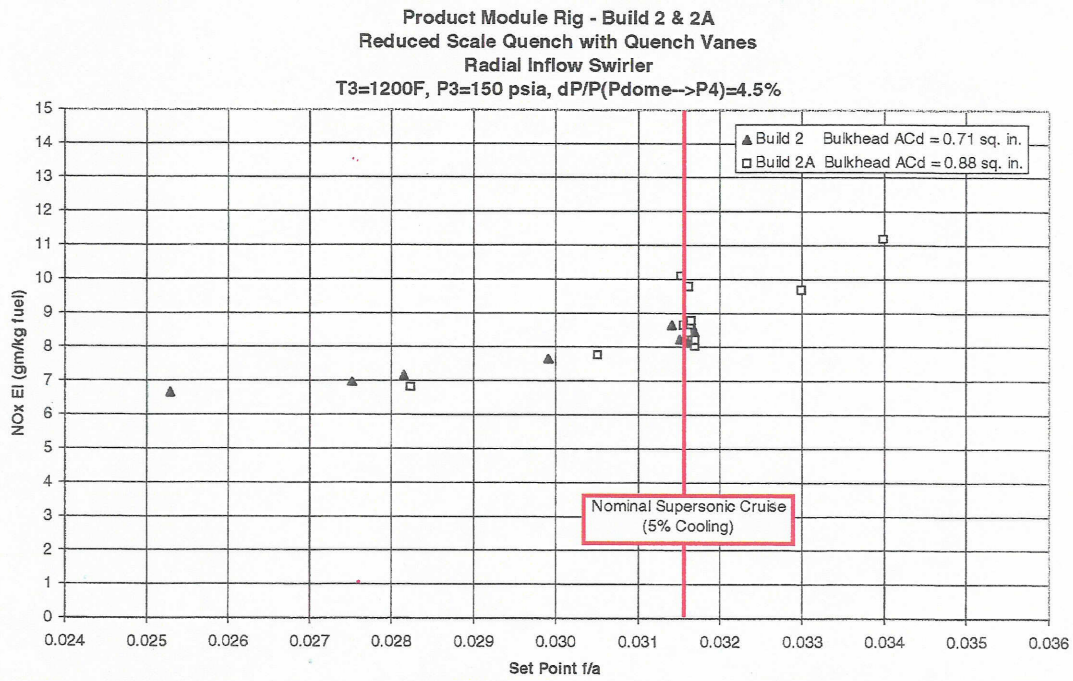


Figure VI - 58 NO<sub>x</sub> Emission Comparison at Nominal Supersonic Cruise Condition for Product Module Rig Builds 2 & 2A

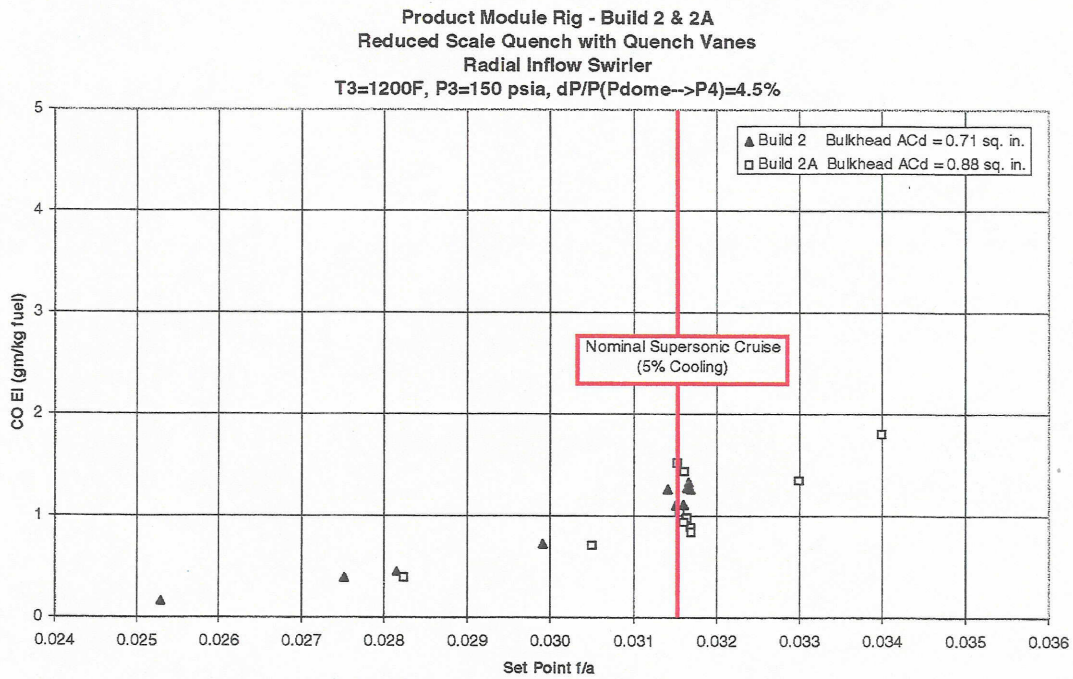


Figure VI - 59 CO Emission Comparison at Nominal Supersonic Cruise Condition for Product Module Rig Builds 2 & 2A

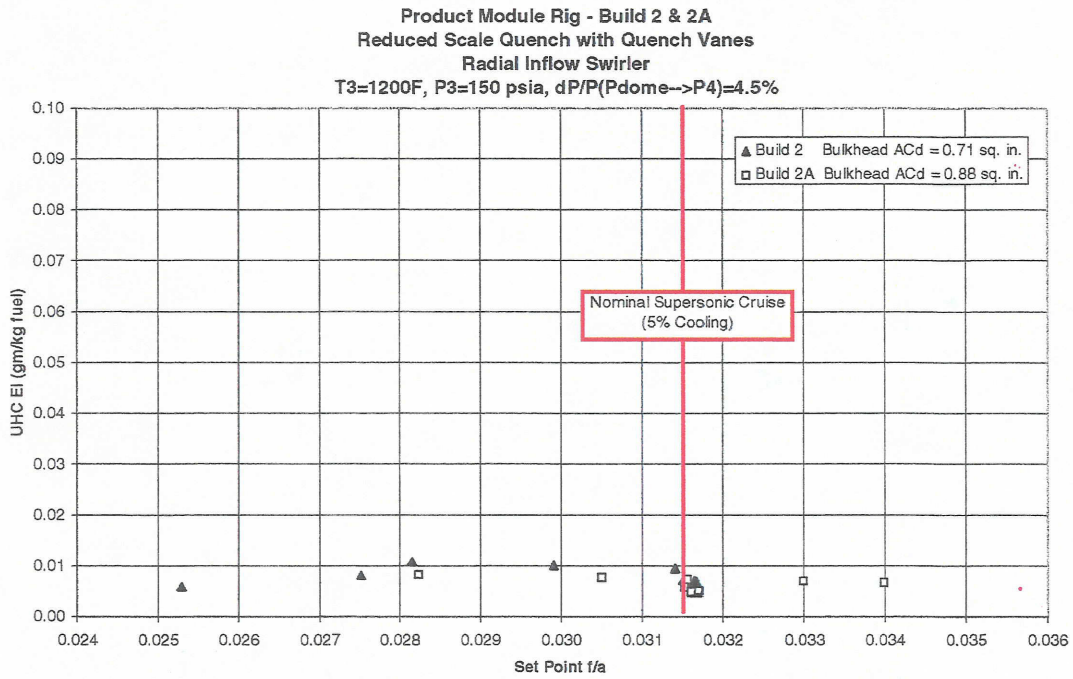


Figure VI - 60 UHC Emission Comparison at Nominal Supersonic Cruise Condition for Product Module Rig Builds 2 & 2A

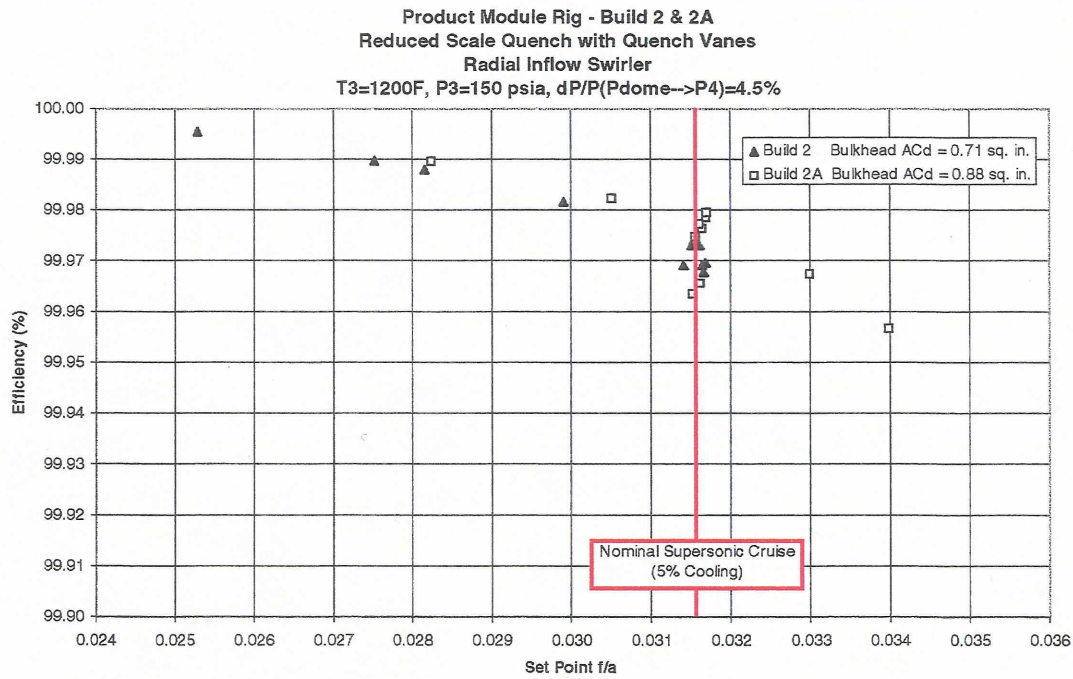


Figure VI - 61 Efficiency Comparison at Nominal Supersonic Cruise Condition for Product Module Rig Builds 2 & 2A

# REPORT DOCUMENTATION PAGE

*Form Approved*  
OMB No. 0704-0188

Public reporting burden for this collection of information is estimated to average 1 hour per response, including the time for reviewing instructions, searching existing data sources, gathering and maintaining the data needed, and completing and reviewing the collection of information. Send comments regarding this burden estimate or any other aspect of this collection of information, including suggestions for reducing this burden, to Washington Headquarters Services, Directorate for Information Operations and Reports, 1215 Jefferson Davis Highway, Suite 1204, Arlington, VA 22202-4302, and to the Office of Management and Budget, Paperwork Reduction Project (0704-0188), Washington, DC 20503.

<b>1. AGENCY USE ONLY</b> <i>(Leave blank)</i>	<b>2. REPORT DATE</b> February 2004	<b>3. REPORT TYPE AND DATES COVERED</b> Final Contractor Report	
<b>4. TITLE AND SUBTITLE</b>  Product Module Rig Test		<b>5. FUNDING NUMBERS</b>  WBS-22-714-01-39 NAS3-27235	
<b>6. AUTHOR(S)</b>  Louis Chiappetta, Jr., Donald J. Hautman, John T. Ols, Frederick C. Padget IV, William O.T. Peschke, John A. Shirley, and Kenneth S. Siskind			
<b>7. PERFORMING ORGANIZATION NAME(S) AND ADDRESS(ES)</b>  Pratt & Whitney P.O. Box 109600 West Palm Beach, Florida 33410		<b>8. PERFORMING ORGANIZATION REPORT NUMBER</b>  E-14294	
<b>9. SPONSORING/MONITORING AGENCY NAME(S) AND ADDRESS(ES)</b>  National Aeronautics and Space Administration Washington, DC 20546-0001		<b>10. SPONSORING/MONITORING AGENCY REPORT NUMBER</b>  NASA CR-2004-212880 MTD211AA	
<b>11. SUPPLEMENTARY NOTES</b>  Project Manager, James D. Holdeman, Turbomachinery and Propulsion Systems Division, NASA Glenn Research Center, organization code 5830, 216-433-5846.			
<b>12a. DISTRIBUTION/AVAILABILITY STATEMENT</b>  Unclassified - Unlimited Subject Category: 07  Available electronically at <a href="http://gltrs.grc.nasa.gov">http://gltrs.grc.nasa.gov</a> This publication is available from the NASA Center for AeroSpace Information, 301-621-0390.		<b>12b. DISTRIBUTION CODE</b>  Distribution: Nonstandard	
<b>13. ABSTRACT</b> <i>(Maximum 200 words)</i>  The low emissions potential of a Rich-Quench-Lean (RQL) combustor for use in the High Speed Civil Transport (HSCT) application was evaluated as part of Work Breakdown Structure (WBS) 1.0.2.7 of the NASA Critical Propulsion Components (CPC) Program under Contract NAS3-27235. Combustion testing was conducted in cell 1E of the Jet Burner Test Stand at United Technologies Research Center. Specifically, a Rich-Quench-Lean combustor, utilizing reduced scale quench technology implemented in a quench vane concept in a product-like configuration (Product Module Rig), demonstrated the capability of achieving an emissions index of nitrogen oxides (NO <sub>x</sub> EI) of 8.5 gm/Kg fuel at the supersonic flight condition (relative to the program goal of 5 gm/Kg fuel). Developmental parametric testing of various quench vane configurations in the more fundamental flametube, Single Module Rig Configuration, demonstrated NO <sub>x</sub> EI as low as 5.2. All configurations in both the Product Module Rig configuration and the Single Module Rig configuration demonstrated exceptional efficiencies, greater than 99.95 percent, relative to the program goal of 99.9 percent efficiency at supersonic cruise conditions. Sensitivity of emissions to quench orifice design parameters were determined during the parametric quench vane test series in support of the design of the Product Module Rig configuration. For the rectangular quench orifices investigated, an aspect ratio (length/width) of approximately 2 was found to be near optimum. An optimum for orifice spacing was found to exist at approximately 0.167 inches, resulting in 24 orifices per side of a quench vane, for the 0.435 inch quench zone channel height investigated in the Single Module Rig. Smaller quench zone channel heights appeared to be beneficial in reducing emissions. Measurements were also obtained in the Single Module Rig configuration on the sensitivity of emissions to the critical combustor parameters of fuel/air ratio, pressure drop, and residence time. Minimal sensitivity was observed for all of these parameters.			
<b>14. SUBJECT TERMS</b>  Gas turbine; Combustor, Rich burn; RQL		<b>15. NUMBER OF PAGES</b> 120	
		<b>16. PRICE CODE</b>	
<b>17. SECURITY CLASSIFICATION OF REPORT</b> Unclassified	<b>18. SECURITY CLASSIFICATION OF THIS PAGE</b> Unclassified	<b>19. SECURITY CLASSIFICATION OF ABSTRACT</b> Unclassified	<b>20. LIMITATION OF ABSTRACT</b>